

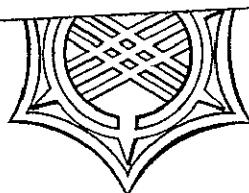
NUCLEAR CHEMISTRY AND GEOCHEMISTRY RESEARCH CARNEGIE-MELLON UNIVERSITY 1969-1970

Truman P. Kohman, Principal Investigator

PROGRESS REPORT

UNITED STATES ATOMIC ENERGY COMMISSION
REPORT NO. NYO-844-81

FACILITY FORM 604	N71-10304	N71-10319
	(ACCESSION NUMBER)	(THRU)
	115	063
	(PAGES)	(CODE)
	CR-111001	06
	(NASA CR OR TMX OR AD NUMBER)	(CATEGORY)



CARNEGIE-MELLON UNIVERSITY

Department of Chemistry

1970 June 30

Pittsburgh, Pennsylvania 15213



Carnegie-Mellon University and
United States Atomic Energy Commission
Contract No. AT(30-1)-844
Report No. NYO-844-81.

N71-10304

N U C L E A R C H E M I S T R Y A N D G E O C H E M I S T R Y R E S E A R C H

C A R N E G I E - M E L L O N U N I V E R S I T Y

Truman P. Kohman, Principal Investigator

PROGRESS REPORT

Sponsors:

United States Atomic Energy Commission

Division of Research

Contract No. AT(30-1)-844

National Aeronautics and Space Administration

Manned Spacecraft Center

Contract No. NAS-9-8073

CARNEGIE-MELLON UNIVERSITY

Department of Chemistry

1970 June 30

Pittsburgh, Pennsylvania 15213

171-1080

C O N T E N T S

PART I.	GENERAL REPORT	1
A.	<u>Introduction</u>	1
B.	<u>Personnel</u>	1
	1. Principal Investigator	1
	2. Research Associates.	1
	3. Graduate Students.	2
	4. Undergraduate Students	2
	5. Technical Assistants	2
	6. Non-technical Assistants	3
C.	<u>Facilities</u>	3
	1. Laboratories	3
	2. Instruments.	3
D.	<u>Publications</u>	4
	1. Published and in Press	4
	2. Presented at National Scientific Meetings.	4
	3. In Preparation	4
E.	<u>Acknowledgments</u>	5
PART II.	RESEARCH PROGRESS REPORT AND PLANS.	6
A.	<u>Nuclear Geochemistry</u>	6
	1. Investigation of the $\text{Sm}^{146}\text{-Nd}^{142}$ and $\text{Sm}^{147}\text{-Nd}^{143}$ System as Dating Methods (Ramzi Y. Saleh).	6 ✓
	2. Tables of Uranium-Thorium-Lead Decay-Growth Functions (Truman P. Kohman)	14 ✓
	3. Search for Long-lived Transuranium Alpha Emitters and Other Anomalous Alpha Emitters in Natural Materials (Nina Landes).	18 ✓
	4. Mössbauer Spectroscopy of Coal-related Minerals (James D. Ulmer)	31 ✓
B.	<u>Nuclear Cosmochemistry</u>	37
	1. Isotopic Composition of Lead and Thallium in Natural Materials (James M. Huey).	37 ✓
	2. Chronology of Galactic Heavy-element Nucleosynthesis (James M. Huey and Truman P. Kohman)	46 ✓
C.	<u>Nuclear Chemistry</u>	57
	1. Search for Natural Radioactivity of Calcium-48 (Mark J. Yeager)	57 ✓

D. <u>Techniques and Instrumentation</u>	65	
1. Instrumentation (Mark Haramic)	65	✓
2. General Scheme of Chemical Analysis of Lunar and Meteoritic Samples (H. Itochi)	69	✓
3. Mass-spectrometry (Lance P. Black and James M. Huey)	76	✓
4. Chemical Procedures for Purification of Uranium and the Alpha-spectroscopy of Uranium (Nancy Kan)	83	✓
5. Alpha-isotope-dilution Analysis of Uranium and Thorium (Brij M. P. Trevedi)	91	✓
6. Least-squares Analysis of Experimental Alpha Spectra (Brij M. P. Trevedi)	97	✓
7. Design and Construction of a Position-sensitive Proportional Counter (John R. Yocum, Jr. and John F. Monahan)	105	✓
E. <u>Miscellaneous</u>	110	
1. A Universal Magnitude System for Astronomical Objects (Truman P. Kohman)	110	✓

SECRET

N U C L E A R C H E M I S T R Y A N D G E O C H E M I S T R Y
R E S E A R C H

C A R N E G I E - M E L L O N U N I V E R S I T Y

1 9 6 9 - 1 9 7 0

PART I. GENERAL REPORT

A. Introduction

This report describes research in the areas of nuclear chemistry, geochemistry, and cosmochemistry carried out on the main campus of Carnegie-Mellon University from summer 1969 through spring 1970 under the principal sponsorship of the United States Atomic Energy Commission under Contract No. AT(30-1)-844.

We include in this document also reports on the progress of research sponsored by the National Aeronautics and Space Administration under its Lunar Samples Analysis Program under Contract No. NAS-9-8073 for "Radiogenic Isotope Studies of Lunar Materials". From the viewpoint of nuclear chemistry, this work is an extension of studies of nuclear phenomena in nature utilizing terrestrial and particularly meteoritic materials, and an opportunity to apply analytical and interpretative techniques to some extent already developed to a new and important class of materials.

The principal part of this Report is a series of contributions authored by the students, research associates, and other research personnel who have participated in one phase of the work or another. Some of the contributions describe incomplete work, plans, ideas, and calculations. Many of the numerical data and suggested interpretations presented here are preliminary or tentative. Those wishing to use or quote such information are requested to treat it as such, and if possible to check as to whether final results have been published or prepared for publication. We will be happy to supply additional information through correspondence, preprints, or reprints as available.

B. Personnel

1. Principal Investigator

Truman P. Kohman: A.B. (1938) Harvard College; Ph.D. (1943), University of Wisconsin; Professor of Chemistry.

2. Research Associates

Dr. Lance P. Black: B.S. (1966) The Australian National University; Ph.D. (1969) The Australian National University; Research Geochemist and Co-Investigator, Lunar Sample Analysis Program.

Dr Haruhiko Ihochi: B.S. (1963) St. Paul's University, Tokyo; Ph.D. (1969) University of Arkansas; Research Chemist and Co-Investigator, Lunar Sample Analysis Program.

2.
300-01-1271
Dr. Brij M. P. Trivedi: B.Sc. (1962) Indian Institute of Technology, Kanpur, India; Ph.D. (1969) Indian Institute of Technology, Kanpur, India; Research Chemist.

3. Graduate Students

Mr. James M. Huey: B.S. (1966) University of Kentucky; M.S. (1969) Carnegie-Mellon University; fourth-year graduate student in Chemistry. For the past three years Mr. Huey has been a NASA Graduate Trainee.

Mr. Ramzi Y. Saleh: B.S. (1963) Ain Shams University, Cairo, Egypt, U.A.R.; second-year graduate student in Chemistry until May 1970. (See below).

Mrs. Nancy Man-Na (née Kuo) Kan: B.S. (1969) National Taiwan University; first-year graduate student in Chemistry.

4. Undergraduate Students

Miss Nina A. Landes: Chemistry, '70; full-time during summer 1969, part-time during academic year. (See below).

Mr. Charles J. Vukotich: Chemistry-Psychology '71; full-time during summer 1969, part-time during academic year.

Miss Sarah E. Weber: Chemistry, '71; part-time during academic year.

Mr. Mark J. Yeager: Chemistry, '71; full-time during summer 1969, part-time during academic year and summer 1970.

Mr. John R. Yocum: Chemistry, '73; part-time during academic year and summer 1970.

5. Technical Assistants

Mr. Mark W. Haramic: Diploma (1968) Air Force Electronics Course for Aircraft Radio; Diploma (1969) Penn Technical Institute; Research Electronics Technician.

Miss Nina A. Landes: B.S. in Chemistry (1970) Carnegie-Mellon University; Junior Research Chemist, summer 1970 (see above).

Mr. Ramzi Y. Saleh: (see above); M.S. in Chemistry (1970) Carnegie-Mellon University; Junior Research Chemist, summer 1970.

Mr. J. David Ulmer: B.S. in Physics (1970) Carnegie-Mellon University; Junior Research Physicist, summer 1970.

Mrs. Ignez de Carvalho: B.S. (1961) Universidade Federal de Minas Gerais, Minas Gerais, Brazil; Instructor, Universidade Federal de Minas Gerais (1964-1968); Assistant Professor of Chemistry, Universidade Federal de Minas Gerais (1968); Laboratory Technician.

6. Non-Technical Assistants

Mrs. Gail R. Chasey: Secretary through April 1970.

Mrs. Judith W. Watt: Secretary beginning May 1970.

C. Facilities

1. Laboratories

All of the work described herein has been conducted in the laboratories in Doherty Hall on the main campus which have been described in previous reports. These include three chemical laboratories and an electronics laboratory on the third floor; a radiochemical laboratory, parts of several chemical laboratories, and a clean room on the second floor; and a large air-conditioned room in the basement which houses the mass spectrometer and the low-level counting instruments. Although this space has served us well, it is now remote from the main focus of advanced study and research of the Department of Chemistry, which has now shifted to the Mellon Institute Building. Moreover, it has become increasingly apparent that the clean room, with ordinary air-conditioning and air filters, is inadequate for work with extremely low levels of trace elements, particularly lead.

The space allocated to this research group in the Mellon Institute Building is now undergoing renovation and preparation for all aspects of our work. It consists of the following units, all but the last of which are on the northeast corner of the fifth floor of the building:

An office suite for professor, research associates, and secretary, including a library and reading room which can be used also for conferences.

An electronics laboratory with a small instruments room.

A large conventional chemical laboratory.

A radiochemical suite consisting of a "hot" and a "warm" area.

A clean laboratory, within which are a walk-in hood and a fume hood each with HEPA (High-Efficiency Particulate-Air) filters.

On the north side of the first floor (basement), a large nuclear measurements laboratory, which will house the mass spectrometer and most of the counting instruments and nuclear spectrometers.

All of this space is air-conditioned, the clean laboratory being provided with specially-filtered room air in addition to the HEPA filters. According to present plans, the renovations will be completed during July and the move will be made during August.

2. Instruments

The radiation detection instruments available are essentially the same as described in last year's Report. Their present status is described in Section II. D. 1. of this Report.

The most important improvement during the year has been in the signal-handling part of the mass spectrometer, which has been equipped with a digital voltmeter, digital printer, and rapid beam-switching device; see Section II. D. 3. of this Report.

D. Publications

1. Published and in Press

ISOTOPIC COMPOSITION OF METEORITIC THALLIUM

R. G. Ostic, H. M. El-Badry, and T. P. Kohman

Earth and Planetary Science Letters 7, 72-76 (1969 Oct.)

NYO-844-78

LEAD AND THALLIUM ISOTOPES IN MARE TRANQUILLITATIS SURFACE MATERIAL

T. P. Kohman, L. P. Black, H. Itochi, and J. M. Huey

Science 167, 481-483 (1970 Jan. 30); Geochimica et Cosmochimica Acta 34,

in press (1970 Supplement)

CMU-NASA-21-3 (Revised)

LEAST-SQUARES FITTING OF DATA WITH LARGE ERRORS

T. P. Kohman

Journal of Chemical Education 47, in press (1970 July ?)

NYO-844-77

TABLES OF URANIUM-THORIUM-LEAD DECAY-GROWTH FUNCTIONS

T. P. Kohman

NYO-844-79

2. Presented at National Scientific Meetings

LEAD AND THALLIUM ISOTOPES IN MARE TRANQUILLITATIS SURFACE MATERIAL

T. P. Kohman, L. P. Black, H. Itochi, and J. M. Huey

Apollo 11 Lunar Science Conference, Houston, Texas, 1970 January 8.

CMU-NASA-21-3

A UNIVERSAL MAGNITUDE SCALE FOR ASTRONOMICAL OBJECTS

Truman P. Kohman

American Astronomical Society Meeting, Boulder, Colorado, 1970 June 10.

NYO-844-80

3. In Preparation

EXTINCT NATURAL RADIOACTIVITY AND POSSIBLE LUNAR MANIFESTATIONS

T. P. Kohman

A UNIVERSAL MAGNITUDE SYSTEM FOR ASTRONOMICAL OBJECTS

T. P. Kohman

CHRONOLOGY OF GALACTIC HEAVY-ELEMENT NUCLEOSYNTHESIS

J. M. Huey and T. P. Kohman

RADIONUCLIDE DISTRIBUTIONS IN THICK IRON TARGETS WITH 0.1 TO 6.1-GeV PROTONS

G.V.S. Rayudu and T.P. Kohman

RADIONUCLIDE DISTRIBUTIONS IN THICK SILICATE TARGETS BOMBARDED BY 0.1-, 0.4- 1.0-, AND 3.0-GeV PROTONS

J. P. Shedlovsky and G. V. S. Rayudu

20201-174

MERCURY AND BISMUTH ABUNDANCES IN IRON METEORITES BY NEUTRON ACTIVATION

J. T. Tanner and T. P. Kohman

MERCURY, THALLIUM, AND BISMUTH IN THE METAL AND TROILITE PHASES OF IRON METEORITES

S. N. Tandon and T. P. Kohman

COSMOGENIC RADIONUCLIDES IN STONE METEORITES

P. J. Cressy, Jr. and T. P. Kohman

COSMOGENIC X-RAY AND β -RAY EMITTERS IN IRON METEORITES

J. H. Kaye, M. M. Chakrabartty, and T. P. Kohman

THORIUM ISOTOPES METHOD FOR DATING MARINE SEDIMENTS

I. Almódovar and T. P. Kohman

DATING OF MARINE SEDIMENTS BY IONIUM AND PROTACTINIUM METHODS

T. P. Sarma and T. P. Kohman

E. Acknowledgments

The persons whose research activities, scientific training, and professional development have benefitted from the support of the Project through AEC Contract AT(30-1)-844 express their appreciation to the Atomic Energy Commission and to the personnel of the Chemistry Programs Branch of the Division of Research for their interest and assistance.

Those of us who have been involved in the Lunar Samples Analysis Program under NASA Contract No. NAS-9-8073 are grateful to the National Aeronautics and Space Administration and to its many personnel who have contributed to the opportunity to participate in this activity, including especially the Apollo 11 and Apollo 12 astronauts.

James M. Huey is indebted to the National Aeronautics and Space Administration for a NASA Graduate Traineeship.

Various individuals who have contributed materials, information, and advice during the past year, whether specifically mentioned in the individual sections of this Report or not, are hereby thanked for their contributions. This includes many professional colleagues who have sent us reports, preprints, and reprints of their publications.

PART II. RESEARCH PROGRESS REPORT AND PLANSA. Nuclear Geochemistry**N71-10305**

II. A. 1

INVESTIGATION OF Sm^{146} - Nd^{142} AND Sm^{147} - Nd^{143} AS DATING METHODS

Ramzi Y. Saleh

I. Introduction

Investigation of Sm^{146} - Nd^{142} and Sm^{147} - Nd^{143} systems for their potential applications to geochronology (1,2,3) has been continued.

The utilization of these systems as dating methods will depend on the extent of Sm-Nd fractionations in natural materials. Sm-Nd fractionations in various types of natural materials have been discussed previously (3).

The discussion of the ion-exchange separation of neodymium and samarium from each other as well as from the other rare-earth elements has been reported previously (3).

Mass spectrometry of 1-5- μg samples of standard solutions of natural neodymium and samarium (4) has been found to be quite feasible.

II. Chemical Procedure

Dissolution of rock samples and group separation of the rare-earth elements has been described elsewhere (3).

The separation of samarium and neodymium from each other as well as from other elements using 1-M ammonium lactate as eluant, Dowex 50W-X8 50-100 mesh as a resin, and 67°C as an operating temperature (1,2,3,6) has been found to be difficult due to the fact that hot columns require specialized equipment and techniques. Moreover, the separability of these two cations, which is a function of the ratio of their distribution coefficients, was not of the right order of magnitude for the elution (7).

Another technique was used in this laboratory for the separation of samarium and neodymium (5). Bio Rad AG-50W-X4 200-400 mesh was used as a resin. 0.4-M ammonium α -hydroxy isobutyrate was the eluant used. The design of the column was the same as that used for the 1-M ammonium lactate separation (3) but different dimensions (30-cm height and 0.6-cm diameter). A coarse fritted-glass disc was sealed at the bottom of the column to support this small-particle size resin instead of using glass wool. The cation-exchange elution curve of samarium and neodymium was determined using two different methods.

A. Determination of Sm and Nd Peak Positions by Visual Inspection of Their Oxalate Precipitates and Pm^{147} Tracer Peak by Beta-Counting

The rare-earth preparation consisted of a mixture of 5 mg Sm, 5 mg Nd, and Pm^{147} tracer. A solution of 0.4-M ammonium α -hydroxy

isobutyrate of pH 4.2 was used as eluant. Ten ml was the fraction size collected at room temperature. The resulting elution curve showed that there was no separation at all, which can be attributed to the high pH value (4.2).

The same experiment has been repeated, using the same concentration of the rare-earth elements and the same technique, with the exception that the pH was reduced to 3.8. The resulting data showed incomplete separation, which might be explained by the same reason given above.

The separation of Sm, Pm¹⁴⁷, and Nd was improved when the pH was reduced to a lower value of 3.6. Figure 1 is an ion-exchange elution curve of macroscopic amounts of Sm, Nd, and Pm¹⁴⁷ tracer. The resulting elution curve obtained using the technique given above showed that a sharp separation between the three rare-earth peaks has been obtained. The results of this experiment were confirmed when the same experiment, with the same technique and conditions, was repeated.

B. Tracer Experiments

The next preparation consisted of a mixture of Sm¹⁴⁵, Pm¹⁴⁵, and Nd¹⁴⁷ gamma-emitting tracers. One mg La was added as a carrier. This experiment was done at room temperature, and the flow rate was 3 drops/min. The same technique was repeated with the exception that the volume of the fraction collected was 5 ml each. Gamma counting was done on every 5-ml test tube, using a Ge(Li) gamma-ray detector and a 512-channel analyzer. Sm¹⁴⁵ was detected by 61-keV γ -rays, Pm¹⁴⁵ by 72-keV x-rays, and Nd¹⁴⁷ by 91-keV γ -rays. Figure 2 is a semi-logarithmic plot of counting rate versus the volume of the eluate. This figure shows that a sharp separation has been obtained.

Another tracer experiment has been done using a rare-earth mineral. A 0.5-g sample of allanite was decomposed using the chemical procedure described elsewhere (1,3). The total rare-earth elements were separated as a mixture, dissolved in HCl, and kept as a stock solution. A mixture of one-tenth of this stock solution, which is equivalent to 50-mg allanite, and which contained about 10-mg rare-earth elements, and tracers of Sm¹⁴⁵, Pm¹⁴⁵, and Nd¹⁴⁷ was prepared. The previous conditions for the Sm and Nd separation were repeated. The data obtained are shown in Figure 3-a. It is observed from this figure that Sm, Pm, and Nd were eluted rather more rapidly than the corresponding peaks in Figure 2. This can be attributed to the fact that in the present experiment there was an appreciable fraction of the column volume nearly saturated by the rare-earth content.

The rare-earth concentration was reduced, when a mixture of 5-mg allanite (one hundredth of the stock solution was used which contained 1000 μ g rare-earth elements) and tracers of Sm¹⁴⁵, Pm¹⁴⁵, and Nd¹⁴⁷ (containing ~ 15 μ g rare-earth elements) was loaded on the column. Figure 3-b is the resulting elution curve.

The concentration of the rare-earth in the ion-exchange column was still further reduced so as to determine the concentration range in which the Sm, Pm, and Nd peak positions will be independent of the amount

present. A mixture of 0.5-mg allanite (containing approximately 100 μg rare-earth elements) and the three radioactive tracers (containing $\sim 15 \mu\text{g}$ rare-earth elements) were loaded on the column. The resulting elution curve is shown in Figure 3-c. Moreover, one more experiment was done using Sm^{145} , Pm^{145} , and Nd^{147} tracers. The total rare-earth element content in the column was $\sim 15 \mu\text{g}$. The data of this experiment which are represented in Figure 3-d were found to be close to those in Figure 3-c. These close results obtained (Figures 3-c and 3-d) may result in the conclusion that if the rare-earth concentration in the ion-exchange column is $\leq 0.1 \text{ mg}$, the Sm, Pm, and Nd peaks will be located at the same positions in the elution curve.

III. Mass Spectroscopy

The technique of mass spectrometry of samarium and neodymium is described elsewhere in this report (4).

IV. Isotope Dilution Analysis of Sm and Nd

Isotope dilution technique will be used to determine the concentrations of samarium and neodymium in natural materials.

Samarium spike enriched in 150 (Sm^{150} fraction and $\text{Sm}^{150}/\text{Sm}^{149}$ ratio as provided from the analysis sheet were 95.1% and 80.59, respectively) and neodymium enriched in 150 (Nd^{150} atom and $\text{Nd}^{150}/\text{Nd}^{146}$ ratio were 94.75% and 86.14, respectively) were obtained from Oak Ridge National Laboratory, Oak Ridge, Tennessee. Each spike was dissolved in 10 ml dil. nitric acid kept in a clean 10-ml volumetric flask, and designated as Sm^{150} spike, 1970 and Nd^{150} spike, 1970.

Standard nitrate solutions of reagent samarium and neodymium oxides of accurately known concentrations were prepared for use in calibration of the spikes. A very sensitive Sartorius Balance was used to determine the accurate weights of these reagents. These nitrate solutions will be standardized using gravimetric techniques, since the stoichiometric composition has not been verified. These reagents were manufactured by Alfa Inorganics, Inc., Beverly, Massachusetts. The concentrations of these nitrate solutions were 77 μg Sm/10 μl and 39.99 μg Nd/10 μl and labeled as Sm-STD. SOLN. 1970 and Nd-STD. SOLN. 1970.

A mixture of 10 μl Sm^{150} spike solution ($\sim 4.3 \mu\text{g}$ Sm^{150}) and 10 μl of the standard reagent (77.00 μg natural Sm) estimated to yield a $\text{Sm}^{150}/\text{Sm}^{149}$ ratio of unity was prepared and analyzed by mass spectrometry (4). Another mixture of 10 μl Nd^{150} spike solution ($\sim 4.1 \mu\text{g}$ Nd^{150}) and a 10 μl of natural neodymium solution, (39.99 μg natural Nd) was prepared and analyzed in a similar manner.

Table I shows the different measured isotope ratio of samarium and neodymium and their mean standard deviations (σ). Sm^{149} and Nd^{146} were selected as reference isotopes for the calculations of the Sm and Nd ratios, respectively. The exact concentrations of both Sm^{150} and Nd^{150} spike solutions were 4.35 μg Sm^{150} /10 μl and 4.11 μg Nd^{150} /10 μl , respectively. The $\text{Sm}^{150}/\text{Sm}^{149}$ and $\text{Nd}^{150}/\text{Nd}^{146}$ ratios used for this calculation were 0.5340 and 0.3291, respectively (4).

IV. Plans for Applications

About 1 g of very old materials (Precambrian rocks and minerals, meteorites, and lunar samples) will be chemically decomposed according to the procedure described elsewhere (3). This solution will be divided into two fractions. One of these fractions will be spiked for the determination of Sm and Nd concentrations. The other fraction will be used for the determination of the isotopic composition of neodymium. It is conceivable that very careful neodymium measurements in very old materials might reveal Nd^{143} and Nd^{142} abundance variations which may be useful for chronological interpretations, particularly if attention is paid to variation in the Sm/Nd ratio. Each of these two fractions will be subjected to the procedure described in part II. B of this section.

References

- (1) R. Y. Saleh, Semi-Annual Progress Report to NASA, Contract NAS-9-8073 (1 May, 1968 - 31 October, 1968), Report CMU-NASA-21-1, Section VI.
- (2) R. Y. Saleh, Semi-Annual Progress Report to NASA, Contract NAS-9-8073 (15 May, 1969), Report CMU-NASA-21-2, Section VI.
- (3) R. Y. Saleh, 1968-1969 Progress Report, USAEC Report NYO-844-76, II. B. 2.
- (4) L. P. Black, This Report, II. D. 3.
- (5) H. L. Smith and D. C. Hoffman, J. Inorg. Chem., 3, 243-247 (1956).
- (6) R. A. Schmitt and R. H. Smith, "A Program of Research for the Determination of Rare-Earth Elemental Abundances in Meteorites", General Atomic Report 3411, September 15, 1961 through August 14, 1962.
- (7) O. Samuelson, Ion Exchange Separation in Analytical Chemistry, (John Wiley & Sons, Inc., New York, 1963) Chapter 3.

TABLE I
MASS SPECTROMETRIC DATA FOR SPIKE CALIBRATION

Samarium			Neodymium		
Ratio	Mean Value	σ of Mean	Ratio	Mean Value	σ of Mean
$\text{Sm}^{144}/\text{Sm}^{149}$	0.2277	± 0.0002	$\text{Nd}^{142}/\text{Nd}^{146}$	1.5941	± 0.0076
$\text{Sm}^{147}/\text{Sm}^{149}$	1.0884	± 0.0008	$\text{Nd}^{143}/\text{Nd}^{146}$	0.7104	± 0.0004
$\text{Sm}^{148}/\text{Sm}^{149}$	0.8157	± 0.0005	$\text{Nd}^{144}/\text{Nd}^{146}$	1.3879	± 0.0008
$\text{Sm}^{150}/\text{Sm}^{149}$	1.0841	± 0.0008	$\text{Nd}^{145}/\text{Nd}^{146}$	0.4837	± 0.0009
$\text{Sm}^{152}/\text{Sm}^{149}$	0.5212	± 0.0005	$\text{Nd}^{148}/\text{Nd}^{146}$	2.9665	± 0.0087
$\text{Sm}^{154}/\text{Sm}^{149}$	0.6197	± 0.0004	$\text{Nd}^{150}/\text{Nd}^{146}$	1.1545	± 0.0003

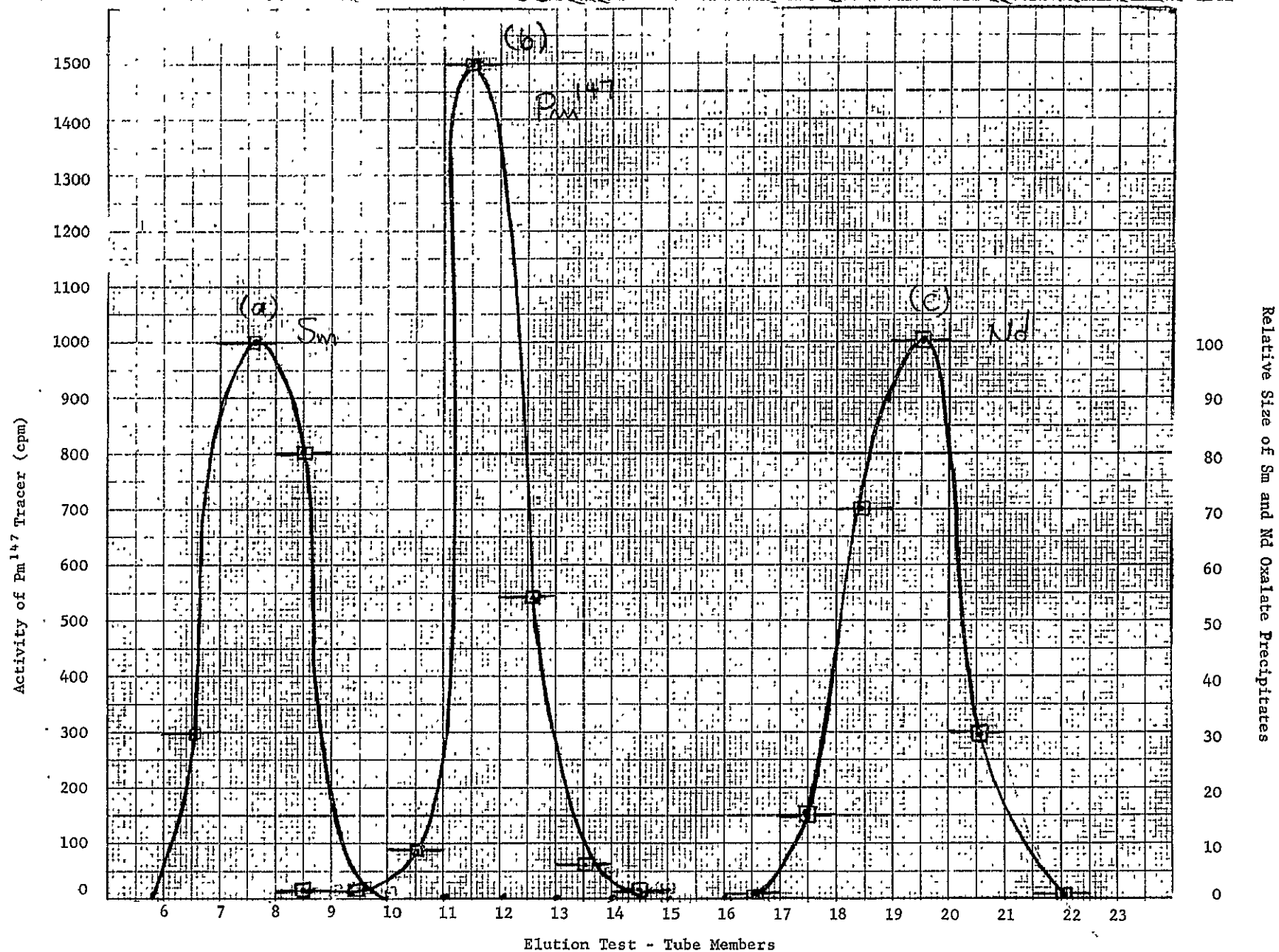


Figure 1. Cation-exchange separation of macroscopic amounts of Sm and Nd and tracer amounts of Pm^{147} . (Exchanger, AG 50W-X4, 200-400 mesh; column, 30 cm long by 0.6 cm diameter; eluant, 0.4-M ammonium α -hydroxy isobutyrate, pH = 3.6; flow rate = 3 drops/min; T = room temperature; each test tube contains 10 ml). (a) 5 mg Sm. (b) Pm^{147} tracer. (c) 5 mg Nd.

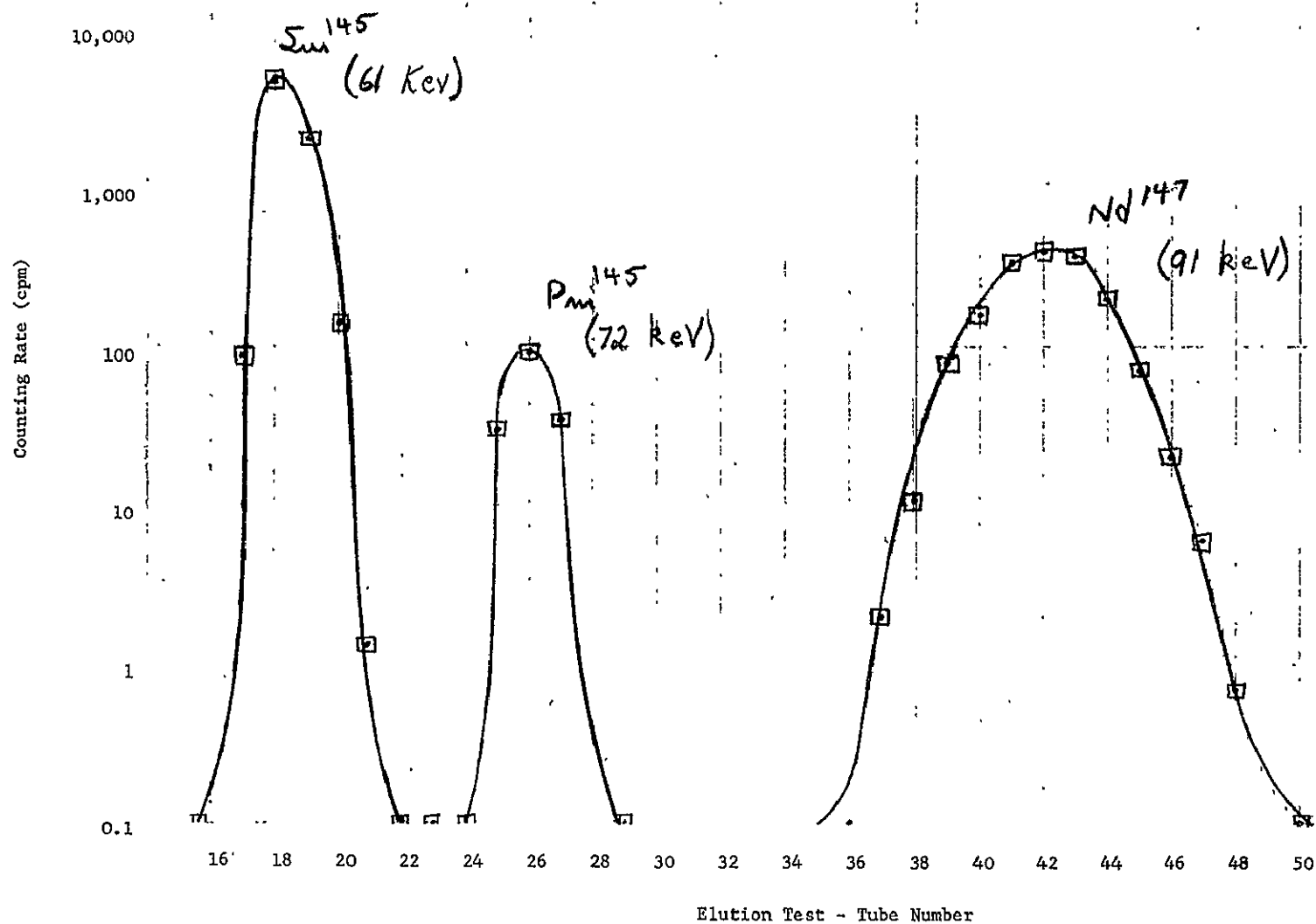


Figure 2. Plot showing Sm^{145} , Pm^{145} , Nd^{147} tracer activities and 1 mg La versus volume of eluate at room temperature. (Each test tube contains 5 ml; exchanger, eluate, and column are same as in Fig. 1)

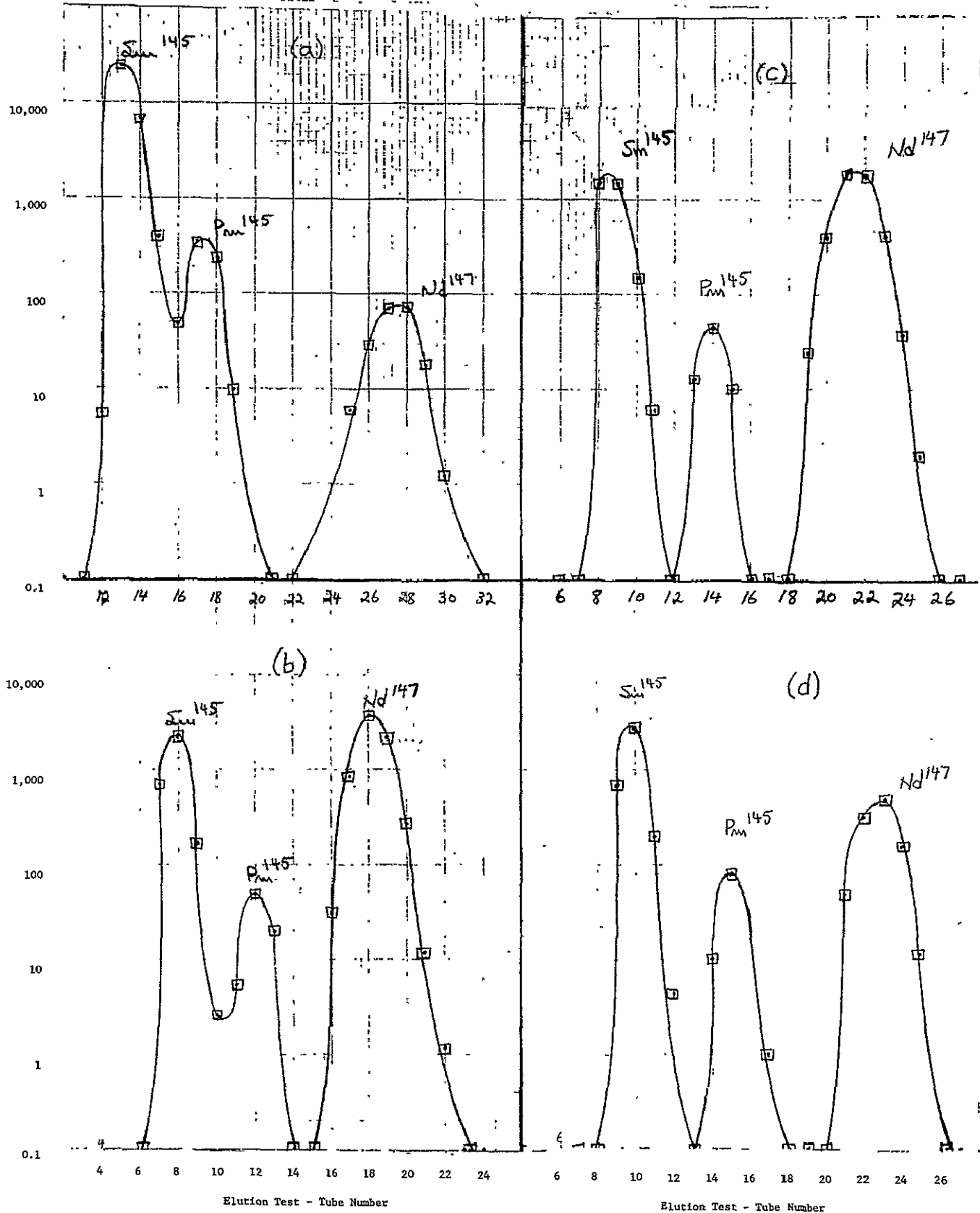


Figure 3. Ion-exchange elution curve of microscopic amounts of Sm, Pm and Nd and their tracers.

- (a) Sm, Pm, and Nd recovered from 50 mg allanite.
 - (b) Sm, Pm, and Nd recovered from 5 mg allanite.
 - (c) Sm, Pm, and Nd recovered from 0.5 mg allanite.
 - (d) Sm, Pm, and Nd tracers only.
- (Other conditions are same as for Fig. 2).

TABLES OF URANIUM-THORIUM-LEAD DECAY-GROWTH FUNCTIONS

Truman P. Kohman

Introduction

Calculations involving the U^{238} - Pb^{206} , U^{235} - Pb^{207} , and Th^{232} - Pb^{208} radioactive systems, particularly in geochronology applications, involve the use of exponential decay or growth functions, singly or in combinations of two or four exponentials involving a single time or two different times. Often the times are the quantities to be evaluated by means of these functions, but the combination functions cannot be solved analytically for the times. Consequently the solutions are usually obtained by successive trials or graphical methods, requiring that the functions be computed several times.

To eliminate some of the tedium of these calculations, a set of six tables giving a total of approximately 15,000 values of functions have been computed and printed with an electronic computer.

Functions Computed

The following quantities are parameters or arguments of the various functions which were computed:

λ_5 = disintegration constant of U^{235}

λ_8 = disintegration constant of U^{238}

λ_2 = disintegration constant of Th^{232}

ζ = $(U^{238}/U^{235})_{\text{present}}$ (atomic ratio)

α = $1/\zeta = (U^{235}/U^{238})_{\text{present}}$ (atomic ratio)

T = age of beginning of single-stage interval ending at present

T_1 = age of end of multiple-stage interval in past

T_2 = age of beginning of multiple-stage interval in past

The single-stage-model functions tabulated in Table I are:

$$e^{\lambda_5 T}$$

$$e^{-\lambda_5 T}$$

$$e^{\lambda_8 T}$$

$$e^{-\lambda_8 T}$$

$$e^{\lambda_2 T}$$

$$e^{-\lambda_2 T}$$

$$\begin{aligned}
 R(\alpha, \lambda_5, \lambda_8, T) &= \alpha \frac{\lambda_5 e^{\lambda_5 T}}{\lambda_8 e^{\lambda_8 T}} & U(\lambda_2, \lambda_8, T) &= \frac{\lambda_2 e^{\lambda_2 T}}{\lambda_8 e^{\lambda_8 T}} \\
 S(\alpha, \lambda_5, \lambda_8, T) &= \alpha \frac{e^{\lambda_5 T} - 1}{e^{\lambda_8 T} - 1} & V(\lambda_2, \lambda_8, T) &= \frac{e^{\lambda_2 T} - 1}{e^{\lambda_8 T} - 1}
 \end{aligned}$$

The multiple-stage functions tabulated are:

Table II: $e^{\lambda_5 T_2} - e^{\lambda_5 T_1}$

Table III: $e^{\lambda_8 T_2} - e^{\lambda_8 T_1}$

Table IV: $e^{\lambda_2 T_2} - e^{\lambda_2 T_1}$

Table V: $S(\alpha, \lambda_5, \lambda_8, T_2, T_1) = \alpha \frac{e^{\lambda_5 T_2} - e^{\lambda_5 T_1}}{e^{\lambda_8 T_2} - e^{\lambda_8 T_1}}$

Table VI: $V(\lambda_2, \lambda_8, T_2, T_1) = \frac{e^{\lambda_2 T_2} - e^{\lambda_2 T_1}}{e^{\lambda_8 T_2} - e^{\lambda_8 T_1}}$

The physical significance of some of these functions is as follows:

- $R(\alpha, \lambda_5, \lambda_8, T)$ = instantaneous production-rate ratio of Pb^{207} to Pb^{206} in natural uranium at time $-T$ (present time = 0).
- $S(\alpha, \lambda_5, \lambda_8, T)$ = slope of single-stage isochron for interval from $-T$ to present on $\text{Pb}^{207}/\text{Pb}^{204}$ versus $\text{Pb}^{206}/\text{Pb}^{204}$ diagram.
- $U(\lambda_2, \lambda_8, T)$ = instantaneous production-rate ratio of Pb^{208} to Pb^{206} at time $-T$ in system with equal numbers of Th^{232} and U^{238} atoms at present.
- $V(\lambda_2, \lambda_8, T)$ = factor which, when multiplied by present $\text{Th}^{232}/\text{U}^{238}$ ratio, gives slope of single-stage isochron for interval from $-T$ to present on $\text{Pb}^{208}/\text{Pb}^{204}$ versus $\text{Pb}^{206}/\text{Pb}^{204}$ diagram.
- $S(\alpha, \lambda_5, \lambda_8, T_2, T_1)$ = slope of multiple-stage isochron for interval from $-T_2$ to $-T_1$ on $\text{Pb}^{207}/\text{Pb}^{204}$ versus $\text{Pb}^{206}/\text{Pb}^{204}$ diagram.
- $V(\lambda_2, \lambda_8, T_2, T_1)$ = factor which, when multiplied by present $\text{Th}^{232}/\text{U}^{238}$ ratio, gives slope of multiple-stage isochron for interval from $-T_2$ to $-T_1$ on $\text{Pb}^{208}/\text{Pb}^{204}$ versus $\text{Pb}^{206}/\text{Pb}^{204}$ diagram.

Nuclear Data Used

The computations have been made for the values of the nuclear constants adopted by Russell and Farquhar (1):

$$\lambda_5 = 0.9722 \times 10^{-9} \text{ y}^{-1}$$

$$\lambda_8 = 0.1537 \times 10^{-9} \text{ y}^{-1}$$

$$\lambda_2 = 0.0499 \times 10^{-9} \text{ y}^{-1}$$

$$\zeta = 137.8$$

These are very close to the earliest reasonably accurate values (2,3,4,5,6). There is some evidence that more accurate values are available (1,7,8). However, these are probably not far from the true values, and they have been recommended again recently by Kanasewich (9). Since most workers in lead isotope geochronology use these values, it seems best to retain them for all calculations until agreement can be reached on a better set.

Description of Tables

The single-stage functions are evaluated at intervals of 0.01 Gy = 10 My for ages up to 6 Gy = 6,000 My. Linear interpolation should be quite adequate for age intervals of 0.001 Gy = 1 My.

The multiple-stage functions are evaluated for $T_2 > T_1$ at intervals of each argument of 0.1 Gy = 100 My for the same range. For 0.01-Gy (10-My) intervals linear interpolation should suffice except for functions involving λ_5 and $T_1 \sim T_2$. In such cases, and in all cases where accurate values are required for 0.001-Gy (1-My) intervals, Table I can be used with an intermediate amount of tedium. Alternatively, tabulated values in the region of interest can be plotted and connected by smooth curves, and intermediate values can be determined by graphical interpolation.

The computations were made by the Carnegie-Mellon University Computation Center's UNIVAC 1108 computer with a FORTRAN V program designated UPTHLE. The exponentials in the first three columns of Table I were evaluated directly, and all other values in Tables I-VI were computed from them. Appropriate derivative functions were substituted for limiting cases which would lead to 0/0. Compilation and execution required 23 seconds.

Availability of Tables

These tables are available as CMU-AEC Report No. NYO-844-79, dated 1970 May 15. A listing of the program can be supplied on request.

708 01 - 18W

References

1. R. D. Russell and R. M. Farquhar, Lead Isotopes in Geology (Interscience Publishers, Ltd., London, 1960), pages 6-7.
2. A. O. Nier, Phys. Rev. 55, 150-153 (1969).
3. A. F. Kovarik and N. I. Adams, Jr., J. Appl. Phys. 12, 296-297A (1941).
4. A. F. Kovarik and N. I. Adams, Jr., Phys. Rev. 98, 46. (1955).
5. A. F. Kovarik and N. I. Adams, Jr., Phys. Rev. 54, 413-421 (1938).
6. M. Lounsbury, Canadian J. Chem. 34, 259-264 (1956).
7. E. K. Hyde, I. Perlman, and G. T. Seaborg, The Nuclear Properties of the Heavy Elements. II. Detailed Radioactivity Properties. (Prentice-Hall, Inc., Englewood Cliffs, N. J., 1964), pages 434-438 and 489-492.
8. C. M. Lederer, J. M. Hollander, and I. Perlman, Table of Isotopes, Sixth Edition (John Wiley and Sons, Inc., New York, 1967).
9. E. R. Kanasewich, Chapter 4 (pages 147-223) in Radiometric Dating for Geologists (E. I. Hamilton and R. M. Farquhar, Eds.; Interscience Publishers, John Wiley and Sons, London, 1968).

II. A. 3.

SEARCH FOR LONG-LIVED TRANSURANIUM ALPHA EMITTERS AND OTHER ANOMALOUS
ALPHA EMITTERS IN NATURAL MATERIALS

Nina Landes

I. Introduction

Any discussion of a search for unknown transuranium elements in natural materials must necessarily begin with a theoretical justification for their survival as possible primary alpha emitters. First it must be shown that superheavy elements could have been formed in nucleosynthesis. Then, it must be proven that the elements thus formed could not only have outlasted the period Δt when the elements reacted, fractionated, and condensed into the minerals composing the planets and meteorites, thus qualifying them to be classified as "extinct natural radioactivity" (1), but also be around today. Nilsson et al., point out that $t_{1/2}$ must be greater than 2×10^8 years to be detected by the techniques previously tried by Thompson, by Ghiorso, and by Fowler (2).

Superheavy elements could have been produced in the r-process during a Type I supernova explosion (3), as evidently were considerable portions of the known heavy elements, besides all the isotopes of uranium and thorium, and Pu^{244} . Difficulties arise because the heavier the intermediates formed by neutron bombardment, the more likely they are to fission spontaneously before they can beta decay to stable superheavy nuclides. Still, the possibility that some would have survived cannot be ruled out. Once formed, the nuclide must be sufficiently stable to alpha and beta decay and to spontaneous fission, the latter tending to assume more and the second less importance with increasing mass number in the transuranium region (3). An account of the projected half lives for all three modes led Nilsson (2) to propose that the nuclide $^{294}110$ is likely to be around today. Large uncertainties in the calculations give leeway for other elements instead of $^{294}110$. Seaborg concluded that it is feasible to expect the survival of a small number of primary emitters, particularly in the islands of stability around $Z = 126$, $N = 184$, and $Z = 114$, $N = 184$ (3).

Studies have been made of the newly discovered phenomenon of shape isomerism, in which a relative minimum can exist in the potentials of known elements due to a stable vibrational state conducive to fission (4). This opens up the possibility of various modes of decay from this state in the known elements, which have previously been predicted to be energetically unlikely, and poses a rationale for anomalous alpha activity.

Many investigators have reported evidences of what they interpret as extinct natural radioactivity, some of which might otherwise be interpreted as being caused by previously unknown primary radioactive emitters. Observances of an unusual abundance of Xe^{129} have been interpreted as evidence of "in situ" beta decay of an extinct I^{129} parent, which is itself a daughter of spontaneous fission from Pu^{244} (5). Unusual abundances of Xe^{136} have variously been attributed to extinct Pu^{244} fissioning (6) and to an extinct transuranium element (7).

In addition, some investigators detected evidence of anomalous alpha activity. Cherdyn'tsev et al., attributed an excess of U^{235} to either extinct Cm^{147} or to an extinct transuranium element (8), and they also reported an anomalous abundance of Pu^{239} (9,10). They reported anomalous alpha activity in the 4.2-4.6 MeV and 5.0-5.3 MeV regions for U^{235} -rich samples, and in the 4.4-4.6 MeV region for Pu^{239} -rich samples.

Cherry, Richardson, and Adams (11) also reported anomalous alpha activity in the 4.4 MeV region, in thorite and huttonite isolated from Conway granite from Conway, New Hampshire.

Gentry in his studies of pleochroic halos found "giant halos" (12), and an anomalous halo designated as "type Y" in a sample also containing Po^{210} , Po^{214} , and Po^{218} halos, without the halos of their usual uranium and thorium parents (13).

Our investigations are being conducted by two separate techniques. The first technique is designed to isolate the volatile elements, because elements 114-118, likely candidates for stable transuranium elements, are analogs to the volatile elements 82-86, and would thus probably be volatile (3), and because the excess xenon which Anders and Heymann found was in a chondrite containing the volatile fraction of the elements (7). Another procedure is being used to observe non-volatile elements.

We feel that studies of alpha activity are likely to be revealing as a search method. Most heavy nuclides ($Z \geq 83$) emit alphas. In particular, since some of our studies are on rocks containing pleochroic halos, which are produced by alpha particles, it is essential that we study this mode of emission. Alpha counting is attractive because of its high sensitivity, good resolution, low background, and high counting yields for small samples.

Our studies range from 3-15 MeV, with particular attention being focused on the 4.4 MeV region cited by Cherry, Richardson, and Adams, and on the energies corresponding to anomalous pleochroic halos, the giant halos representing alphas of energy 9-10 MeV (12) and the Y type of energy 6.55 MeV (13). In general, we first scan the entire 3-15 MeV range, and then observe in detail the energies less than 9 MeV, where known peaks tend to obscure other activity.

II. Physical and Chemical Procedures

A. Procedure for Non-Volatile Elements (see reference 14)

The technique makes use of the knowledge and presumption that heavy elements tend to substitute themselves into the cation positions of thorite [$Th(SiO_4)$] and zircon [$Zr(SiO_4)$]. Both of these minerals are very dense, with a specific gravity of 6.7 for thorite and 4.6-4.7 for zircon (15) and both are non-magnetic. There is little else in igneous rock with both these characteristics. For example, quartz and many silicates are non-magnetic but have low densities. Minerals rich in iron are heavy, but they are all slightly to strongly magnetic. Consequently, the technique centers around a heavy liquid separation followed by a magnetic separation. A flow chart is given below (Figure 1).

The sample is first crushed in a large manual press, such as the one in the Metallurgy Department of Carnegie-Mellon University, further crushed with a hollow tube, rod, and hammer assembly, and finally ground with an electrically operated mortar and pestle. Sieving is done at every step of the way to remove the grains which are small enough. A too-fine sample cannot be separated in the heavy-liquid step because of colloidal effects, and the grains in a too-coarse sample tend to be non-homogeneous. The samples used ranged from 40-200 mesh.

A 30-g portion of a sample of the proper grain size is washed with distilled water, dried in an oven, and poured into a 250-ml separatory funnel previously filled with 70 ml of bromoform ($d = 2.89 \text{ g/cm}^3$). The funnel is shaken, and the contents up to the interface with the floating layer are emptied into a 60-ml sintered-glass funnel over a 250-ml vacuum flask. The heavy and intermediate density material is dried with acetone, following which it undergoes an identical separation with methylene iodide ($d = 3.325 \text{ g/cm}^3$). Both heavy liquids can be saved and re-used.

The heavy fraction is further separated with a strong permanent hand magnet. The magnet is covered with a piece of plastic and tediously run over the spread-out sample as close as possible without touching. The attracted particles fall off the plastic onto a piece of paper when the magnet is removed from the plastic.

The technique of sample deposition for alpha counting varies depending on whether or not it is desired to include volatile elements with the non-volatile. Both techniques use Pt discs 1 inch in diameter. As much as possible of a 1-mg aliquot of the final separation fraction is dissolved in 4-N HNO_3 and deposited with a dropper on the planchet. At this point, if the object is to count only non-volatiles, a few drops of TEG (tetra-ethylene glycol) are added to raise the boiling point, as the TEG monomer boils at 276°C and the polymers formed with heating boil even higher. The slow evaporation and precipitation which results gives a uniform deposit (16,17). A heat lamp is placed over the planchet to dry it, and the planchet is then flamed to remove any remaining organic matter. Unfortunately, this last step, necessary with TEG, may lose the volatile elements. Thus when volatiles are to be included, the sample is evaporated from straight nitric acid. Plans are being made for setting up an electro-deposition unit, so that volatile elements can be counted with better resolution than that obtained by nitric acid deposition.

B. Procedure for Volatile Elements

This approach is particularly useful in that uranium, thorium, and many of their decay products, plus most bulk elements, which tend to mask other alpha activity are absent from the spectrum. The sample is ground, sieved, and separated with the two heavy liquids. It is then placed in the furnace, in a boat in a fused-quartz tube (18). The volatile material dissolved from the fused-quartz condensation tube with 4-N HNO_3 is ready to be deposited on the planchet.

III. Alpha Counting

All samples were counted on one of the two ORTEC detectors available for this research (19). Energy calibrations were made for the narrow ranges with a natural uranium standard, and for the wide ranges with Sample D (See section V-C of this report.), which is dominated by Th^{232} and its decay products, with lesser contributions from the U^{238} series. Linearity within the standardized ranges was confirmed by plotting the known energies of the nuclides postulated to correspond to the peaks obtained, against the channel numbers of the peaks, and checking to see if all the points fall on a straight line.

A voltage divider was added to the alpha system to extend its range. It was discovered that if the post amplifier bias on the alpha system is set at "1", the voltage divider could be used without destroying linearity. It was then possible to obtain energies up to 21.7 MeV.

IV. Results

A. Conway Granite, by Procedure for Non-Volatiles

Samples A and B were prepared from a core sample of Conway granite, similar to that used by Cherry, Richardson, and Adams (11). Sample A was deposited with TEG and analyzed in the range 3.59-5.74 MeV. Sample B was deposited with plain nitric acid and analyzed in the range 3.73-5.79 MeV. The spectra are given below in Figures 2 and 3. Note that no activity was observed in the 4.4 MeV region. Sample A was run again at a wider range, 2.00-7.56 MeV (Figure 4).

B. Conway Granite, by Procedure for Volatiles

The samples were obtained from a surface rock which Dr. Kohman collected at a quarry at Conway, New Hampshire, and which has been designated "green" Conway granite because of its coloration. A preliminary sample volatilized at 800°C produced a spectrum so dominated by Po^{210} that it was difficult to resolve other details. It was decided to first distill out the Po^{210} at a low temperature. A Sample C was prepared and heated at 600°C, a new quartz condensing tube was inserted, and the sample was reheated at 700°C. The alpha spectra for Sample C at the two temperatures are shown in Figures 5 and 6. Po^{210} was present in relatively smaller amounts in the second spectrum. In addition, since the overall activity of the second spectrum was lower than that of the first, it was suspected that most of the polonium volatilized at 600°C, and that the radon, radium, and bismuth are only partially volatilized even at 700°C. Sample C will be run at 800°C and 900°C in the future.

C. Chaines Anoxyennes Biotite and Monazite by Procedure for Non-Volatiles

A Sample D was prepared from a biotite and monazite rock containing pleochroic halos, from Chaines Anoxyennes, Madagascar, obtained from Dr. Robert Gentry. The sample was analyzed at various ranges, the narrowest of which ran

from 0.80-8.16 MeV, and the widest from 2.1-21.7 MeV. Figure 7 shows Sample D analyzed for a range of 1.085-11.505 MeV, which was narrow enough to preserve the details of the spectrum.

V. Conclusions and Plans

No anomalous alpha activity has so far been detected at this early stage of our studies. In the future we will look at many rock types, including more rocks containing pleochroic halos which Dr. Gentry sent, and also meteorites.

References

- (1) T. P. Kohman, Ann. New York Acad. Sci. 62, Art. 21, 503 (1956).
- (2) S. G. Nilsson, S. G. Thompson, and C. F. Tsang, Physical Letters 28B, 458 (1969).
- (3) G. T. Seaborg, Annual Review of Nuclear Science 18, 53 (1969).
- (4) D. H. Wilkinson, Comments on Nuclear and Particle Physics II (5), 146-50 (1968).
- (5) R. O. Pepin, in The Origin and Evolution of Atmospheres and Oceans (P. J. Brancazio and A. G. W. Cameron, Eds.; Wiley Company, New York, 1964), pp. 191-234.
- (6) P. K. Kuroda, Nature 187, 36 (1960).
- (7) E. Anders and D. Heymann, Science 164, 821-3 (1969).
- (8) V. V. Cherdyntsev and V. F. Mikhailov, Geochemistry 1, 1-13 (1963).
- (9) V. V. Cherdyntsev, I. V. Kazachevskiy, L. D. Sulerzhitskiy, and Ye. A. Kuzmina, Geochemistry International 2 (9), 8-20 (1965).
- (10) V. V. Cherdyntsev, V. L. Zverev, V. M. Kuptsov, and G. I. Kistlitsina, Geochemistry International 5 (2), 355-61 (1968).
- (11) R. D. Cherry, K. A. Richardson, and J. A. S. Adams, Nature 202, 639-41 (1964).
- (12) R. V. Gentry, Applied Physics Letters 8 (3), 65-67 (1966).
- (13) R. V. Gentry, Nature 213, 487-9 (1967).
- (14) J. Zussman, Physical Methods of Determinative Mineralogy, (Academic Press, New York, 1967), pp. 1-30.
- (15) B. Mason and L. G. Berry, Elements of Mineralogy, (W. H. Freeman and Company, 1959), pp. 504-7.

- (16) I. Almodóvar, Carnegie Institute of Technology, USAEC Report No. AT(30-1)-844 (1960), pp. 57-59.
- (17) D. L. Hufford and B. F. Scott, in The Transuranium Elements Part II, 1st ed., (G. T. Seaborg, J. J. Katz, and W. M. Manning, Eds.; McGraw-Hill Book Co., Inc., 1949), pp. 1158-61.
- (18) J. Huey, 1968-69 Progress Report, USAEC Report NYO-844-76, II. B. I.
- (19) M. Haramic, This Report, II. D. 1.

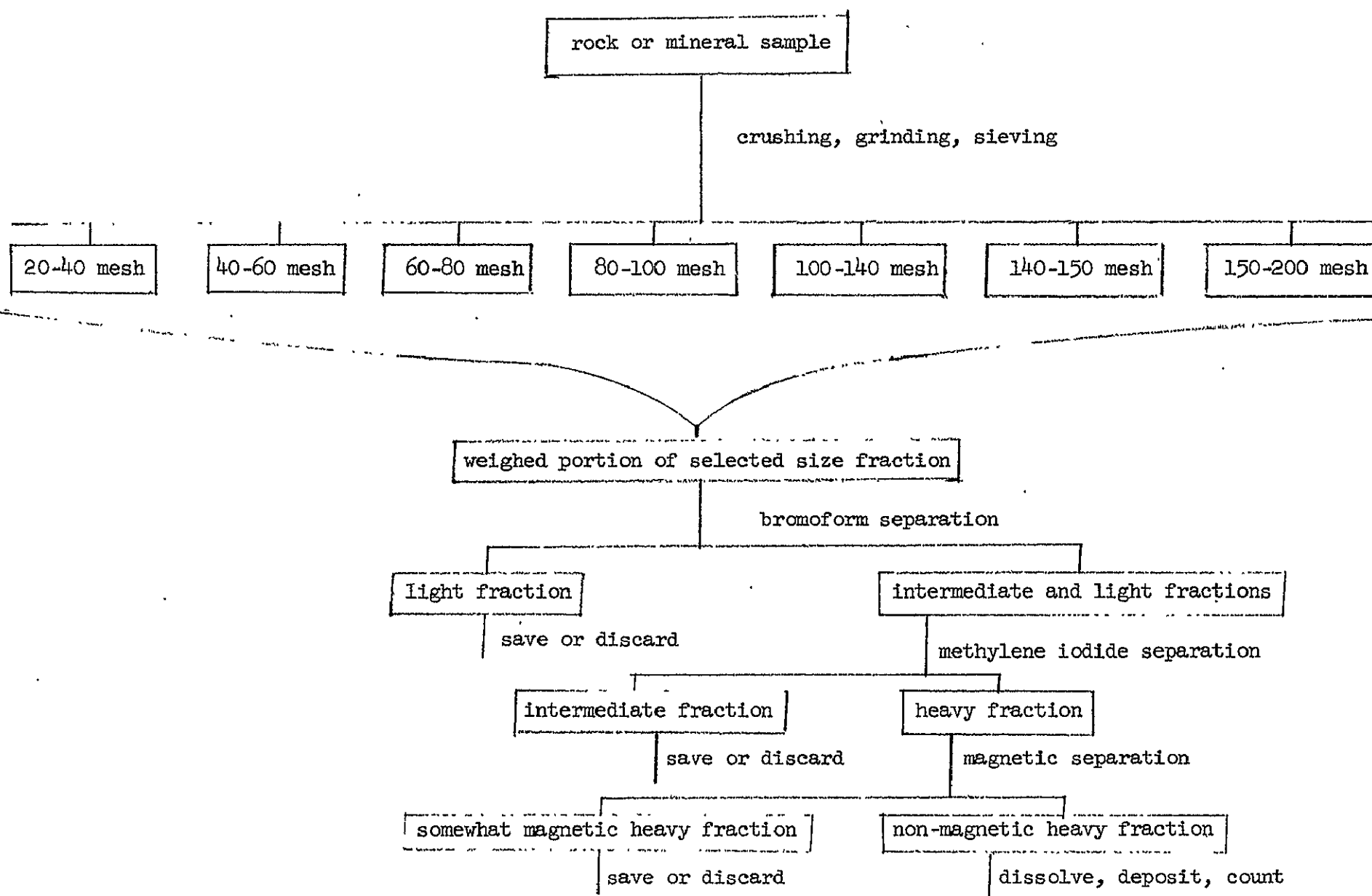


Figure 1. Flow chart for separation of high-density non-magnetic minerals from rock or mineral sample for alpha-activity measurements.

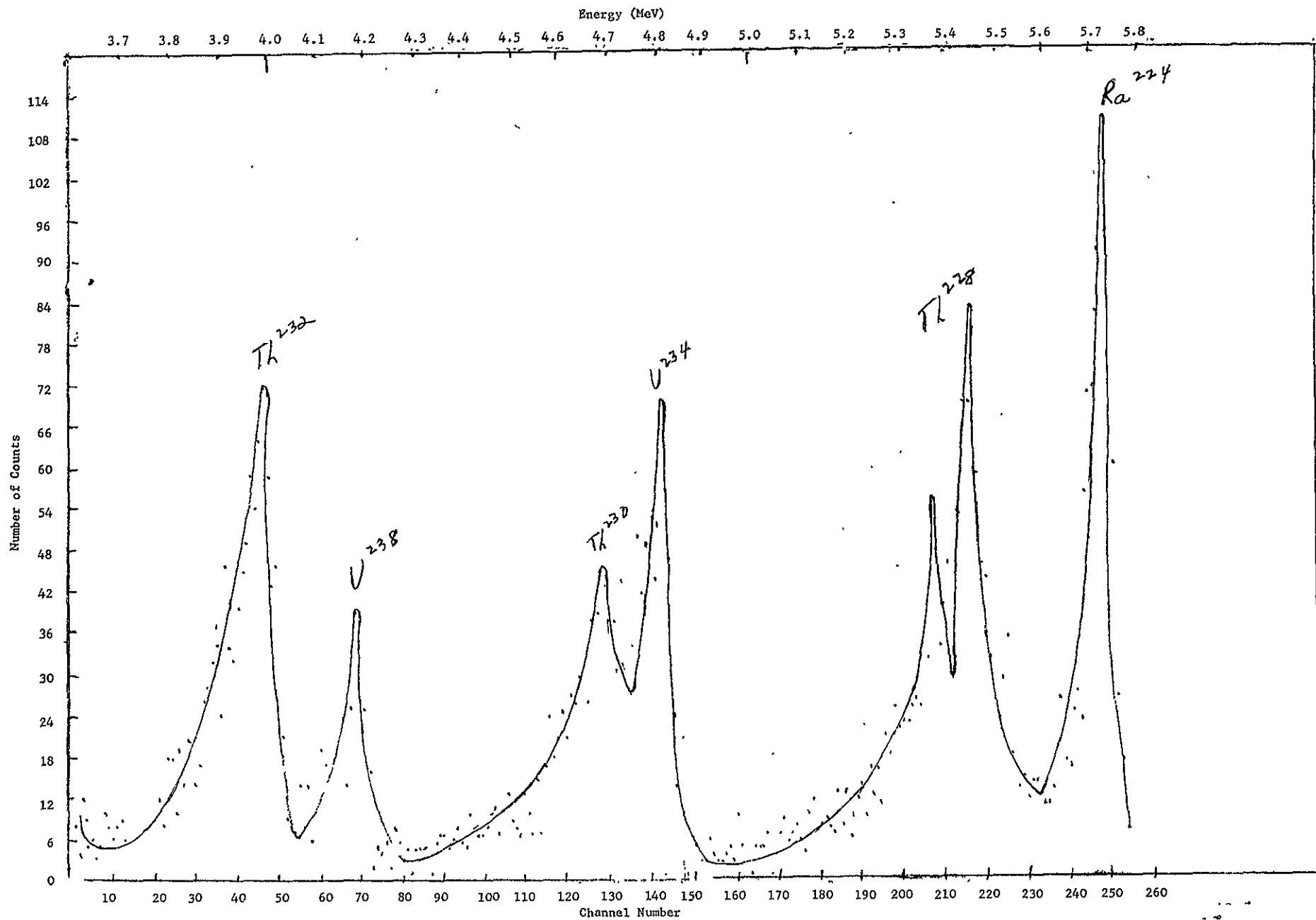


Figure 2. Alpha spectrum of non-volatile, non-magnetic, heavy mineral, 40-100 mesh fraction from Conway granite (Sample A) in range 3.59-5.74 MeV, deposited with TEG.

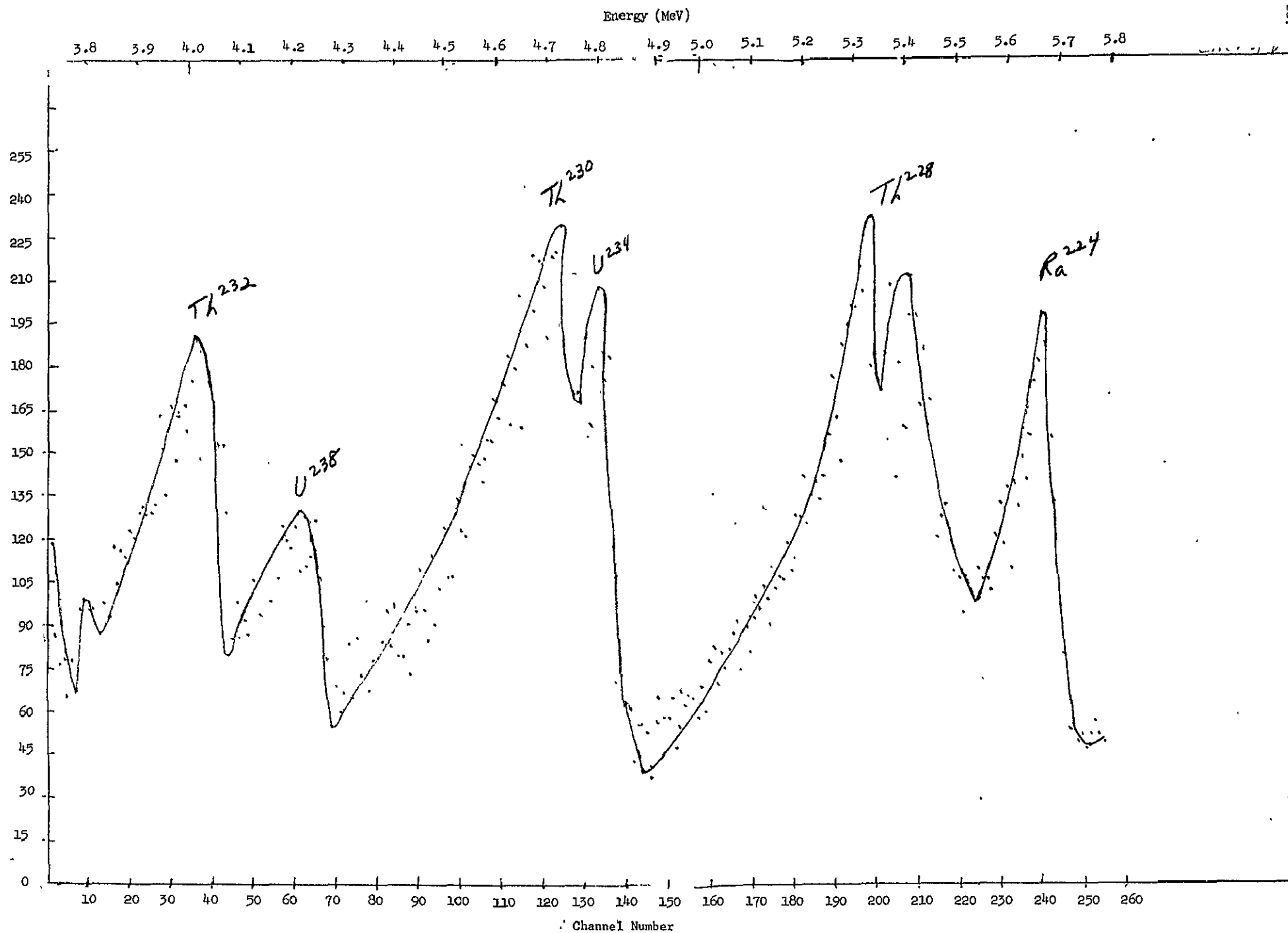


Figure 3. Alpha spectrum of non-volatile, non-magnetic, heavy mineral, 150-200 mesh fraction from Conway granite (Sample B) in 3.73-5.79 MeV, deposited with HNO_3 .

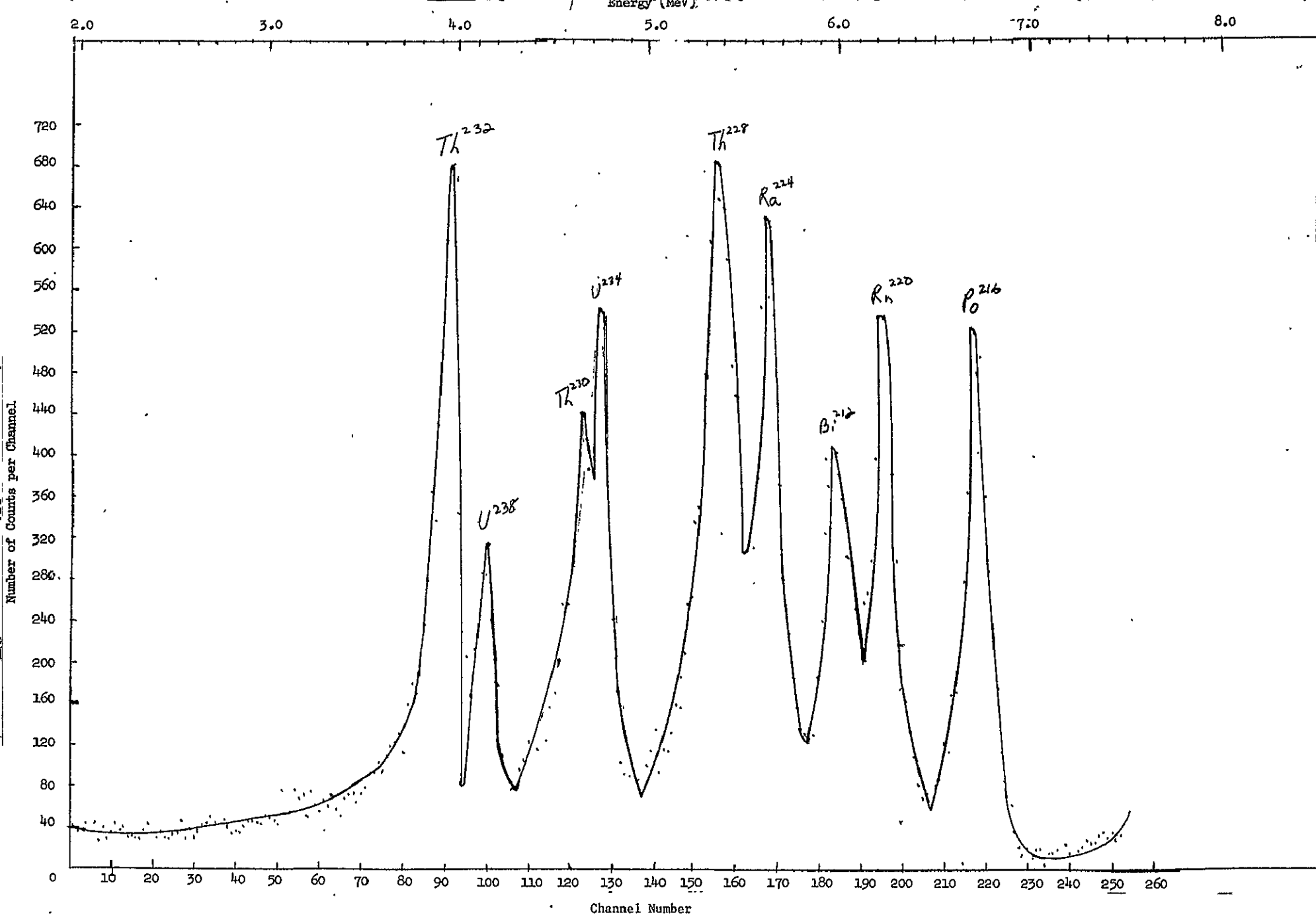


Figure 4. Alpha spectrum of non-volatile, non-magnetic, heavy mineral, 40-100 mesh fraction from Conway granite (Sample A) in range 2.00-7.56 MeV, deposited with TEG.

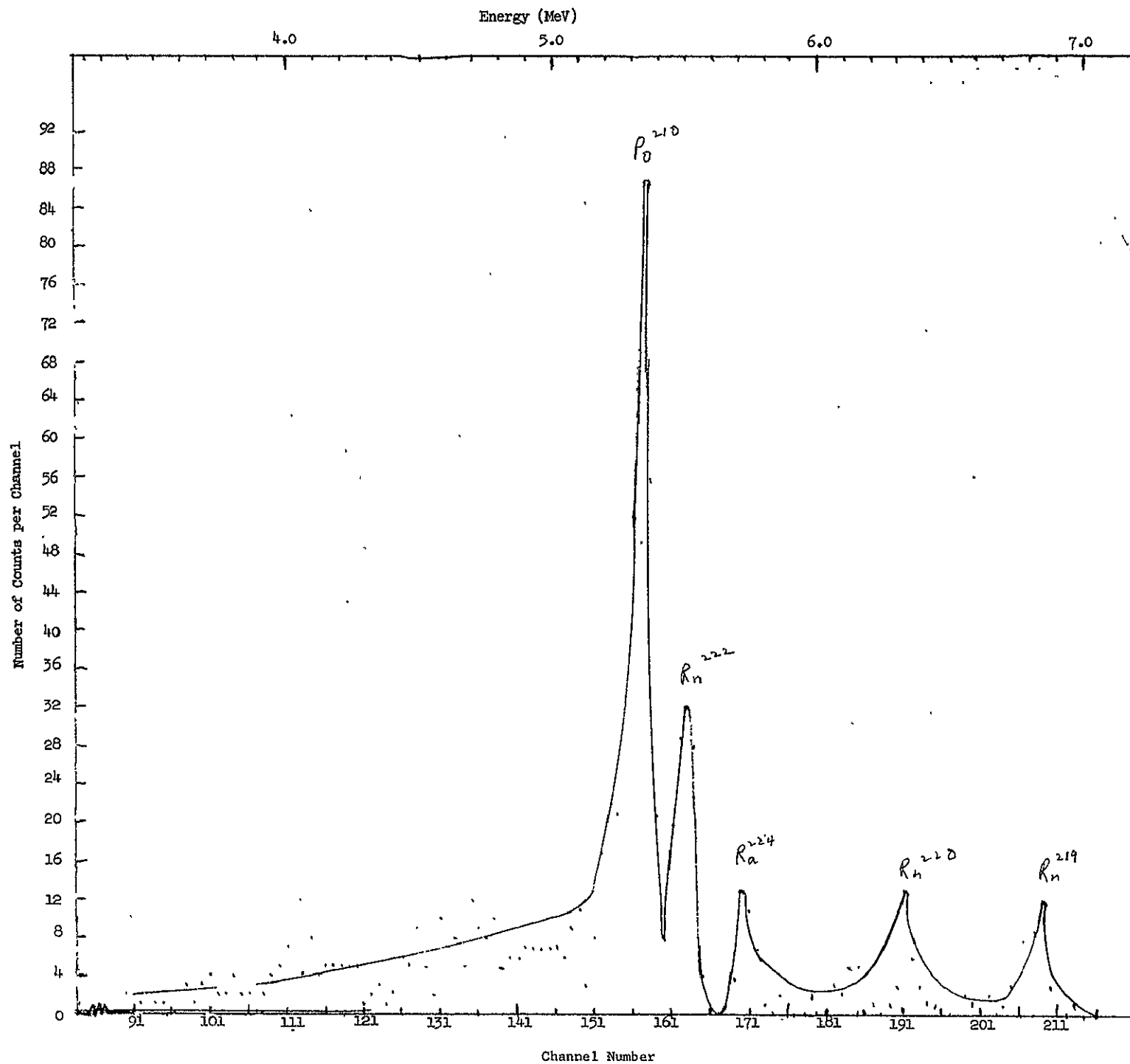


Figure 5. Alpha spectrum of volatile (600°C), heavy mineral, 80-100 mesh fraction from

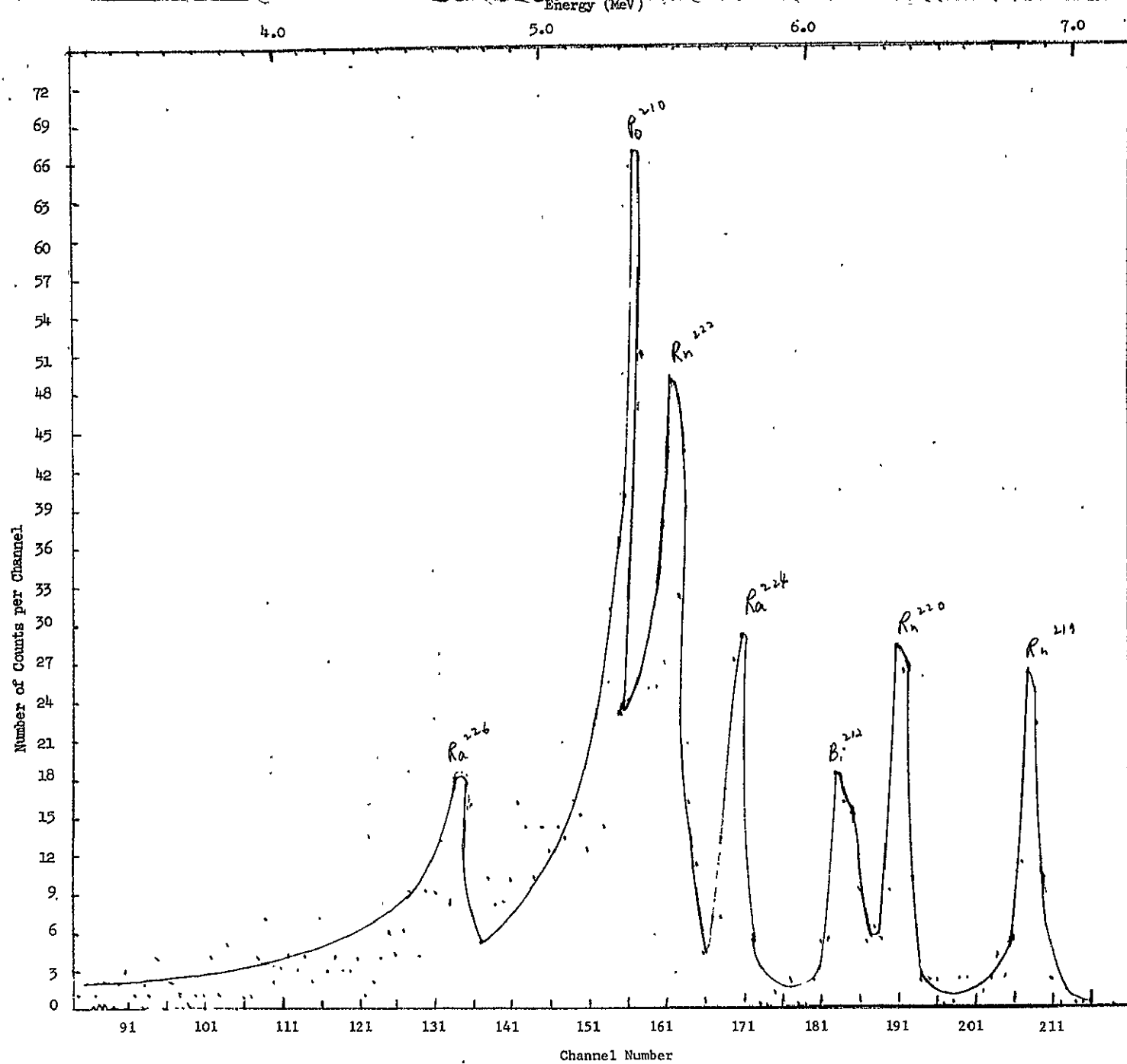


Figure 6. Alpha spectrum of volatile (700°C), heavy mineral, 80-100 mesh fraction of Conway granite (Sample C) in range 0.80-8.16 MeV.

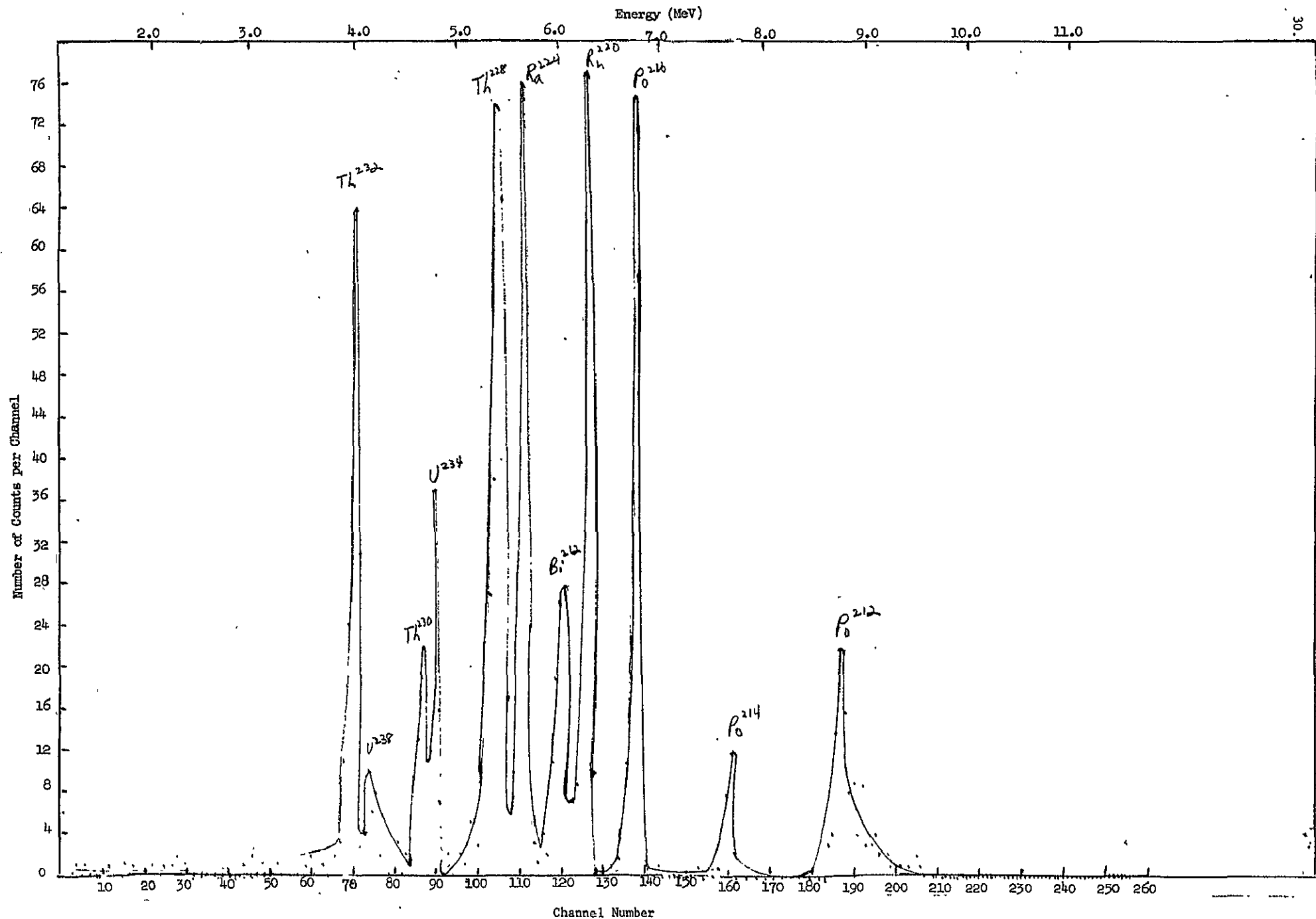


Figure 7. Alpha spectrum of non-volatile, non-magnetic, heavy mineral, 60-140 mesh fraction from Chaines Anoxyennes biotite and monazite (Sample D) in range 1.085-11.505 MeV, deposited with TEG.

II. A. 4.

MÖSSBAUER SPECTROSCOPY OF COAL-RELATED MINERALS

James D. Ulmer

I. Introduction

This project is a continuation of and expansion on earlier work that tried to identify iron-containing mineral constituents of coals, including possible "organically bound" iron compounds (1,2,3).

The method is to obtain Fe^{57} Mössbauer spectra of various iron-containing compounds and minerals and to identify those in coal by comparing their Mössbauer spectra.

The parameters obtained from Mössbauer spectra that are most readily used for identification of chemical compounds are the isomer shift and the quadrupole splitting. Other parameters, line width and fractional absorption, for example, can also be used to identify a compound. These parameters, however, depend not only on the nuclear and atomic configuration of iron atoms in the compound, but also on the nature of the particular sample. For example, sample thickness and concentration of iron atoms in the sample can affect line width and fractional absorption (4,5), and, therefore, these parameters are not so easily used for identification.

In addition to the quadrupole splitting, Fe^{57} displays a magnetic splitting in ferromagnetic materials. Observation of splitting of this nature, then, would help to identify such minerals or compounds.

II. Techniques and Instrumentation

The samples of coals, coal fractions, minerals, and compounds which have been utilized so far were previously prepared by Edgar Pérez, and their preparation and chemical and thermal treatment are described elsewhere (2).

The instrumentation consists of an International Chemical and Nuclear Corp. Model NS-1 Mössbauer Effect Spectrometer, a Type 745 Amperex 303 PC proportional counter, and the following Nuclear Data, Inc. equipment: Model ND-537 High Voltage Supply; Model ND-533 Preamplifier; Model ND-532 Amplifier; Model ND-522 Single-Channel Analyzer; and Model ND-510 Series 1100 multichannel Analyzer System used as a multiscaler. In addition, there are three pieces of peripheral equipment used for displaying and recording the Mössbauer spectra: an oscilloscope for immediate display of the spectrum; a Houston Instrument Model 6550 Omnigraphic Recorder for a graphic record of the spectrum; and a Teletype Corp. Model 33 teletype for recording the spectrum as number of counts per channel on paper and paper tape. A tape reader and a card

punch are available in the Physics Department of Carnegie-Mellon University (CMU), and they are used to convert data from paper tape to cards.

There is also a Janis Research Company Model 6-5/8" D.T. Super Varitemp Dewar with Optical Tails for obtaining spectra at low temperatures, and an Eastern Scientific Company Model 4HF Laboratory Electromagnet for obtaining spectra at various magnetic field strengths.

A computer program that corrects for the parabolic shape of the spectrum baseline when obtained using the moving-source mode of the spectrometer has been written for use on the UNIVAC 1108 computer. The program also corrects for small, non-random differences in counting rates (less than 1%) for different channels and a larger difference (still less than 1%) in counting rates between the first 256 channels and the last 256 channels of the multiscaler caused by some malfunctioning of the multiscaler equipment. The data are corrected for these effects by dividing each channel of the absorption spectrum by its corresponding channel of a blank spectrum. Because the difference in counting rates between the first half and the second half of the channels of the multiscaler is dependent on the counting rate, the blank spectrum and absorption spectrum must be obtained using the same counting rate. This program, then, determines the baseline and normalizes the spectrum with respect to this line. After the data have been corrected and normalized, they are printed graphically and numerically on the computer listing and punched on cards.

A second program has been obtained from the Mössbauer group in CMU's Physics Department that fits a Lorentzian curve to each absorption peak in a Mössbauer spectrum by the method of least-squares.

III. Project Status and Plans

Currently, spectra have been obtained for three samples of Jewell Valley coal and two samples of lignites. Spectra of these samples were previously obtained by Edgar Pérez, and the values for the isomer shift and quadrupole splitting of the doublet peaks in each sample are in reasonably good agreement with values obtained by him. Table I lists the values of the isomer shift and quadrupole splitting obtained.

These spectra have not as yet been fit by Lorentzian curves because the computer program obtained from the Physics Department is currently being revised to use our data as input. When this program is working, the values for the quadrupole splitting and isomer shift will be determined more precisely.

It is believed that the peaks in the Jewell Valley coal spectra represent the presence of "non-pyrite iron", as designated by Lefelhocz (1). Further, comparison of values for the isomer shift (δ) and quadrupole splitting (Δ) of the lignite samples with the values of δ and Δ for pyrite indicate that the peaks in the lignite spectra probably represent the presence of pyrite in the lignite samples. Values of δ and Δ for the

coal samples investigated here can be compared with values obtained for the same coal samples by Pérez and with non-pyrite iron and pyrite by referring to Table I.

In one of the samples of Jewell Valley coal (JVC-4 sink) investigated, there is a third absorption peak at approximately $+0.8$ mm/sec, relative to the center of the sodium nitroprusside spectrum (Fig. 1). The fractional absorption of the third peak is approximately one-fourth that of the low velocity peak of the doublet. It is suspected that this third peak is the high-velocity peak of a second doublet in the spectrum, and that the low-velocity peak of this second doublet is obscured by the low-velocity peak of the first doublet. The low-velocity peak of the second doublet appears to be at approximately $+0.3$ mm/sec., relative to the center of the sodium nitroprusside spectrum. In comparison, the low-velocity and high-velocity peaks of pyrite are located at $+0.24$ mm/sec. and $+0.84$ mm/sec., respectively, relative to the center of the sodium nitroprusside spectrum. The second doublet observed in this sample, then, may or may not be an indication of pyrite in the sample, depending on how well the position of the low-velocity peak was determined. Fitting Lorentzian curves to the spectra of this sample will determine the location of the low-velocity peak more precisely and it will be possible to decide whether the second doublet is caused by the presence of pyrite or not.

Mössbauer spectra of many coal-related minerals and compounds have been obtained. However, none of these spectra appear to match the spectrum of non-pyrite iron in coal (1). This non-pyrite iron has been determined to be iron (II), in a high spin configuration, and, very probably, in octahedral symmetry (1). Mössbauer spectra will be obtained for coal-related minerals and compounds which may have iron with these characteristics.

It has been suggested that the correlation between iron and silicon, aluminum, and magnesium in coal, observed by Dr. L. F. Vassamillet using the electron microprobe x-ray analyzer at the Mellon Institute (8), would make it profitable to obtain spectra of chlorites (2). This reasoning will be pursued, and various chlorite minerals will be investigated.

The investigation of coal-related minerals and compounds at liquid nitrogen temperature will give additional parameters to use as identification because the isomer shift and the quadrupole splitting are temperature dependent (6,7). Furthermore, the magnitude of absorption can increase with decreasing temperature (5), and unobserved peaks at room temperature may be observed at liquid nitrogen temperature.

It is also hoped that an external magnetic field will induce magnetic splitting in spectra of coals and coal fractions and thus help locate overlapping and unresolved absorption peaks.

References

- (1) J. F. Lefelhocz, R. A. Friedel, and T. P. Kohman, *Geochim. Cosmochim. Acta* 31, 2261-2273 (1967).
- (2) E. A. Páez, 1967-1968 Progress Report, USAEC Report NYO-844-75, II. A. 2.
- (3) E. A. Páez, 1968-1969 Progress Report, USAEC Report NYO-844-76, II. A. 1.
- (4) H. Frauenfelder, The Mössbauer Effect, (W. A. Benjamin, Inc., New York, N. Y., 1962), p. 45.
- (5) R. H. Herber, *Journal of Chemical Education* 42, 180-187 (1965).
- (6) S. DeBenedetti, F. deS. Barros, and G. R. Hoy, *Ann. Rev. Nucl. Sci.*, 16, 31-88 (1966).
- (7) E. Fluck, W. Kerler, and W. Neuwirth, *Angew. Chem. Internat. Ed.* 2, 277-287 (1963).
- (8) L. F. Vassamillet, Mellon Institute, unpublished results mentioned by Páez (Ref. 2).

TABLE I
MÖSSBAUER SPECTRAL PARAMETERS OF COALS AND COAL-RELATED MINERALS AND COMPOUNDS

Sample #	Description	This Work		Other Work		
		$\delta^{\dagger*}$	$\Delta^{\dagger\dagger}$	$\delta^{\dagger*}$	$\Delta^{\dagger\dagger}$	Ref.
JVC-3 Float.	Jewell Valley Coal, physically fractionated	$1.34 \pm .08$	$2.68 \pm .08$	1.41	2.60	(a)
JVC-4 Sink.	Same, physically fractionated	$1.24 \pm .06$	$2.75 \pm .06$	1.393	2.575	(a)
JVC-11	Same, heat treatment 200°C in air for 3 hrs.	$1.34 \pm .08$	$2.75 \pm .06$	1.35	2.575	(a)
	Non-pyrite iron in coal			1.38	2.62	(b)
L-2	Gascoyne, Grand Forks, N. Dak., high-iron lignite	$0.50 \pm .08$	$0.68 \pm .05$	0.4	0.63	(a)
L-3	Beulah lignite, Hoot Lake Grand Forks, N. Dak.	$0.55 \pm .05$	$0.63 \pm .04$	0.5	0.6	(a)
	Pyrite, FeS_2			0.54	0.60	(b)

Designation of Páez (2).

† In mm/sec.

* Isomer shift with respect to center of sodium nitroprusside.

‡ Full velocity difference between paired peaks.

(a) Páez (1967).

(b) Lefelhocz et al., (1967).

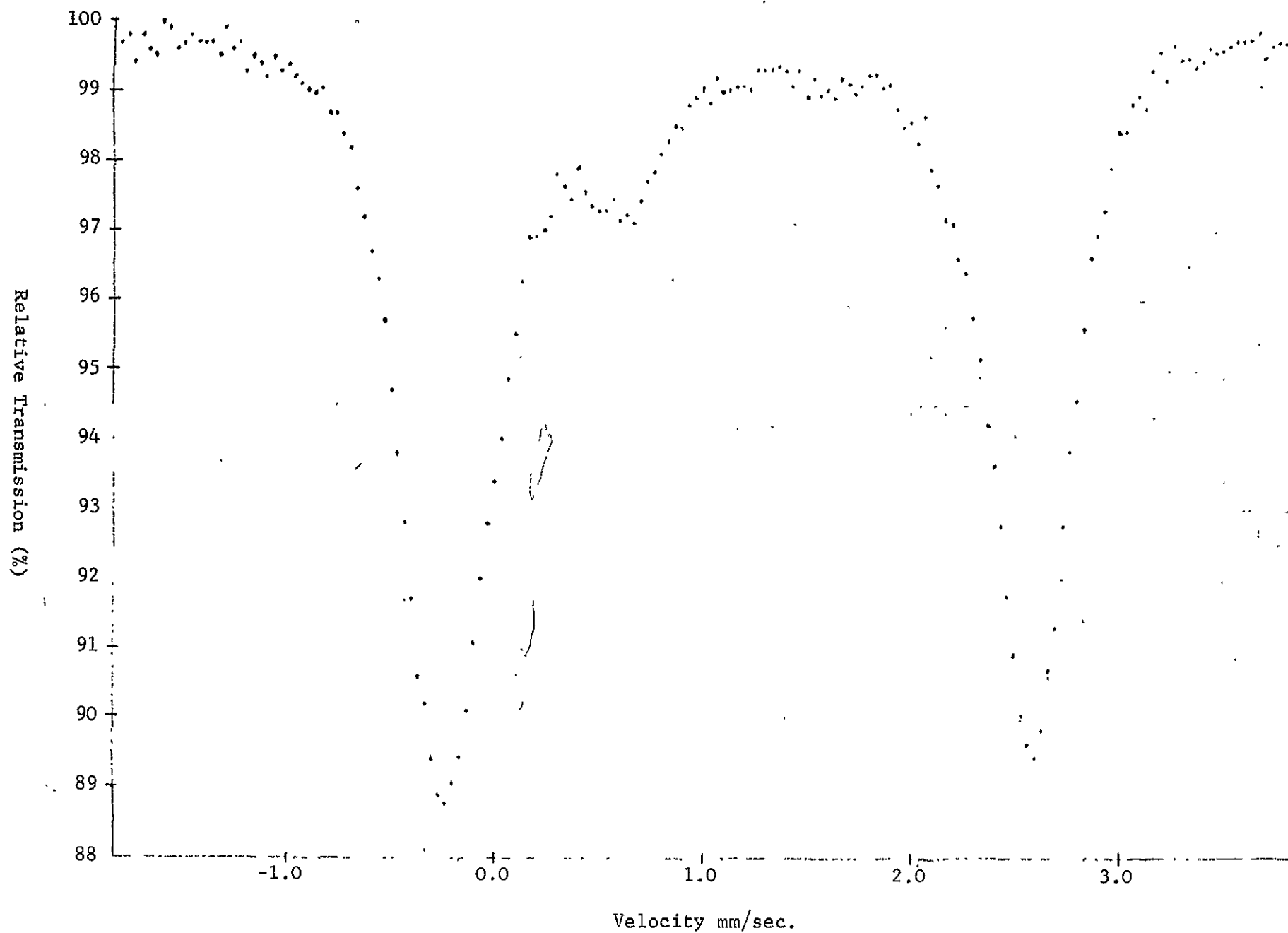


Figure 1. Spectrum of Jewell Valley Coal (WV-4 sink). Zero of velocity is for

II. B. 1.

ISOTOPIC COMPOSITION OF LEAD AND THALLIUM
IN NATURAL MATERIALS

.. James M. Huey

I. Introduction

Data obtained from the isotopic analysis of lead in many natural materials have already found widespread interpretations in the field of geochronology and have been applied in the development of theories of nucleosynthesis. In addition, it may be possible to extend the fine time-resolution of the interval following nucleosynthesis through application of the principles of extinct natural radioactivity to the ^{205}Pb - ^{205}Tl system and isotopic analyses of thallium. Data on the isotopic compositions and concentrations of lead and thallium in stone meteorites, particularly the carbonaceous chondrites, should be important in the search for extinct natural radioactivity of ^{205}Pb , and lead data, when coupled with uranium and thorium concentration values will further the understanding of the history of these extra-terrestrial bodies. The objectives and potentialities of lead and thallium isotopic studies including the work of previous investigators has been described in detail previously (1).

II. Chemical Procedures

The following scheme for isolation of lead and thallium from natural materials, separation, and conversion to suitable form for mass spectrometry was proposed previously (1):

- (1) Volatilization of crushed sample in gas stream to separate Tl and Pb from the matrix.
- (2) Dissolution of volatiles in dilute HCl and reduction of Tl^{+3} with SO_2 .
- (3) Ion-exchange separation of lead and thallium from each other and from other volatile elements.
- (4) Preparation of thallium for mass-spectrometry as the nitrate.
- (5) Preparation of lead for mass-spectrometry, either as the nitrate or as the sulfide.

Several additions and modifications in the chemical procedure have been necessary. The procedure which has been applied to the analysis of standard rocks, lunar fines, and meteorites is briefly discussed and outlined below:

- (1) Sample crushed in agate mortar and pestle to pass through 200-mesh nylon screen.

The use of a tungsten carbide capsule and pestle (Wig'l-Bug) was abandoned when chips of the pestle were discovered in crushed material, thus creating a potential source of lead contamination.

- (2) Volatilization of sample in vacuo (~ 0.1 mm Hg) in fused quartz combustion tube.

Adequate yields of lead based on analyses of NBS standards AGV-1 (Andesite) and BCR-1 (Basalt) could not be obtained by heating of the crushed sample in a stream of oxygen. The use of a vacuum system produced a substantial increase in yields of both lead and thallium.

- (3) Dissolution of volatiles in a mixture of 5 ml 7.9-N HCl + 2 ml redistilled 70% HNO_3 and evaporation to dryness; when concentrations are to be determined, spikes (92.26% Tl-203, NBS-983 lead std.) are added at this point.

- (4) Dissolution in 1.8-M HCl and reduction of Tl^{+3} to Tl^{+1} with SO_2 passed first through concentrated sulfuric acid traps for purification.

- (5) Solution placed on a 20-cm long (0.7-cm diameter) anion-exchange column (Dowex 1-X8, 100-200 mesh) and Tl eluted with 30-ml SO_2 -saturated 1.8-M HCl.

- (6) Lead eluted with 20 ml triply distilled water.

- (7) Solutions evaporated to dryness in quartz beaker.

- (8) Electrodeposition of lead.

The use of a silica-gel-phosphoric-acid technique has been necessary for mass-analysis of small quantities of lead. However, lead must be removed from interfering hydrocarbons by electrodeposition prior to mass analysis. Lead is deposited in 90-100% yield on a platinum anode from a 0.1-M HNO_3 solution at 1.85 V for 24 hrs. Lead is dissolved from the anode in 4-N HNO_3 and evaporated to dryness in preparation for mass analysis.

- (9) Refluxing of thallium with redistilled 70% HNO_3 in quartz crucible.

Hydrocarbon contamination is reduced, and the solution is evaporated to dryness in preparation for mass analysis using a triple filament-silica-gel technique.

If hydrocarbon contamination in small samples cannot be eliminated, refluxing with perchloric acid may be necessary.

Tests of the yields of lead and thallium obtained incorporating all parts of the chemical procedure except volatilization have been made using small quantities of reagent solutions. The results, reported in Table 2, show average yields of ~ 85% for thallium and 70-75% for lead. It is not necessary to know yields exactly since isotope dilution techniques are used and samples are spiked prior to chemical separation, but high yields are desirable for adequate recovery of the elements for analyses to determine exact isotopic compositions.

These chemical procedures have been developed in particular for the recovery of the volatile elements lead and thallium from silicates, metal and troilite phases, and various separated mineral fractions of natural materials. At some time it may be desirable to incorporate these procedures into a separation scheme involving several other elements, (e.g., Nd, Sm, U, Th, Ag, Pd), which, with the possible exception of Ag will be retained in the residue. Discussion of such a scheme is found elsewhere in this report (2). Some modification of the current procedures may be necessary for this incorporation, but basic techniques will remain the same and should be readily adaptable.

III. Mass Spectrometry

Much time in this laboratory has been devoted to experimentation with mass analysis of microgram quantities of lead and nanogram quantities of thallium. Results of these experiments are described elsewhere in this report (3).

IV. Blank Analyses

Analyses of various parts of the chemical procedure to determine chemical blanks for lead and thallium have been made at intervals between processing of samples. Table 1 shows the results of several analyses. Blanks for both elements approach a constant value, but it is desirable to obtain a lower and more consistent lead blank. An analysis of various components of the blank, including reagent contamination, quartz tubing, and atmospheric fallout contamination has been initiated. Blank levels for quantities of various reagents used in an individual separation are reported in Table I.

V. Results

A. NBS Standard Rocks BCR-1 and AGV-1

To determine the efficiency of the entire chemical procedure including volatilization, several analyses of standard rocks BCR-1 and AGV-1 have been made at various heating times and temperatures. In

Table 3, results of these analyses are reported as elemental concentrations. Comparison of these concentrations with reported values permits the calculation of a chemical yield for the volatilization procedure. Tl yields are $\geq 80\%$ for heating times of ≥ 24 hrs., but longer heating periods ($\sim 6-8$ da) at successive temperatures are necessary to obtain comparable yields of lead.

B. Lunar Fines from Apollo-11 and Apollo-12

Preliminary results obtained in this laboratory on Apollo-11 finds have been published recently (4). A program of differential heating of Apollo-11 and Apollo-12 samples to successively higher temperatures was utilized to isolate various lead fractions of unique isotopic composition. Fractions were collected at 700° , 800° , 900° , 950° , and 1100° . A total sample heating encompassing the entire heating range served as a control for comparison. Analyses of all samples have been completed.

When detailed blank analyses have been completed, interpretations of the data obtained will be possible.* Lead isotopic data in conjunction with U and Th concentrations will aid in the determination of various components of the lunar fines and provide information about the thermal history of the moon.

C. Meteorites

At present, several stone meteorites are being analyzed using total and differential-heating techniques and the chemical procedures described in this report.

The analysis of lead contents of Ladder Creek, an olivine-hypersthene chondrite, is presented in Table 4. Mass-spectrometric data are corrected for a blank of $0.07 \mu\text{g}$. Unfortunately, a very small signal was obtained in the composition analysis of the high-temperature differential fraction (900° , 48 hr; 950° , 48 hr; 1100° , 48 hr), but a comparison of low-temperature (700° , 24 hr; 800° , 24 hr) and total-heating (encompassing heating range of low and high temperature fractions) samples show only a small compositional variation. This is apparently in contrast to the behavior of samples of lunar material subjected to similar treatment.

Further examination of other meteoritic samples should prove invaluable in establishing other similarities and differences between meteorites and lunar samples, and indeed, those between various meteorites themselves. Improved lead isotopic composition data will provide information about the process of formation of stone meteorites and their thermal history. If variations in the isotopic composition of thallium can be observed, fine time-resolution of the interval following nucleosynthesis may be possible.

* Preliminary calculations indicate that variable lead isotopic compositions do exist among the various temperature fractions of both Apollo-11 and Apollo 12.

References

- (1) J. M. Huey, 1968-1969 Progress Report, USAEC Report NYO-844-76, II. B. 1.
- (2) H. Ihochi, This Report, II. D. 2.
- (3) L. P. Black and J. M. Huey, This Report, II. D. 3.
- (4) T. P. Kohman, L. P. Black, H. Ihochi, J. M. Huey, Science, 167, 481-3 (1970).
- (5) B. M. P. Trivedi, This Report, II. D. 5.
- (6) F. J. Flanagan, Geochim. Cosmochim. Acta 33, 81 (1969); M. Tatsumoto, private communication to F. J. Flanagan.
- (7) J. C. Laul, I. Pelly, and M. E. Lipschutz, in preparation.

TABLE I
BLANK ANALYSES

Procedure	Pb Contamination (μ g)	Tl Contamination (ng)
Chemical Scheme Beginning with Sample Dissolution	.096	13.5
Chemical Scheme Beginning with Sample Dissolution	.075	1.48
40 hr Heating at 950° + Chemistry	.049	12.02
Electroplating Only	.021	---*
Heating (42 hr, 900°; 28 hr, 975°; 27 hr, 1050°C) + Chemistry	.084	14.7
Heating (23 hr, 800°; 24 hr, 850°; 20 hr, 900°) + Chemistry	.13	.78
Heating (24 hr, 700°; 24 hr, 800°; 48 hr, 900°; 48 hr, 950°; 48 hr, 1100°) + Chemistry	.17	.64
Heating (24 hr, 700°) + Chemistry	.090	2.58
Heating (24 hr, 800°) + Chemistry	.068	.45
Heating (24 hr, 900°) + Chemistry	.058	1.09
Heating (24 hr, 950°) + Chemistry	.053	.81
Heating (24 hr, 1100°) + Chemistry	.053	.54

* Electroplating not used for Tl.

TABLE II

YIELDS OF COMPLETE CHEMICAL PROCEDURE FOLLOWING VOLATILIZATION

Sample	Electroplating Time	Amt. Recovered (μg)	Yield
2.31 μg Pb	50 hr	1.61	69.7%
2.31 μg Pb	50 hr	1.67	72.3%
2.31 μg Pb	24 hr	1.68	72.8%
2.31 μg Pb	24 hr	2.17	93.9%
6.04 μg Tl	None	5.23	86.6%
6.04 μg Tl	None	5.37	89.0%

TABLE III
NBS STANDARD ROCK ANALYSES

Sample	Amt. (g)	Treatment of Sample to Remove Volatiles Prior to Chemistry	Amt. Recovered (μ g)		Derived Mass Fraction (ppm)		Yield (%)	
			Pb	Tl	Pb	Tl	Pb	Tl
BCR-1*	2.77	Heat (1200°, 3 hr in O ₂)	2.02	.230	.73	.083	5.4	25.1
BCR-1	2.65	Heat (1100°, 4-1/2 hr in O ₂)	2.05	.347	.77	.131	5.7	39.8
BCR-1	1.39	Heat (1000° for 3 hr; in O ₂ used cold trap)	4.02	.503	2.90	.364	21.0	110.0
BCR-1	2.78	Heat (1000° for 3 hr; in O ₂ used cold trap)	3.44	.344	1.24	.124	9.2	37.6
BCR-1	2.47	Heat (1000° for 3 hr; in O ₂ used cold trap)	.66	.329	.27	.134	2.0	40.5
BCR-1	3.023	Heat (1000° for 3-1/2 hr; vacuum)	14.7	.640	4.86	.212	35.8	64.4
BCR-1	1.995	Heat (1000° for 4 hr; vacuum)	21.2	.422	10.6	.212	78.3	64.2
BCR-1	1.082	Heat (900°, 10 hr)	11.7	.282	10.8	.260	79.6	79.0
BCR-1	3.61 g	Heat (900°, 30 hr)	42.3	.754	11.7	.209	86.5	63.4
AGV-1 [‡]	1.817	Heat (1000°, 24 hr)	18.8	.534	10.4	.294	28.4	86.1 [‡]
AGV-1	2.000	Heat (900°, 72 hr)	43.2	.622	21.6	.311	59.2	94.5
AGV-1	2.502	Heat (800°, 20 hr; 900°, 20 hr; 1050°, 20 hr)	43.1	.750	17.2	.299	47.1	87.5
AGV-1	2.630	Heat (900°, 24 hr)	23.7	.750	9.0	.285	24.7	83.5
AGV-1	2.009	Heat (800°, 20 hr; 900°, 20 hr; 1050°, 20 hr)	65.8	.645	32.8	.321	89.8	94.0
AGV-1	3.227	Heat (800°, 20 hr; 900°, 20 hr; 1050°, 20 hr)	31.8	.905	9.9	.280	27.0	81.9

*Yields of BCR-1 based on 13.56 ppm Pb(6) and .330 ppm Tl(7).

[‡]Yields of AGV-1 based on 36.53 ppm Pb(6) and .342 ppm Tl(7).

TABLE IV
LEAD ISOTOPIC DATA OBTAINED FROM DIFFERENTIAL
HEATING OF LADDER CREEK METEORITE

Sample	Mass (g)	206/204	207/204	208/204	207/206	208/206	Pb Mass Fraction (ppm)
Total Heating (Sum of Low + High Temp.)	3.994	19.63	16.30	38.74	.8304	1.9733	.518
Low Temp. Fraction (700°, 24 hr; 800°, 24 hr)	5.300	19.08	15.96	38.47	.8363	2.0158	.123
High Temp. Fraction (900°, 48 hr; 950°, 48 hr; 1100°, 48 hr)	5.300	---	---	---	---	---	.226

45. 10-18-70

N71-10310

II. B. 2.

CHRONOLOGY OF GALACTIC HEAVY-ELEMENT NUCLEOSYNTHESIS

James M. Huey and Truman P. Kohman

I. Introduction

Three quite independent methods for obtaining quantitative estimates or lower limits of the "age of the universe" have been discussed by Fowler (1) and Sandage (2), with the conclusion that each of these methods yields results consistent with an age between about 8 and 25 Gy: (a) calculation of model ages of the oldest stars from the main-sequence cut-off points in color-luminosity diagrams for star clusters; (b) determination of model parameters for a monotonically expanding universe from galactic red-shifts; and (c) evaluation of parameters in models of galactic nucleosynthesis from relative abundances of radioactive and stable products.

We have undertaken a refinement of the third method, using chiefly a model for galactic nucleosynthesis proposed earlier by one of us (3,4) with recent values of cosmochemical and nuclear-physical data.

II. Multi-parameter Models of Galactic Nucleosynthesis

In models of the time-dependence of nucleosynthesis, the number of astronomical parameters which can be evaluated is equal to the number of critical observable quantities which can be related to them through certain nuclear parameters. A number of models having different numbers of astronomical parameters have been proposed, and these are summarized in Table I. The numerical part of each Model Number is the number of astronomical parameters.

The symbolism is an extension of that used earlier (3):

Capital Greek letters:	Time intervals.
Small Latin letters:	Specific times.
Small Greek letters:	Model and nuclear parameters.
Capital Latin letters:	Extensive quantities related to matter.

The symbols in Table I and the ensuing discussion have the following significance:

t = time

o = present time ($t = 0$)

m = time of meteorite formation (as cool solids capable of retaining rare gases)

- s = time of beginning of solar-system formation (defined as end of galactic nucleosynthesis of any solar-system matter, presumably the time of eruption of the last contributing r-process, Type I, supernova)
- f = time of beginning of formation of r-process nuclides
- g = origin of our galaxy (and of the universe)
- M = $o - m$ = age of meteorites (as cool solids)
- E = $m - s$ = decay interval for extinct natural radioactivity (especially with radiogenic Xe)
- Σ = $o - s$ = age of solar system = $E + M$
- Δ = $s - f$ = duration of galactic nucleosynthesis of heavy elements of the solar system
- E = $f - g$ = average evolutionary time for Type I supernovae
- Γ = $o - g$ = age of galaxy = $E + \Delta + E + M$
- A = mass number of nuclide
- N_A = number of atoms of nuclide of mass number A
- ρ_A = cumulative r-process production rate of nuclide of mass number A
- λ_A = decay constant for radionuclide of mass number A
- λ = decay constant for general galactic stellar activity
 * (assumed proportional to r-process nucleosynthetic activity)
- ϕ = fraction of total r-process elements in terminal spike
 (from last Type I supernova contributing to solar system)
- α = fraction of total r-process elements in initial spike
 (from massive first-generation stars during collapse of galaxy to disc configuration)
- $\chi_U = (N_{235}/N_{238})_O / (\rho_{235}/\rho_{238})$
- $\chi_{Th} = (N_{232}/N_{238})_O / (\rho_{232}/\rho_{238})$
- $\chi_I = (N_{129}/N_{127})_m / (\rho_{129}/\rho_{127})$
- $\chi_{Pu} = (N_{244})_m / (N_{238})_O / (\rho_{244}/\rho_{238})$

As explained earlier (3), the abundance ratio of two isotopes or otherwise related nuclides always enters into the mathematical equations as the ratio to the corresponding production-rate ratio, and we have adopted Clayton's (5,6) designation of such ratio-ratios by the symbol χ with a subscript for the element in the numerator of each ratio.

III. Evaluation of Parameters

The general equation for each pair of related nuclides is

$$\chi_{El} = \frac{(N_Y)_x / (N_Z)_0}{\rho_Y / \rho_Z}$$

Here we have adopted the philosophy of relating the astronomical parameters of a nucleosynthesis model as directly as possible to observed quantities. Thus, the abundances of stable and extant radioactive nuclides are taken at the present time; for extinct natural radionuclides the time x in the above equation is taken as m , which is when the observable abundances of the radiogenic products (Xe isotopes in all cases so far) were established. $\chi = 0 - x$ is the corresponding interval, 0 or M .

In addition to the four critical observable isotope or nuclide ratios already mentioned, there is a fifth, which may formally be taken as the ratio of radiogenic Pb^{207} to radiogenic Pb^{206} produced from uranium in meteorites during the interval M . Actually, there is a large body of evidence based on five radioactive systems ($U^{238}-Pb^{206}$, $U^{235}-Pb^{207}$, $Th^{232}-Pb^{208}$, $Rb^{87}-Sr^{87}$, $K^{40}-Ar^{40}$) which give more-or-less concordant estimates of M , the age of the meteorites (the most accurate of which actually does come from radiogenic Pb^{207} and Pb^{206} via the slope of the meteoritic Pb^{207}/Pb^{204} versus Pb^{206}/Pb^{204} isochron). —

One could set up a fifth equation for the radiogenic Pb^{207}/Pb^{206} ratio and solve the five simultaneous equations for the five parameters of Model 5a or 5b. However, the solution of the equation for M is completely independent of the other equations and input quantities, so we choose instead to accept the previous estimates of M by other workers, and consider M instead as an input quantity. This leaves four simultaneous equations (for χ_U , χ_{Th} , χ_I , χ_{Pu}) involving four additional parameters to be solved for (see Table I).

As the "nominal" value of M , we have taken 4.56 Gy, which is the best value of the age of chondrite meteorites from Pb-Pb isochrons (7). The nominal values of the other input quantities, with the abundance ratios and production-rate ratios from which they were derived, are listed in Table II. According to recent observations of Podosek (8), there are definite differences in the ratio of radiogenic Xe^{129} to stable I^{127} in different chondrite and achondrite meteorites, indicating differences in formation (cooling) times amounting to as much as 50 My.

Therefore, for consistency, we have used values of $(N_{129}/N_{127})_m$ and $(N_{244})_m/(N_{238})_o$ derived from the same meteorite, St. Severin (whole-rock) in the same laboratory (8,9).

The four simultaneous equations have been solved using the CMU UNIVAC 1108 computer and a FORTRAN V program designated CHRONs. The program provides solutions for either Model 5a or 5b. It is based on the Newton-Raphson method of successive approximations starting with estimates of the values of the parameters. Each input quantity, including M , is systematically varied through the physically interesting or possible range on both sides of its "nominal" value, and separate solutions are obtained. Variations of a χ correspond to variations in either the abundance ratio or the production rate or both.

IV. Results and Discussion

The "nominal" values of the parameters for the two models are given in Table III. Figures 1 and 2 show how the output quantities vary with the input quantities for Models 5a and 5b, respectively. In each plot, each of the curves shows how two of the output quantities vary with one of the input quantities. The numbers on the χ curves represent the ratio of the input value to the nominal value. The numbers on the M curve represent the absolute values used for the age of the meteorites expressed in Gy.

We feel that Model 5a is the more realistic of the two 5-parameter models which have been proposed so far. Contrary to some opinions, we feel that this model, with parameters in the ranges of derived values, is in satisfactory concordance with astrophysical data on the build-up of heavy elements in the galaxy, with the ages of galactic halo and disc star clusters, and estimates of the age of the universe based on galactic red-shifts. Unfortunately, the derived value of Δ , the duration of galactic nucleosynthesis, is very sensitive to χ_{Th} , and hence to both the Th/U ratio and ρ_{232}/ρ_{238} . Therefore, precise statements about the age of the universe (Γ) by this method cannot be made. Similarly, the value of λ_x or α depends strongly on both χ_{Th} and χ_U . Thus, to obtain information about the early phases of galactic nucleosynthesis will require very good observational and theoretical information about the very long-lived radionuclides, U^{235} , U^{238} , and Th^{232} , whose present abundances reflect in part the early time-dependence of r-process nucleosynthesis in the galaxy.

After completing these calculations, we learned that Fowler (10) has made an almost identical set of calculations for what we have designated as Model 5a. His "standard" input values differ somewhat from our "nominal" values, so that his best output values differ somewhat from ours. His ranges of values for the parameters overlap ours, and confirm that Δ and λ_x are very uncertainly determined by this method. His "standard" results $\phi = 8.8\%$ and $E = 175$ My are both considerably higher than our "nominal" values, and we are investigating the reason for this apparent disagreement.

We feel that neither Fowler's "standard" input quantities nor our "nominal" values are the best that can be used at the present time, and we are continuing with an evaluation of all available abundance data and production-rate estimates as a preliminary to repeating the calculations for both Models 5a and 5b.

References

1. W. A. Fowler, Proceedings of the Rutherford Jubilee International Conference, Manchester, England, 1961, September.
2. A. Sandage, in Galaxies and the Universe, (L. Woltjer, ed., Columbia University Press, New York, 1968) pp. 75-112.
3. T. P. Kohman, J. Chem. Ed. 38, 73-82 (1961).
4. T. P. Kohman, Proceedings of Conference on Problems Related to Interplanetary Matter, Highland Park, Illinois, 1960, June, NAS-NRC Publication 845, 7-8 (1961).
5. D. Clayton, Science 143, 1281-1286 (1964).
6. D. Clayton, Ap. J. 139, 637 (1964).
7. E. R. Kanasewich, in Radiometric Dating for Geologists (E. I. Hamilton and R. M. Farquhar, eds., Interscience Publishers, New York, 1968) pp. 147-224.
8. F. A. Podosek, in preparation.
9. F. A. Podosek, in preparation.
10. W. A. Fowler, New Observations and Old Nucleocosmochronologies, Contribution to George Gamow Memorial Volume, February, 1970.
11. F. G. Houtermans, Z. Naturforsch 2a, 322-328 (1947).
12. E. M. Burbidge, G. R. Burbidge, W. A. Fowler, and F. Hoyle, Rev. Mod. Phys. 29, 547-650 (1957).
13. J. H. Reynolds, Phys. Rev. Let. 4, 8-10 (1960).
14. G. J. Wasserburg, W. A. Fowler, and F. Hoyle, Phys. Rev. Let. 4, 112 (1960).
15. W. A. Fowler and F. Hoyle, Ann. Physics 10, 280-302 (1960).
16. R. H. Dicke, Nature 194, 329-330 (1962).

17. G. J. Wasserburg, D. N. Schramm, and J. C. Huneke, Ap. J. 157, L91-L96 (1969).
18. C. M. Hohenburg, Science 166, 212-215 (1969).
19. P. A. Seeger, W. A. Fowler, and D. D. Clayton, Ap. J. Supplement, XI, 121-166 (1965).

Table I
MODELS FOR THE TIME-DEPENDENCE OF GALACTIC NUCLEOSYNTHESIS OF SOLAR-SYSTEM HEAVY ELEMENTS

Model No.	Description of Model	Reference to Model	Parameters	Input Quantities
1	Single-event	Houtermans 1947 (11)	Σ	X_U
2a	Continuous uniform	Burbidge, <u>et al.</u> 1957 (12)	$\Sigma \Delta$	$X_U X_{Th}$
2b	Single-event	Reynolds 1960 (13)	$M E$	$[M] X_I$
3	Continuous uniform	Wasserburg, <u>et al.</u> 1960 (14)	$M E \Delta$	$[M] X_I$ (*)
4a	Continuous decaying	Fowler and Hoyle 1960 (15)	$M E \Delta \lambda_x$	$[M] X_I X_U X_{Th}$
				$[M][X_I] X_U X_{Th} \text{ Os}^{187}/\text{Re}^{187}$ (+)
4b	Continuous uniform with initial spike	Dicke 1962 (16)	$M E \Delta \alpha$	$[M] [X_I] X_U$ (#)
4c	Continuous uniform with terminal spike	Wasserburg, <u>et al.</u> 1969 (17)	$M E \Delta \phi$ E	$[M] X_I X_{Pu} X_U X_{Th}$ (§)
4d	Initial and terminal spikes with no continuous	Wasserburg, <u>et al.</u> 1969 (17)	$M E \Delta \phi$	$[M] X_I X_{Pu} X_U X_{Th}$ (§)
5a	Continuous decaying with terminal spike	Kohman 1961 (3,4)	$M E \Delta \lambda_x \phi$	$[M] X_I X_{Pu} X_U X_{Th}$
5b	Continuous uniform with initial and terminal spike	Hohenberg 1969 (18)	$M E \Delta \alpha \phi$	$[M] X_I X_{Pu} X_U X_{Th}$ (§)

* Model not completely evaluated.

+ Clayton 1964 (5,6); system over-determined and consistent solution not obtained.

Model not independently evaluated.

§ Unique solution not obtained.

Table II
NOMINAL INPUT QUANTITIES FOR SIMULTANEOUS EQUATIONS

Abundance Ratio	Ref.	Production-Rate Ratio	Ref.	Resultant
$(N_{235}/N_{238})_o = .00726$	(7)	$\rho_{235}/\rho_{238} = 1.46$	(19)	$x_U = .00497$
$(N_{232}/N_{238})_o = 3.66$	(7)	$\rho_{232}/\rho_{238} = 1.74$	(19)	$x_{Th} = 2.10$
$(N_{129}/N_{127})_m = .0000773$	(8)	$\rho_{129}/\rho_{127} = 1$		$x_I = .0000773$
$(N_{244})_m/(N_{238})_o = .0256$	(9)	$\rho_{244}/\rho_{238} = .67$	(19)	$x_{Pu} = .038$
$(N_{207}/N_{206})_{m-o}^{rad} = .5946$	(7)	$M = 4.56 \text{ Gy}$		

Table III
NOMINAL VALUES FOR ASTRONOMICAL PARAMETERS

Quantity	Model 5a (Kohman 1961)	Model 5b (Hohenberg 1969)
[M]	4.56 Gy	4.56 Gy
E	146 My	142 My
φ	3.5%	2.9%
α	---	65%
λ_{eff}	0.61 Gy ⁻¹	---
Δ	3.92 Gy	3.17 Gy

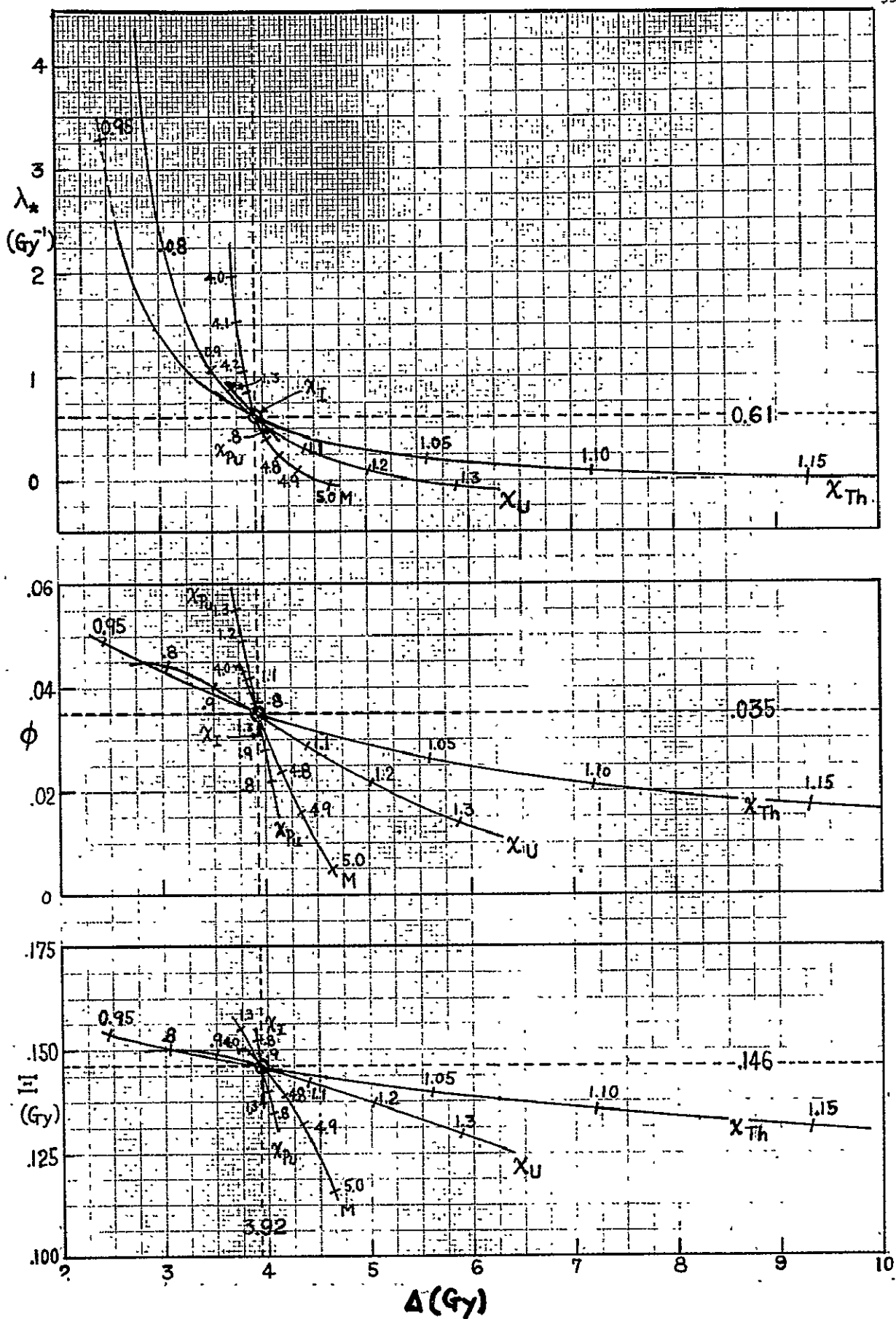


Figure 1. Astronomical parameters and their dependence on input quantities for galactic nucleosynthesis Model No. 5a (continuous decaying nucleosynthesis with terminal spike).

C. Nuclear Chemistry

II. C. 1.

SEARCH FOR NATURAL RADIOACTIVITY OF CALCIUM-48

Mark J. Yeager

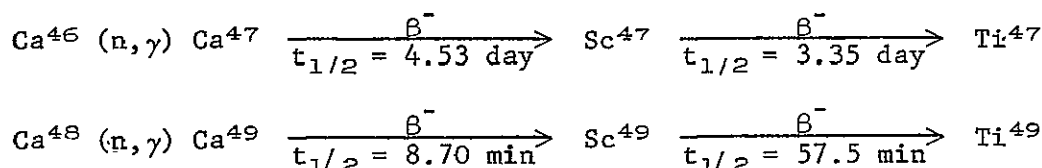
I. Introduction

In searching for single beta decay of Ca^{48} , we are employing the active daughter extraction technique proposed by Jones and Kohman (1,2): Sc^{48} activity is chemically isolated from large amounts of calcium. Thus far the work has been concerned with the development of a procedure which removes any radioactive impurities and which can be conducted in a time which allows detection of the 44-hr half-life of Sc^{48} .

Rajagopalan (3) has recently placed a lower limit of 0.9×10^{20} yr for single beta decay of Ca^{48} . This value is an increase by a factor of 36 over the latest limit determined in this laboratory by Van Itallie *et al.* (4), 2.5×10^{18} yr. In his investigation, Rajagopalan employed a β - γ coincidence counting system, and the Sc^{48} activity was coprecipitated with $\text{Fe}(\text{OH})_3$ from ~ 240 kg CaCl_2 (78 kg natural Ca).

In order to improve Rajagopalan's estimate or detect Sc^{48} activity, counting sensitivity and the amount of calcium used are critical. The large-scale experiments will be conducted using ~ 100 kg of natural calcium (184 g Ca^{48}). A Sharp Laboratories Model LB-100 LowBeta proportional counter with a background of $.8 \pm .2$ cpm has been utilized for all sample counting. The Sharp system contains two side-window Geiger counters, each mounted directly below a guard Geiger counter. The new detectors installed in 1965 have a window diameter of 2-1/4 inches (5). Samples are counted on aluminum planchets with a 5-cm diameter.

Five 1-Curie plutonium-beryllium neutron sources have been used to promote neutron-capture reactions of Ca^{46} and Ca^{48} . The Sc^{47} activity (3.4-day half-life) and the Sc^{49} activity (1-hr half-life) serve as radioactive tracers for testing radiochemical procedures (6). The reactions involved are (7):



The procedure for homogeneous irradiation has been discussed by Fang (6).

II. Dependence of Scavenging Efficiency of Sc Activity on pH

Several initial experiments have been conducted using the neutron sources to determine the optimum pH for $\text{Fe}(\text{OH})_3$ scavenging of scandium activity. 4 l of a 5-M $\text{Ca}(\text{NO}_3)_2$ solution were irradiated for one hour, after which .125 g Fe^{+++} was added. The $\text{Fe}(\text{OH})_3$ precipitate was centrifuged, and a second precipitation from the $\text{Ca}(\text{NO}_3)_2$ solution was made using .125 g Fe^{+++} . The precipitates were dried on separate planchets and counted. The time for extraction of both precipitates was ~ 4 hours. A graph of initial activity of Sc^{49} versus pH indicates that the optimum pH for scavenging is $7.5 \pm .1$ (Fig. 1). At $\text{pH} < 7.5$ the $\text{Sc}(\text{OH})_3$ has probably not completely precipitated; it has been reported that $\text{Sc}(\text{OH})_3$ does not begin to precipitate until pH 7 (8). And at $\text{pH} > 7.5$ Sc^{+++} has probably complexed with ammonia, which was used to adjust the pH of the $\text{Ca}(\text{NO}_3)_2$ solution; the existence of a hexamino scandium cation in the presence of excess ammonium ion has been established (8). Because of the possibility of such complexing, $\text{Ca}(\text{OH})_2$ has been used to raise the pH in all succeeding experiments.

III. Scavenging Efficiency of $\text{Fe}(\text{OH})_3$

To determine the scavenging efficiency of $\text{Fe}(\text{OH})_3$, three successive precipitations were made using a 4 l aliquot of 5-M $\text{Ca}(\text{NO}_3)_2$ solution (pH 7.5) and .125 g Fe^{+++} . The initial Sc^{49} activities for the three samples were respectively 639 ± 10 cpm, 70 ± 7 cpm, and 12 ± 6 cpm. Assuming that the sum of these three activities represents virtually 100 percent of all Sc^{49} activity, the recovery from the first precipitation is $88.8 \pm 2.2\%$.

IV. Radiochemical Purification Procedure

The main structure of the procedure was provided by Van Itallie et al. (4,9) and Fang (6), and their procedures originated from The Radiochemistry of the Rare Earths, Scandium, Yttrium, and Actinium (8). The procedure was perfected using 4-l aliquots of 5-M $\text{Ca}(\text{NO}_3)_2$ solution (pH 7.5) irradiated to saturation activity with the neutron sources. .125 g Fe^{+++} was used to precipitate $\text{Fe}(\text{OH})_3$, and the solid was collected by centrifuging and washed with ~ 10 ml H_2O . After dissolving the iron in 9-M HCl , 10 mg scandium carrier was added, and the Fe^{+++} was removed as FeCl_3 using a 15-cm anion-exchange column with a diameter of 2.2 cm (Dowex 1-X10; 200-400 mesh). The effluent HCl was evaporated to ~ 10 ml and diluted with H_2O to ~ 50 ml. Drops of 6-M NaOH were then added to precipitate $\text{Sc}(\text{OH})_3$. Because the sodium salt of ScF_6^{---} is insoluble in aqueous solution, the solid was washed twice with ~ 5 ml H_2O to remove any traces of Na^+ . After dissolving the $\text{Sc}(\text{OH})_3$ in drops of 6-M HNO_3 , the volume of the solution was doubled with H_2O , and an equal volume of 6-M NH_4F was added. By adding 10 mg lanthanum carrier and heating the solution, LaF_3 and any rare earth contaminants such as YF_3 precipitated, and the scandium remained in solution as ScF_6^{---} . The volume of the solution was then doubled with concentrated HClO_4 and heated to keep the majority of the insoluble ammonium perchlorate dissolved. ScF_3 , the resulting precipitate, was isolated by centrifuging and washed with

~ 20 ml H_2O to remove any traces of ammonium perchlorate. The ScF_3 was dissolved using ~ 5 ml saturated boric acid and ~ 2 ml concentrated HNO_3 . Drops of 6-M NaOH were added to precipitate $Sc(OH)_3$, and the solid was washed twice with ~ 5 ml H_2O and once with the same amount of acetone. The precipitate was transferred to a counting planchet using acetone to facilitate drying under an infrared lamp; the sample was then counted. The average time for purification was ~ 5 hours.

V. Results and Conclusions

To indicate the success of the procedure, unirradiated experiments were conducted, and the blank samples were counted. Some short-lived activity and a long-lived component with an activity of ~ .2 cpm are indicated (Fig. 2). Possibly these impurities will be removed after several successive $Fe(OH)_3$ precipitations. In order to improve the procedure, a TTA extraction is presently being added as an additional purification step, and triply-distilled H_2O will be used in future experiments.

Both 57.5-min Sc^{49} activity and 3.4-day Sc^{47} activity were detected in the irradiated samples for testing the chemical procedure (Fig. 3). Since both of these scandium activities are generated by beta decay of calcium, they would be in the same chemical state as Sc^{48} . Thus, it is reasonable to consider the chemical procedure applicable for Sc^{48} extraction and purification. By comparing the initial activities for Sc^{49} between a purification experiment and for the experiment in which three successive $Fe(OH)_3$ precipitations were made, a value of ~ 16% is obtained for the overall chemical yield.

VI. Future Large-Scale Experiments

The $Ca(NO_3)_2$ solution used by Van Itallie et al. (4), has been homogenized and purified by $Fe(OH)_3$ precipitation. Because NH_4OH was used to adjust the pH, it is possible that a significant portion of any scandium present would be complexed. For this reason a fresh solution of $Ca(NO_3)_2$ is being prepared.

Because of the high $Ca(NO_3)_2$ concentration in Van Itallie's solution (5-M), $Fe(OH)_3$ settling is severely inhibited: instead of taking a few hours for the precipitate to settle in the 50-gal tanks, it takes ~ 5 days. A Helixtractor manufactured by International Equipment Company was fitted to the centrifuge, but the device failed to collect the precipitate. An alternative procedure is presently being investigated: larger amounts of Fe^{+++} will be used to scavenge the scandium from a more dilute solution of $Ca(NO_3)_2$; and after collecting the precipitate, the Fe^{+++} will be removed by anion exchange. If anion exchange fails to remove all the iron, the majority of the Fe^{+++} will be separated by solvent extraction with di-isopropyl ether. The remainder of the iron will then be removed by anion exchange. In recent experiments the precipitation time has been reduced to 20 hours by using 1.0 g Fe^{+++} per 50 gal 4-M $Ca(NO_3)_2$ solution. To coagulate the precipitate quicker,

the solution containing the Fe^{+++} [$\text{Fe}(\text{NO}_3)_2 \cdot 4\text{H}_2\text{O}$ in 1-M HNO_3] has been heated to 70°C before addition to the $\text{Ca}(\text{NO}_3)_2$ solution. Immersion heaters will eventually be tested as a means of reducing the settling time by inducing coagulation of the $\text{Fe}(\text{OH})_3$.

A single extraction experiment using Van Itallie's solution has been conducted, but no 44-hr Sc^{48} activity was detected (Fig. 4). After determining the proper conditions for $\text{Fe}(\text{OH})_3$ settling, large-scale experiments will be carried out in search of single beta decay of Ca^{48} . More elaborate counting conditions will eventually be employed to improve sensitivity.

References

- (1) T. P. Kohman, Phys. Rev. 73, 1223 (1948).
- (2) J. W. Jones and T. P. Kohman, Phys. Rev. 85, 941 (1952).
- (3) G. Rajagopalan, High Sensitivity Radiation Counting and Its Applications in Nuclear Physics, Ph.D. thesis at U. of Bombay, Chapter 5 (1969).
- (4) F. J. Van Itallie, R. D. Allerton, and M. R. Rao, 1966-1967 Progress Report, USAEC Report NYO-844-71, II. C. 1.
- (5) M. J. Toia, 1964-1965 Progress Report, USAEC Report, II. D. 6.
- (6) E. Y. Fang, 1967-1968 Progress Report, USAEC Report NYO-844-75, II. C. 1.
- (7) C. M. Lederer, J. M. Hollander, and I. Perlman, Table of Isotopes, 15-16 (1968).
- (8) P. C. Stevenson and W. E. Nervi, National Academy of Sciences, National Research Council, Nuclear Science Series, "The Radiochemistry of the Rare Earths, Scandium, Yttrium, and Actinium," NAS-NS 3020, 18, 21, 201-203, 205.
- (9) F. J. Van Itallie, 1965-1966 Progress Report, USAEC Report NYO-844-67, II. C. 1.

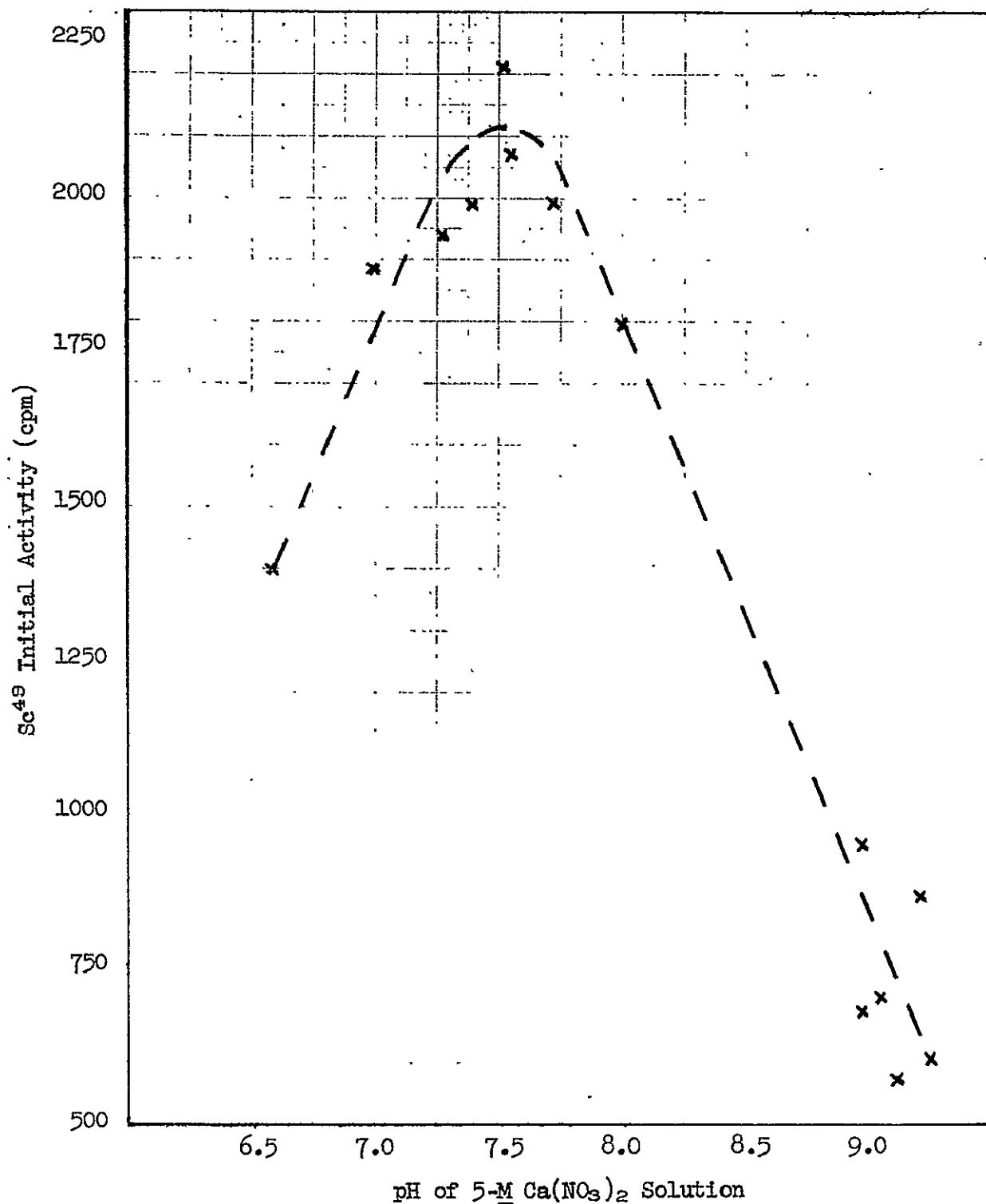


Figure 1. Dependence of scavenging efficiency of scandium activity on pH of 5-M Ca(NO₃)₂ solution.

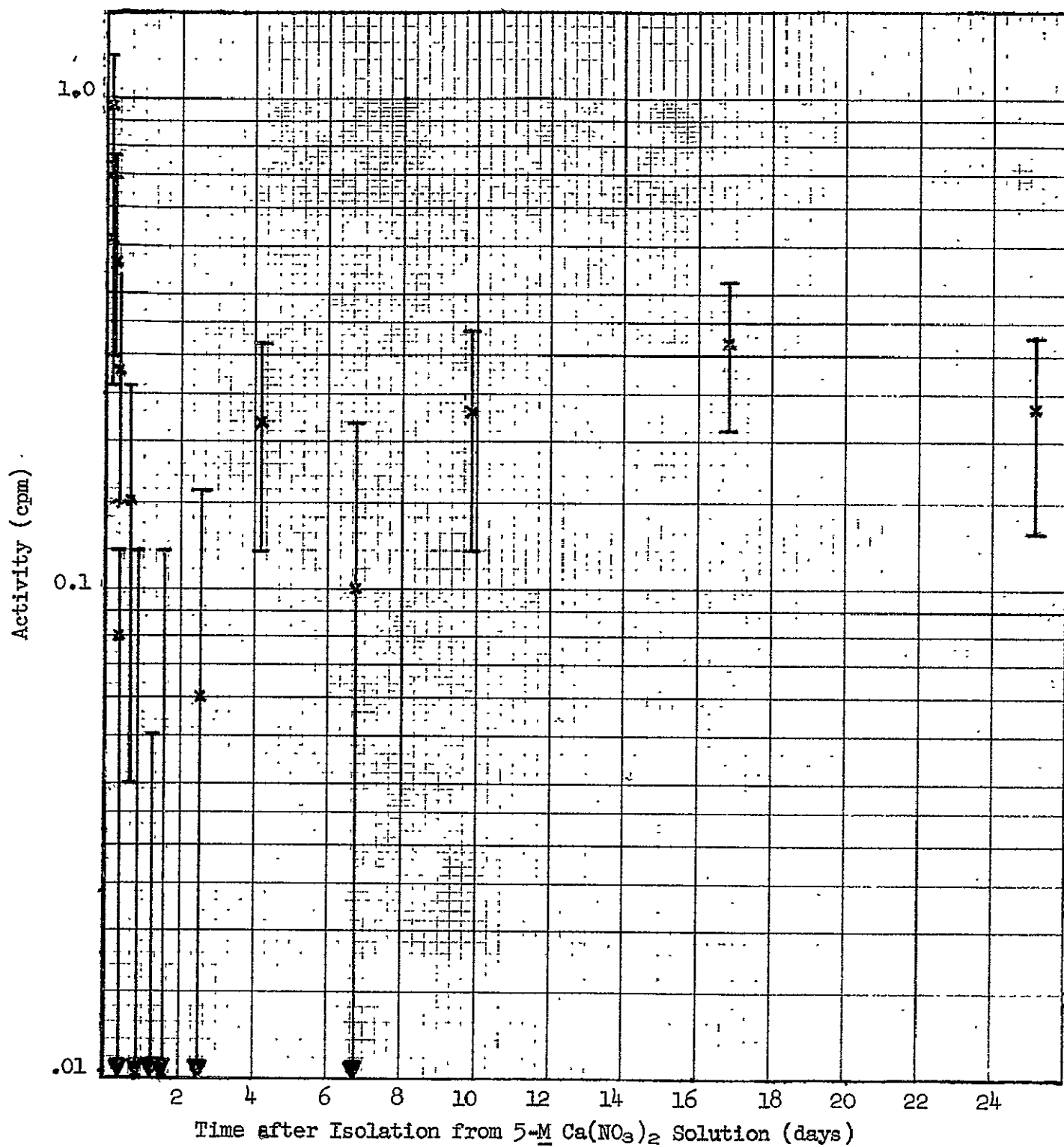


Figure 2. Unirradiated blank displaying low-level contamination.

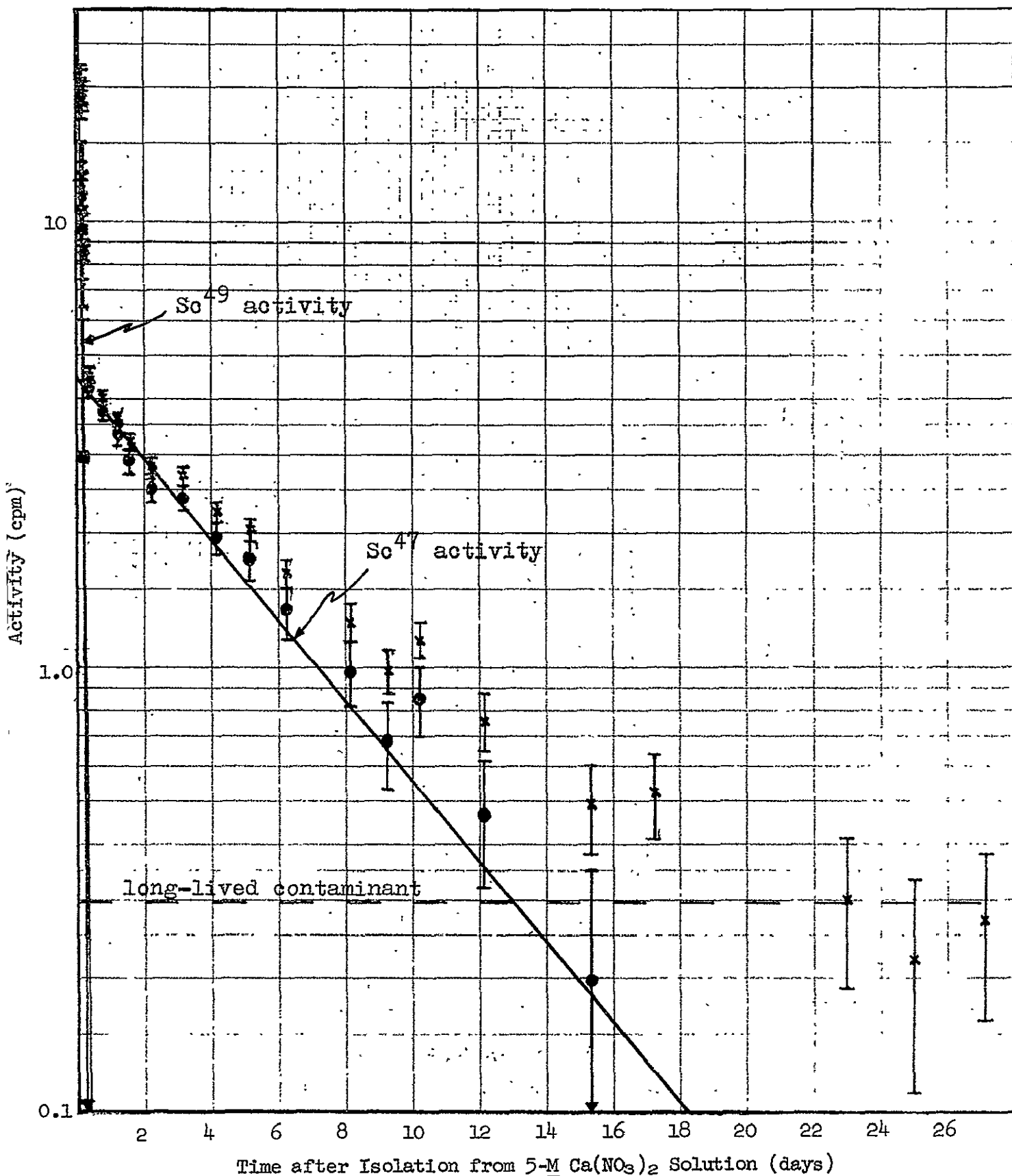


Figure 3. Decay curve of purified $\text{Sc}(\text{OH})_3$ extracted from 4 liters of 5-M $\text{Ca}(\text{NO}_3)_2$ solution irradiated to saturation activity with 5-Curie Pu + Be neutron source.

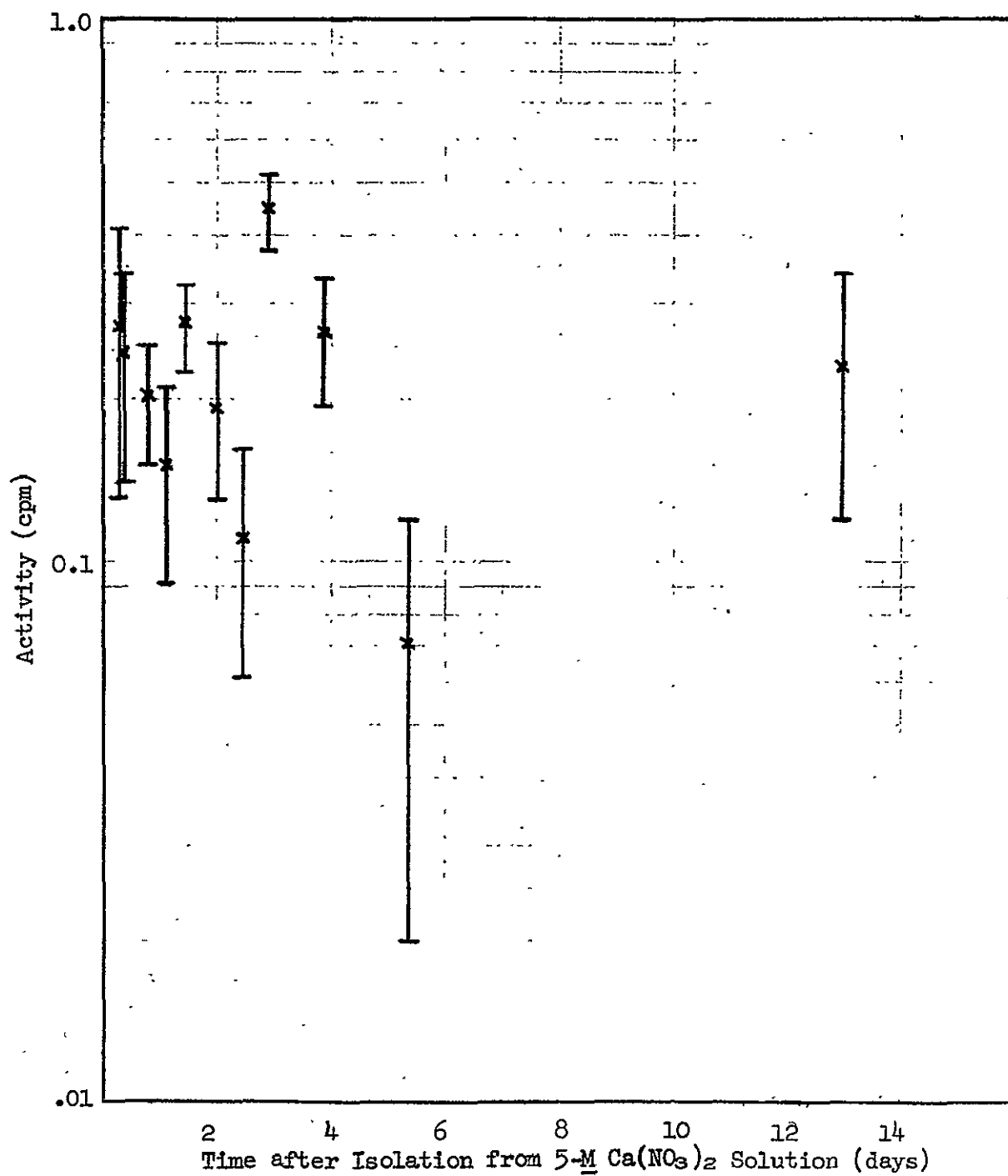


Figure 4. Decay curve of purified $\text{Sc}(\text{OH})_3$ extracted from ~ 80 kg calcium.

D. Techniques and Instrumentation

II. D. 1.

INSTRUMENTATION

Mark Haramic

N71-10312

A brief description of all equipment and plans for modifications and acquisitions will be made. Only equipment not mentioned in previous reports and new modifications will be described in detail. For further information concerning equipment as of the beginning of the year, refer to Toia (1).

A. Mass Spectrometry

A Nuclide Corporation mass spectrometer Model SU 2.4 (2,3) is available to measure abundances of isotopes and their ratios. The instrument has a triple-filament solid-source, with an analyzer tube of a 12-inch radius and 90° deflection. A resolution of less than 1 mass unit at mass 300 can be obtained. Sensitivity can be increased with a 20-stage "ion-electron multiplier" collector.

1. AC Power: Upon original installation, regulated power was supplied to the magnet-accelerator assembly, vibrating-reed electrometer, and ion-electron multiplier to reduce short-term drift. The green power strips located inside the back of the instrument are the regulated power lines. The gray are the unregulated power.

2. Magnetic field: The instrument was supplied with a magnetic field that can be changed with either a sweep control or stepping toggle switch. The sweep control changes the magnetic current at a preselected constant rate; or manual operation of magnet current can be used.

The stepping operation was a modification on the original system. Previously the magnet current was controlled by the difference in voltage between the center taps on two potentiometers in series of 20-k Ω and 200- Ω which are also in series with a 1300- Ω resistor. To this was added a 1-k Ω potentiometer in series with the voltage-divider network shown in modified electronic sweep control for magnet current diagram, Figure 1. The additional resistance, determined by the setting of the potentiometer, will change the magnet current ten times as much as the 200- Ω potentiometer. There is a switch which will bypass the new resistance or leave it in the circuit, enabling a change in magnet current instantly.

A limiting factor of slow response in changing magnetic field arises because of hysteresis losses. When a magnetizing force is applied to a ferromagnetic material there is always a lag in magnetic intensity. The time to reach equilibrium depends on the amount of change in the magnetizing force, in this case the current. A waiting period of four to forty seconds is needed to change from one mass to another.

Solution to the problem of slow response times for magnet equilibrium is to provide a detector to sense the magnetic field. The detector would then send a signal back to a unit that would compare a reference with the actual signal and then make a correction in magnet current. A probe field detector with feedback is the type of device which will do the operation. Plans are being considered to incorporate a detector of this type in our present system.

3. Digital Readout: During the past year a digital-output system from the vibrating-reed electrometer was acquired and installed. It consists of a Hewlett Packard 2212A voltage-to-frequency converter with a zero stability of .0075%. A maximum number of 150,000 pulses full-scale is achieved with a linearity of .01%. Output pulses from the converter are fed to a Monsanto 1510 A counter-timer. Dead-time of the counter is not important because the pulses from the converter are evenly spaced. The counter is equipped with a timer that will open the counter gate and allow pulses to be counted for periods of .1, 1, or 10 seconds. Display of the digital format is either by lit numbers on the face of the counter timer or by a Hewlett Packard 5050 B digital recorder. Numbers from the recorder are printed in sequence on a continuous paper strip.

A paper-tape punching unit or a computer-card punch is being considered. This will allow direct submittal of data to a computer. Already a computer program is being used to calculate isotopic ratios, so the addition of such a unit will greatly increase the efficiency of the projects involved with the use of the mass spectrometer.

B. Radioactivity Measurement Instruments

1. Ge(Li) Gamma-Spectrometry System: The Germanium-Lithium gamma-ray spectrometer system (1) has been running the past year with only a repair on the 512-channel analyzer. During this time a 1/8-inch copper shield was added to the inner walls of the lead shield to reduce the effect of 81-keV X-rays coming from the shield. The X-rays originate from the effect of lead fluorescence resulting from cosmic radiation, natural radioactivity, and sample radiations. The addition of the copper reduced the activity low enough to not be detected in an 80-minute count. Also, a plexiglass frame was constructed to support samples at different distances above the detector. Sample placement at 6 inch intervals with five different locations enabling a maximum distance of 3 feet is obtained.

2. Alpha-Spectrometer Systems: Alpha counting to the present has been done on two identical systems (1) using 200-mm² ORTEC detectors. Recently two 450-mm² silicon surface barrier detectors have been purchased and installed. The present system resolution of system number 2 is 32 keV FWHM. System number 1 seems to have a problem located in the preamplification, causing resolution to fall off to 60 keV FWHM. Maintenance has been started to correct this.

Amplifiers provided with the system enable a maximum width of energy of only 5.5 MeV to be seen at one time using our 256-channel analyzer. By the use of a 10-k Ω potentiometer in parallel with the signal from the amplifier, a smaller signal was taken from the amplifier to increase the energy range that could be seen at one time. For a discussion of the energy ranges obtained refer to the section by Landes in this report (4).

C. Mössbauer Spectrometry

In last year's report (1) it was stated that an International Chemical and Nuclear Corporation Mössbauer spectrometer Model MS-1 was purchased by the Chemistry Department, but there seemed to be a problem with unequal dwell times in the different halves of the memory associated with the Nuclear Data Model 1100 Multichannel Analyzer. Random or pulse-generator pulses fed directly into the multichannel analyzer or fed into the beginning of the electronic Mössbauer network produced a non-random baseline that has repetition with periodicities. Also the

average number of counts in the second half of the memory has a greater amount than the first half producing a step at the 256-257 channel. Originally the step was greater than 1% but has been reduced to ~ 0.2% by Nuclear Data. This is still not satisfactory and arrangements are now being made to have the unit or complete system replaced in the near future.

In the meantime, a computer program has been written to divide each spectrum with a separately determined baseline. Data collected and determined by this method seems to be satisfactory for spectra with relatively few and strong absorption peaks(5).

Unmodified Systems and Equipment

The following equipment and systems are available to project personnel. For further description of equipment and systems refer to reference (1).

Sharp Low-Beta Counter Model LB 101

Gas-flow proportional counter

Harshaw Model 838 "2 x 2" NaI(Tl) detector

4-pi well-type "4 x 4" NaI(Tl) detector

Coincidence system employing two Harshaw detectors Model 12SC12-H "3 x 3" NaI(Tl) detectors.

Coincidence system employing two Harshaw 8S8 "2 x 2" NaI(Tl) Integral-line scintillator detectors.

References

1. M. J. Toia, 1968-1969 Progress Report, USAEC Report NYO-844-76, II. D. 1.
2. M. J. Toia, Semi-Annual Progress Report to NASA, Contract NAS-9-8073, (1 May 1968 - 31 October 1968), Report CMU-NASA-21-1, Section III.
3. M. J. Toia, Semi-Annual Progress Report to NASA, Contract Nas-9-0873 (1 November 1968 - 30 April 1969), Report CMU-NASA-21-2, Section IV.
4. Nina Landes, This Report, II. A. 3.
5. J. D. Ulmer, This Report, II. A. 4.

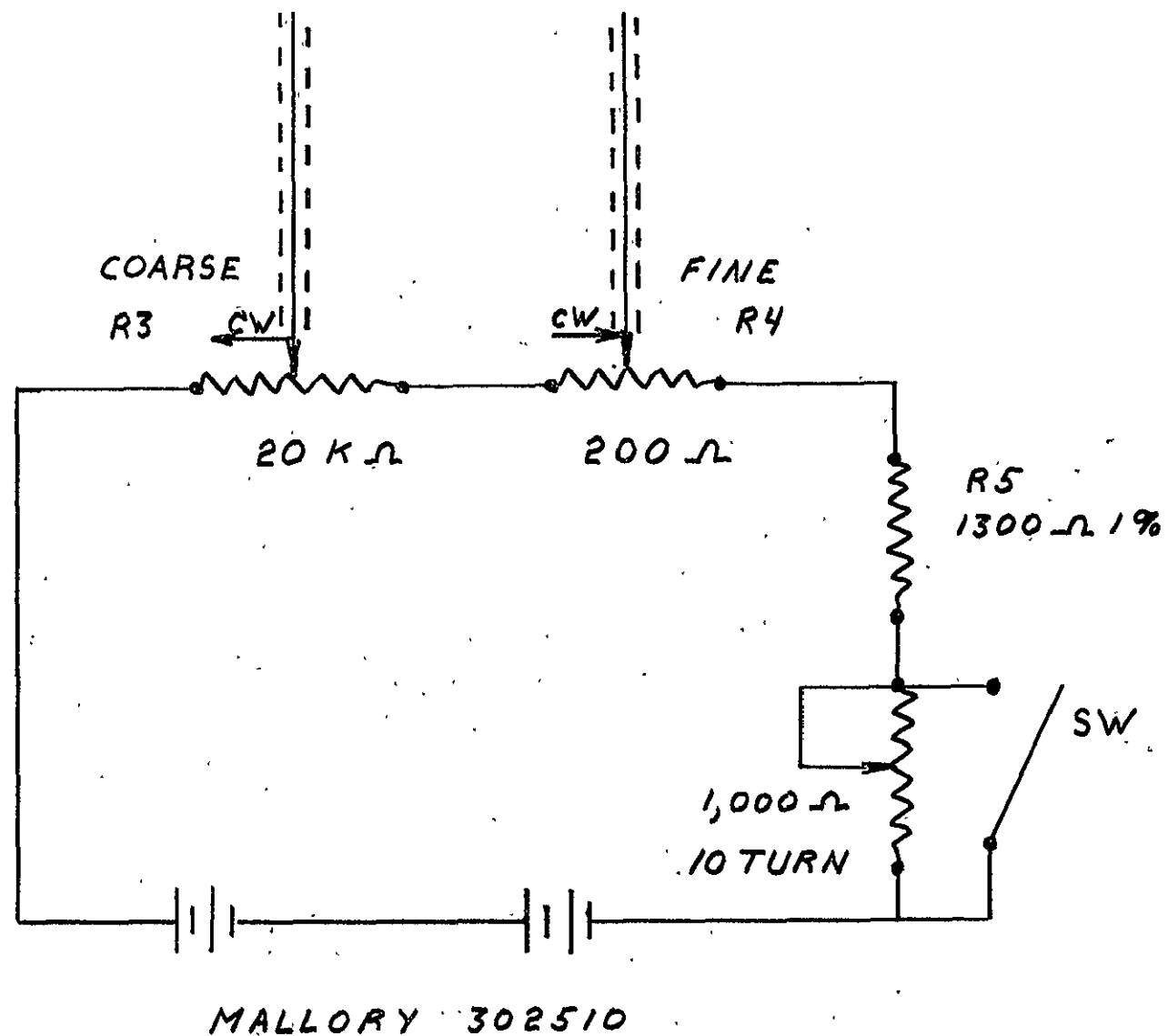


Figure 1. Modified Electronic Sweep Control for Magnet Current

N71-10313

II. D. 2.

GENERAL SCHEME OF CHEMICAL ANALYSIS OF LUNAR AND METEORITIC SAMPLES

H. Ihochi

I. Introduction

Basing on the development of space research, especially with respect to theories about the origin of the solar system and cosmic abundances of the elements, research on extraterrestrial materials has gained considerable importance. Because of limitations in available quantities of such samples, however, a development of a systematic analytical scheme for the determination of the elemental abundances and isotopic compositions of a considerable number of elements from a single sample of a complex matrix is required. As a part of the continuing investigation at Carnegie-Mellon University of the possible existence of additional extinct natural radioactivities, such a general scheme has previously been proposed by J. Tanner (1) for the isolation and determination of the elements, Pd, Ag, Pb, Tl, Sm, Nd, U and Th in lunar materials. Possible extension of this to include W, Hf, Ca, K, Mg, and Al has been discussed by Kohman (2).

In the following section, recent modifications and application of this scheme are discussed.

II. Experimental and ResultsA. Separation of Lead and Thallium by Volatilization

It has been demonstrated that the previously proposed isolation method for separation of Pb and Tl by volatilization in an oxygen flow system as proposed by Huey (3) yielded rather low chemical yields for both lead and thallium. By means of a vacuum volatilization, considerable increase in chemical yields were obtained, and oxidation of sample was avoided. The diagram of the vacuum volatilization system is shown in Figure 1. The results obtained in the above experiments are discussed in detail elsewhere in this report (4).

The behaviors of silver and rare earth elements in this volatilization step were tested by radioactive tracers Ag^{110} and Sm^{145} . The results indicated that silver was partially volatilized and that rare-earth elements were quantitatively retained in the non-volatile residue. The fraction of silver activity in the volatile condensate was found to be very dependent on the condition of sample. When only the silver tracer was used, approximately 100% of the silver activity was found in the volatile fraction. When the same tracer was mixed with basaltic rock, the fraction in the volatile deposit varied from 30% to 70% depending on the operating temperatures of 800°C to 1000°C, respectively.

81801-15N

B. Decomposition and Dissolution of Non-Volatile Residue

Complete decomposition of the non-volatile residue was attained when the residue was repeatedly treated with a mixture of concentrated HF, concentrated HCl, and concentrated HNO_3 of approximately equal volumes. This decomposition procedure was carried out in a teflon beaker covered with a teflon plate at temperature slightly below the boiling point of the mixed acid. Extreme care must be taken in order to avoid complete dryness of the sample during this treatment. Complete dryness of the sample tended to produce insoluble residues.

Treatment of the non-volatile residue with HF- HNO_3 mixture or HF- HClO_4 mixture resulted in formation of insoluble oxides, most probably aluminum oxide. Insoluble sulfate was found when the decomposition was carried out by the HF- H_2SO_4 method. The formation of these insoluble precipitates produced large uncertainty in the abundance determination because of the possibility of loss of trace elements by coprecipitation.

The solution obtained above was then adjusted to 1.5-N HCl by repeated evaporation with concentrated HCl and finally by dilution. The evaporation with concentrated HCl must be repeated until removal of nitrate ions is complete.

For the abundance determinations, appropriate isotopic spikes must be added at the beginning of the decomposition step in order to achieve best mixing of spikes with the samples.

C. Separation of Silver by Ion Exchange

It has been proposed to separate silver from 0.1-N HCl by an anion-exchange column. As mentioned above, it is difficult to obtain complete volatilization of lead and thallium. Thus, the procedure was slightly modified to take this into consideration. Lead, thallium, and silver are absorbed on a Dowex 1 \times 10 anion-exchange column from 1.5-N HCl solution at this point. Preliminary experiments using radioactive tracer indicated that silver is quantitatively absorbed onto the column, and that it can be successfully eluted by 6-N HCl. Lead can be eluted by 0.1-N HCl from the column before the elution of silver. Thallium is then eluted by dilute H_2SO_4 saturated with SO_2 .

Rare-earth elements, uranium, and thorium were observed to remain in the 1.5-N HCl solution in this step. The effects of interfering ions such as Fe^{+++} in this step have not been fully investigated. Thus, further experiments on this procedure will be carried out, and modification of this step may result.

D. Separation of Uranium and Thorium by Ion Exchange

Previously, it was planned to separate uranium and thorium from 8-N HNO_3 solution by an anion-exchange column. The direct conversion of 1.5-N HCl solution into 8-N HNO_3 solution by addition of nitric acid and

heating resulted in the formation of insoluble residues, which might absorb trace amounts of uranium and thorium. Thus, a series of experiments will be carried out to find the most adequate way of conversion. Most likely, hydroxide precipitation and dissolution of the precipitate in several portions of 8-N HNO_3 will be added to the procedure.

Further studies of the isolation technique for uranium and thorium are being carried out at present. The separation of uranium from thorium and purification of each will be performed using procedures such as the ones described elsewhere in this report (5,6).

E. Separation of Rare-Earth Elements

Rare-earth elements are at this point in the 8-N HNO_3 solution with only a few other elements. The rare-earth elements will be separated as a group by fluoride and hydroxide precipitations. The separation of rare-earth elements from this point is discussed in more detail elsewhere in this report (7).

III. Summary

The proposed schemes for the analyses of lunar samples are summarized as block diagrams, in Figures 2 and 3.

The separation scheme for the mass-spectrometric elemental abundance determination is very similar to the scheme for the preparation of samples for the isotopic-composition determination of the elements in question, ~~except that the former includes the addition of isotopic spikes at appropriate steps.~~ For the determination of lead and thallium abundances, spikes are added to an aliquot of the solution of the volatile deposit.

~~The choice of the volatilization method over wet chemical isolation of lead and thallium was based on the following advantages: (a) the smaller chance of contamination from reagents, (b) simplicity of the separation scheme, and (c) merit of additional flexibility, such as differential heating of the sample. The main disadvantage of this volatilization method is that it is extremely difficult to attain complete separation of lead and thallium from the matrix, and the yields in individual runs are unknown.~~

The investigation of the $\text{Pd}^{107}\text{-Ag}^{107}$ system in lunar samples has been discontinued tentatively because of extremely low concentrations of Ag in Apollo 11 samples (8,9,10), and the indications of a rather long time from the termination of r-process nucleosynthesis to the formation of cool meteoritic solids (11). However, because s-process nucleosynthesis may have terminated later than the r-process, and fractionations of non-volatile elements may have occurred earlier than the last cooling to the point of rare-gas retention, the search for extinct natural radioactivity of Pd^{107} continues to appear worthwhile.

The proposed scheme discussed here is not yet completed and is undoubtedly subject to further modifications. Upon completion of various extensions of the scheme, they will be also applied to the analysis of meteorite samples as well as those returned from the moon in the Apollo program.

References

- (1) J. T. Tanner, Semi-Annual Progress Report to NASA, Contract NAS-9-8073 (1 May 1968 - 31 October 1968), Report CMU-NASA-21-1, Section IV.
- (2) T. P. Kohman, Semi-Annual Progress Report to NASA, Contract NAS-9-8073 (1 November 1968 - 31 April 1969), Report CMU-NASA-21-2, Section III.
- (3) J. M. Huey, 1968-1969 Progress Report, USAEC Report NYO-844-76, II. B. 1.
- (4) J. M. Huey, This Report, II. B. 1.
- (5) N. Kan, This Report, II. D. 4.
- (6) B. Trivedi, This Report, II. D. 5.
- (7) R. Saleh, This Report, II. A. 1.
- (8) R. R. Keays, R. Ganapathy, J. C. Laul, E. Anders, G. F. Herzog, and P. M. Jeffery, Science 167, 490-493 (1970).
- (9) A. T. Kashuba, E. V. Gangadharm, A. M. Rothenberg, N. M. Potter, and G. B. Miller, Science 167, 505-507 (1970).
- (10) K. K. Turekian and D. P. Kharkar, Science 167, 507-509 (1970).
- (11) J. M. Huey and T. P. Kohman, This Report, II. B. 3.

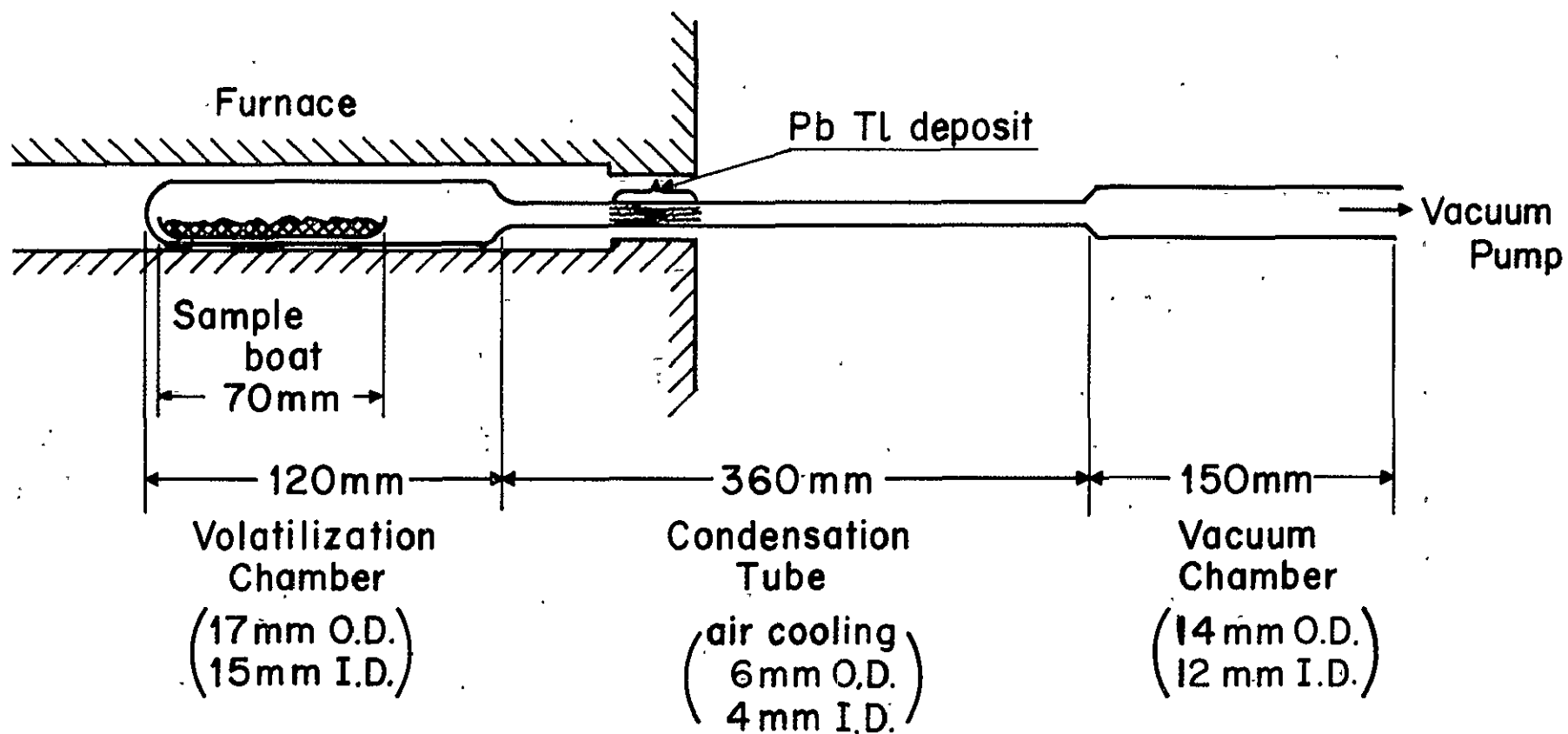


Figure 1. Diagram of the vacuum volatilization system.

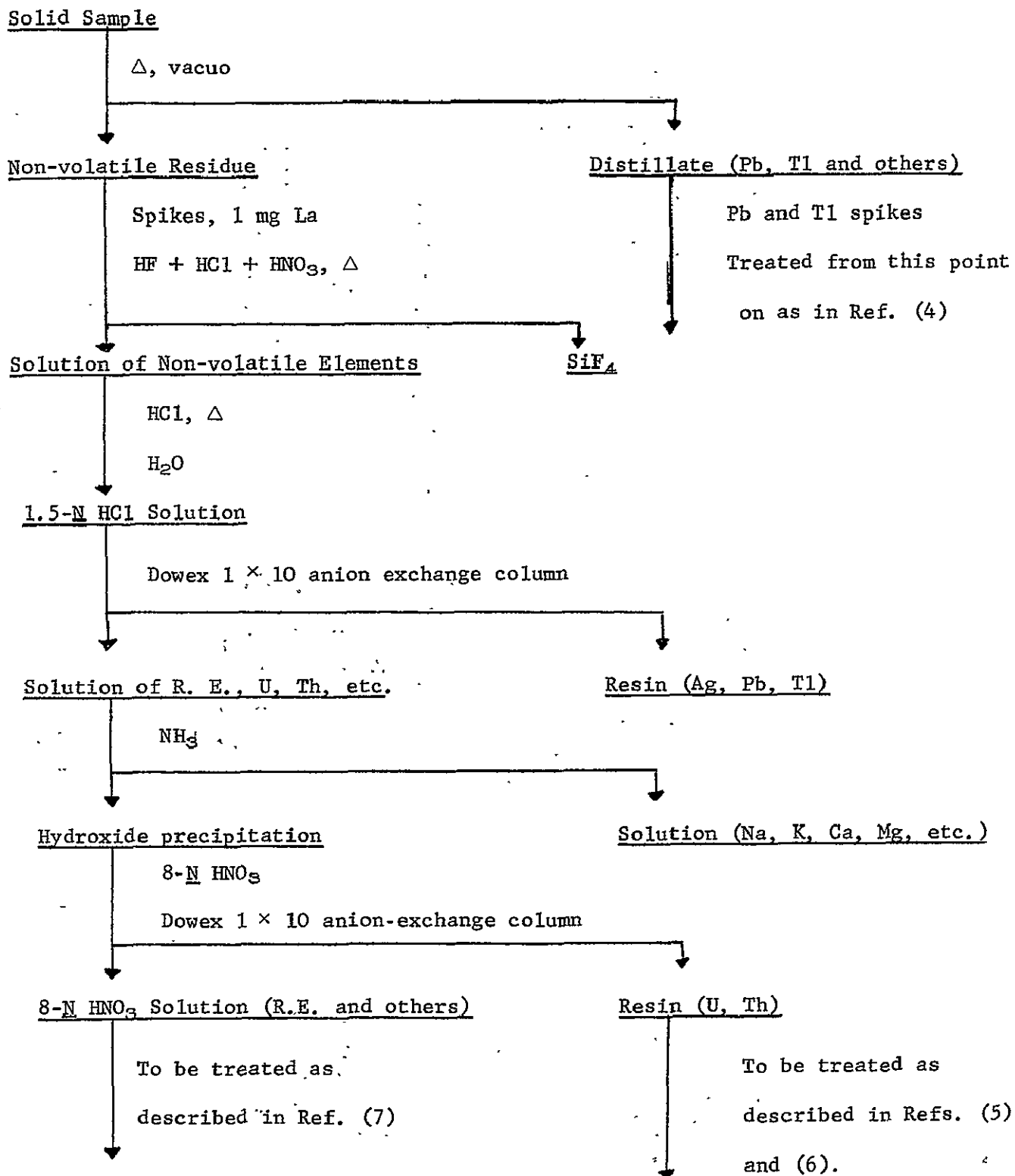


Figure 2.

Block diagram of chemical separation scheme for elemental abundance determinations

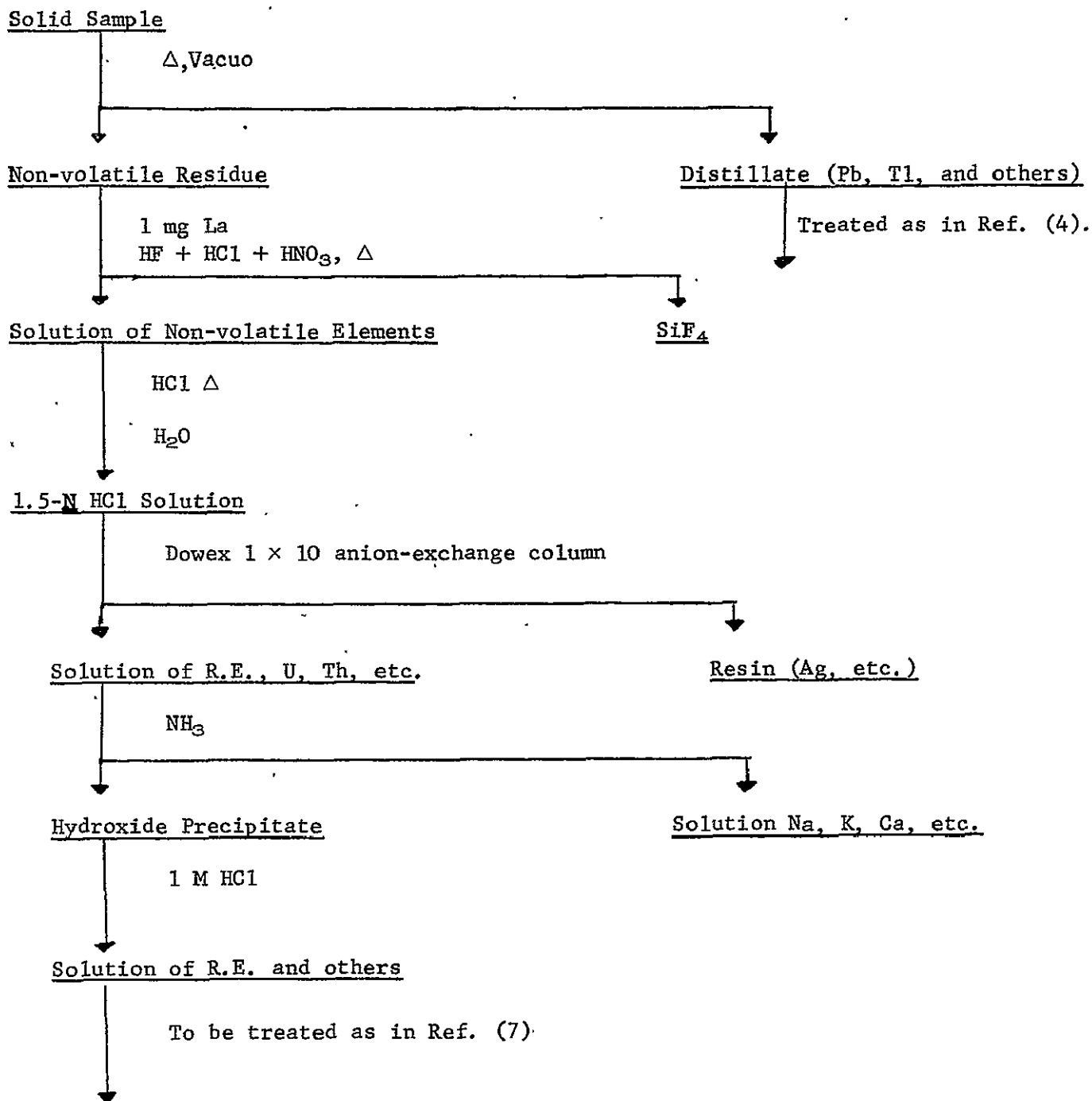


Figure 3. Block diagram of chemical separation scheme for isotopic-composition determinations.

MASS-SPECTROMETRY

Lance P. Black and James M. Huey

I. Additional Instrumentation

The Nuclide model SU-2.4 mass-spectrometer (90° deflection, 30-cm radius), described in a previous report (1), has been upgraded during the past year with the addition of several new systems. This section discusses the reasons for installing these systems; a discussion of their electronic circuitry can be found elsewhere in this report (2).

A. Digital recording system

A digitalizing system, similar to that discussed by Compston, Lovering, and Vernon (3), has been constructed by mating a Hewlett Packard model 2212A voltage-to-frequency converter with a Monsanto model 1510A counter-timer and a Hewlett Packard model 5050B printing digital recorder. This allows an additional output mode besides the normal and expanded-scale circuits of the chart recorder. The system is particularly useful for the measurement of rapidly decaying signals, which cannot be satisfactorily accommodated by the expanded-scale circuit. As the digital voltmeter does not utilize the chart recorder, it is free of any errors arising from non-linearity in this component. In addition to advantages arising from its high sensitivity and precision, the digitalizing system presents the data in a more convenient form than previously.

B. Magnet-switching device

Until recently it was possible to alter the magnetic field during data collection only by continuously varying the magnet current. A control has now been installed which allows the magnet current to be alternately switched between two preset and adjustable values. More time is now spent on-peak rather than at the less important off-peak position; the latter is monitored at the beginning and end of each set of measurements of a particular isotope ratio. Data can now be collected in less time and are less affected by periodic shifts in beam intensity than previously. The combination of the magnet-switching device and the digital-recording system produce data which are readily amenable to statistical analysis.

C. Water pump

A Tuthill 1/4 h.p., 1800 r.p.m. pump is now used to recirculate cooling water to the diffusion pump. This has eliminated the need for the city water supply, which previously caused fouling of the safety cut-off switch after only a few days use. The system is now totally immune to water pressure failure in the mains supply; power failures will cause the diffusion pump to shut off before overheating.

D. Bakeout tapes

Two insulated electrical heating tapes attached to a rheostat control have been wrapped around the source chamber for the purpose of periodically removing volatile material from the walls of the vacuum system. Each tape measures 1" x 96" and has a maximum output of 288 watts. The bake-out system has improved the vacuum within the instrument and considerably reduced the time required for pumpdown after sample introduction.

E. Optical pyrometer

A Pyro micro-optical pyrometer Model No. 95 (manufactured by the Pyrometer Instrument Co., N.J.) has been fitted to a permanent stand opposite the filament-observation portal. The pyrometer is capable of measuring temperatures from 700 °C to 3200 °C on targets which may be smaller than .001" in diameter. With this instrument, filament temperatures can be monitored to approximately ± 5 °C. This allows a precise control on the thermal condition of the source, a parameter which can affect measured isotopic ratios. Precise filament-temperature control is particularly critical in the case of lead (see Part II. A.)

II. Techniques

A large part of many scientific investigations is devoted to developing satisfactory analytical techniques. This is particularly true of mass-spectrometry. The analysis of meteoritic and lunar samples has, in many cases, demanded the analysis of smaller quantities of certain elements than are routinely measured. Thus, relatively new methods have been applied, some of which are still in the developmental stage. In particular, the techniques used for Pb and Tl analysis are still being modified.

A. Lead

The low lead concentrations reported for preliminary analysis of Mare Tranquillitatis surface material (4) necessitated the development of a highly sensitive analytical technique. Following discussions with Drs. Shields and Barnes (5) of the National Bureau of Standards (Washington, D.C.), a method based on the work of Cameron, Smith and Walker (6) was adopted. We have since used this in the analysis of Apollo 11 and 12 lunar fines (7, and unpublished data), and is presently being used for meteoritic lead analyses (8). The technique involves the use of silica gel during the thermal ionisation. This matrix retards the evaporation of lead ions until higher temperature, where there exists a more favorable ionisation-to-evaporation ratio.

The gel is prepared by a method similar to that of Cameron, Smith and Walker (6). However, four heatings of gel with 5% HNO₃ are used instead of two. Great care is also taken during this stage to ensure that the gel does not dry out, as this leads to coarse-grained particles unsuitable for mass-spectrometry. The gel is stored under a shallow water layer (~ 0.25") in glass jars with tightly-fitting plastic caps.

After stirring and a one-minute delay, a 10- μ l aliquot of the overlying aqueous layer, containing gel particles in suspension, is taken and placed on a single filament (zone-refined, high-purity rhenium measuring .030" \times .0012"; supplied by the Rembar Co.). The lead sample in 5% HNO₃ is added, followed by a small quantity (1 μ l) of H₃PO₄. Varying strengths of this acid are used, as some batches of gel emit more stably with weak acid (0.25 M), while others require stronger acid (2.5 M). The sample is dried by resistance heating using a current of about 1.8 A in air for approximately five minutes.

After introduction to the mass-spectrometer ionization chamber, the filament temperature is raised to 800 °C in the space of about ten minutes. It is then adjusted upwards by about 70 °C every five minutes until 1170 to 1190 °C. At these temperatures there is negligible hydrocarbon contamination. Data are taken after a

stabilization period of 10 minutes. In some cases satisfactory stability is not achieved after this time. When this occurs, the filament current is taken to approximately twice its normal reading for about a second, then returned immediately to its normal value (suggested in a personal communication from S. Moorbath (9)). Data taken on the NBS 981 and 983 standards suggest that this treatment does not alter isotopic composition (see Table I).

Unlike the more conventional solid-source procedures employing sulfide (10) or oxalate (11), the silica-gel method can be used for sample sizes in the vicinity of, and less than, one microgram. A one-microgram lead sample yields total ion currents of between 10^{-11} and 10^{-10} A. Ion signals of 10^{-12} A, which persist for more than an hour, can be obtained from less than 100 ng of Pb. Hence we have found it possible to determine the isotopic composition of our chemical blanks (~ 70 ng).

A further advantage is that the method produces no measurable isotopic fractionation (see Table I). This is particularly useful as it avoids the time-consuming and contamination-prone double-spike technique. The table shows that our average composition for NBS 981 is not significantly different from Catanzaro's (12) value (at the 95% confidence level). Our 206/204 and 206/207 ratios of NBS 983 also agree with those obtained from the NBS triple-filament work; our 206/208 ratio, however, appears a little low. In the light of the combined results on both standards, this anomaly is difficult to explain by either contamination or isotopic fractionation.

Ion beams are not as stable as those in the more common solid-source procedures but are generally quite satisfactory, especially as only one mass-spectrometer run per analysis is required.

B. Neodymium

The loading procedures for Nd are relatively simple. The sample, in 5 % HNO_3 , is placed on two rhenium side-filaments and then converted to the oxide by resistance heating at about 1.8 A. Side-filament temperatures between 1300 and 1400 $^{\circ}\text{C}$ are used for data collection; the center filament is set at 1450 to 1500 $^{\circ}\text{C}$. Each isotope is measured relative to that at mass number 146. Total beam current for a 5- μg sample is about 6×10^{-11} A.

The data in Table II have been obtained from three complete mass-spectrometric analyses on commercial reagent neodymium; these are in reasonable agreement with the published compositions (13, 14). Currently analyses are being made to find the reason for the small discrepancies in some of the ratios. Particular attention is being paid to stricter time and temperature controls, as it has been found that the 142/146 ratio, at least, may change by approximately 1% during the early stages of a run.

C. Samarium

Loading procedures are the same as for Nd, with the nitrate being converted to oxide on the filament. However, as with Nd, it is the singly-charged atomic ions that are used for analysis. A center-filament temperature of approximately 1650 $^{\circ}\text{C}$, used in conjunction with side-filament temperatures of around 1300 to 1400 $^{\circ}\text{C}$, appears to give the best results. Each isotope is measured with respect to that at mass number 149. Ion beams are generally about twice as strong as those for Nd. The

reproducibility shown in Table III, which was obtained under a wide range of time and temperature controls, should be improved by experimentation under more rigid conditions.

D. Thallium

Continued experimentation with the triple-filament hydroxide technique reported by Huey (17) has shown it to be inadequate for the analysis of the low-ppb levels of the lunar materials. The single-filament silica-gel method used for lead analysis has been investigated, but has also proved unsatisfactory. Although the technique does have the desired sensitivity, it does not produce consistent isotopic ratios at the relatively low operating temperatures of less than 800 °C. The inability to precisely monitor these filament temperatures appears to lead to variable isotopic fractionation and/or variable amounts of hydrocarbon interference.

A combination of triple-rhenium filament techniques with the silica-gel method of sample preparation provided more consistent results for 25-50 ng samples of thallium. However the low concentrations of thallium observed in many natural materials, including meteorites and lunar fines, makes a method for mass analysis of ≤ 5 ng samples desirable.

Mass analysis of such small samples yielded consistently low 205/203 ratios, $2.386 > R > 2.220$, relative to literature values of 2.390 (18, 21, 22, 23, 24) depending on filament current, time of heating, and amounts of silica gel and phosphoric acid used. The presence of a small peak at mass number 201 suggested that ReO^+ ions (mass numbers 201 and 203) produced during heating with phosphoric acid may be responsible for a low 205/203 ratio. Accordingly, tungsten was substituted as a filament material.

Tungsten-ribbon side filaments are loaded with silica gel, sample, and ~ 2 ul 2.5-M H_3PO_4 . Drying is accomplished by resistance heating (2.0-2.5A, 15 min.). During analysis the ionizing filament is heated to 1000° (~2A) and side-filament currents are turned up slowly. The presence of hydrocarbons is observed at low temperatures, and data are collected after they burn off (side-filament T = 800° (~1.3A)).

Table IV shows the results of several analyses obtained by this technique in comparison with some previous results. There is an apparent increase in the precision of an individual analysis with this technique as compared to previous methods utilized in this laboratory (18). In addition there is a rather large increase in the precision of replicate analyses. This can be attributed to the greater sensitivity of the method (larger signal obtained), the stability of the signal, and the use of a digital readout system.

This technique is being applied presently to the analysis of meteoritic thallium to determine thallium contents (using stable - isotope dilution) and isotopic composition (19).

References

1. M. J. Toia, Semi-Annual Progress Report to NASA, NAS-9-8073
(1 May 1968 - 31 October 1968), Report CMU-NASA-21-1, Section III.
2. M. W. Haramic, This Report, II. D.
3. W. Compston, J. F. Lovering, and M. J. Vernon, Geochim. Cosmochim. Acta 29,
1085-1099 (1965).
4. Lunar Sample Preliminary Examination Team, Science 165, 1211-1227 (1969).
5. W. R. Shields and L. Barnes, personal communication (1969).
6. A. E. Cameron, D. H. Smith, and R. L. Walker, Anal. Chem. 41, 525-526 (1969).
7. T. P. Kohman, L. P. Black, H. Itochi, and J. M. Huey, Science 167, 481-482 (1970)
8. J. M. Huey, This Report, II. B. 1.
9. S. Moorbath, personal communication (1970).
10. B. R. Doe, M. Tatsumoto, M. H. Delevaux, and Z. E. Peterman, U.S. Geol. Survey
Prof. Paper 575-B, 170-177 (1967).
11. J. A. Cooper and J. R. Richards, Earth Planet. Sci. Lett. 1, 58-64 (1966).
12. E. J. Catanzaro, T. J. Murphy, W. R. Shields, and E. L. Garner, Trans. Amer.
Geophys. Union 49, 348 (1968).
13. M. G. Inghram, D. C. Hess, and R. J. Hayden, Phys. Rev. 74, 98-99 (1948).
14. F. A. White, T. L. Collins, and F. M. Rourke, Phys. Rev. 101, 1786-1791 (1956).
15. M. G. Inghram, D. C. Hess, and R. J. Hayden, Phys. Rev. 73, 180 (1948).
16. T. L. Collins, F. M. Rourke, and F. A. White, Phys. Rev. 105, 196-197 (1957).
17. J. M. Huey, 1968-1969 Progress Report, USAEC Report NYO-844-76, II. B. 1.
18. R. G. Ostic, 1966-1967 Progress Report, USAEC Report NYO-844-71, II. B. 3.
19. J. M. Huey, This Report, II. B. 1.
20. E. Anders and C. M. Stevens, J. Geophys. Res. 65, 3043-3047 (1960).
21. A. O. Nier, Phys. Rev. 54, 275-278 (1938).
22. W. Paul, Z. Physik 124, 244-257 (1948).
23. J. R. White and A. E. Cameron, Phys. Rev. 74, 991-1000 (1948).
24. R. F. Hibbs, Mass Spectrometric Measurements of Natural Isotopic Spectra, USAEC
Report AECU-556 (1949).

Table I
Isotopic Analyses of N.B.S. Lead Standards

<u>NBS 981</u>	<u>208/206</u>	<u>206/204</u>	<u>207/206</u>
Analysis 68	2.1684	16.909	.9150; 9136†
102	2.1697	16.909	.9169
106	2.1690; 2.1698	16.954	.9161
127	2.1627	16.924	.9141
168	2.1637; 2.1654‡	16.916	.9150
175	2.1632*	16.916*	.9146*
179	2.1664*	16.948*	.9149*
Average composition	2.1665 ± .0010§	16.925 ± .007§	.9150 ± .0004§
N.B.S. Value (12)	2.1681	16.938	.9146
<u>NBS 983</u>	<u>206/208</u>	<u>206/204</u>	<u>206/207</u>
Analysis 115	72.95	2622	14.040
185	73.25	2835	14.038
187	73.15	2798; 2595‡	14.041
190	73.22	2791; 2829; 2755★	14.033
Average composition	73.14 ± .07§	2748 ± 47§	14.038 ± .002§
N.B.S. Value (12)	73.4	2698	14.04

†Data sets taken at beginning and end of run, respectively.

★Data taken at three stages during run.

*Data taken after sample was briefly subjected to high filament temperature.

§Uncertainties quoted represent the standard deviations of the means.

Table II
Isotopic Analyses of Commercial Reagent Neodymium

	<u>142</u>	<u>143</u>	<u>144</u>	<u>145</u>	<u>146</u>	<u>148</u>	<u>150</u>
Analysis 92	27.08	12.16	23.77	8.30	17.25	5.78	5.66
97	27.09	12.20	23.80	8.30	17.20	5.76	5.65
104	27.05	12.18	23.77	8.30	17.23	5.79	5.69
Inghram et al.(13)	27.13	12.20	23.87	8.30	17.18	5.72	5.60
White et al.(14)	27.3	12.32	23.8	8.29	17.10	5.67	5.56

Table III

Isotopic Analyses of Commercial Reagent Samarium

	<u>144</u>	<u>147</u>	<u>148</u>	<u>149</u>	<u>150</u>	<u>152</u>	<u>154</u>
Analysis 20	3.09	15.00	11.24	13.81	7.38	26.75	22.72
96	3.01	15.00	11.26	13.86	7.43	26.76	22.68
100	3.11	15.07	11.30	13.86	7.38	26.67	22.61
101	3.08	15.02	11.26	13.84	7.39	26.70	22.71
Inghram et al.(15)	3.16	15.07	11.27	13.84	7.47	26.63	22.53
Collins et al.(16)	3.15	15.09	11.35	13.96	7.47	26.55	22.43

Table IV

Isotopic Analyses of Reagent Thallium

	<u>Sample Size</u>	<u>205/203</u>
Analysis 248	≤ 5 ng	$2.389 \pm .004$
252	≤ 5 ng	$2.388 \pm .003$
253	≤ 5 ng	$2.382 \pm .002$
257	≤ 5 ng	$2.386 \pm .001$
259	≤ 5 ng	$2.390 \pm .003$
Weighted Avg.	≤ 5 ng	$2.388 \pm .002$
Avg. of Ostic's Replicate Anal. (18) 40-80 ng		$2.389 \pm .005$
Normal Tl* (20)		$2.36 \pm .02$
Normal Tl (21, 22, 23, 24)		2.390

★ \sqrt{m} correction for electron multiplier applied

II. D. 4.

CHEMICAL PROCEDURES FOR PURIFICATION OF URANIUM AND
THE ALPHA-SPECTROSCOPY OF URANIUM

Nancy-Kan

I. Introduction

Tektites are glassy objects found scattered on the Earth's surface in discrete regions up to thousands of kilometers apart. Their origin is unknown. There are two major hypotheses, lunar origin and terrestrial origin. Schwarcz (1) has demonstrated similarities in the chemical composition of tektites and soils, and assumed that tektites are formed on the earth from soils by the impact of some extra-terrestrial object. In this case, U^{234}/U^{238} isotope ratios differing from unity in tektites might provide strong confirming evidence of this hypothesis (2,3). The U^{234}/U^{238} isotope ratio will be an important clue to the origin of tektites.

If the young tektites showed a U^{234}/U^{238} ratio below unity and old tektites did not, this would prove that tektites are terrestrial in origin. So we have undertaken to determine as accurately as possible the U^{234}/U^{238} ratios in tektites. This will require higher precision than in previous work, ~0.1%. This report describes a chemical procedure of isolation and purification of traces of uranium to determine the U^{234}/U^{238} activity ratio of alpha-particle spectrometry.

II. Chemical Procedure

The techniques of decomposition of silicate rocks and chemical separation are those developed by T. P. Sarma (4). Vassiliki Tsomi (2) followed the same procedure. Thomas J. Thomas (3) modified it by using a thenoyl-trifluoro-acetone (TTA) extraction to deposit uranium onto a planchet, which has also been used by Ku (5). The TTA method was found (3) to yield samples with better alpha-spectrum resolution than samples prepared by electrodeposition. This may be due to the more rapid deposition in the TTA method with correspondingly less granular crystal structure. Also, Thomas changed the planchet material from platinum to titanium (6). The chemical procedure is outlined in Figure 1.

A. Decomposition of Silicates

After treating the 10-g sample with HF, H₂SO₄, and perchloric acid and leaching with HCl as in the procedure of Sarma (4), we still have some residue which cannot be dissolved. For dissolving the residue, instead of using a sodium fusion, to avoid contamination, a mixture of equal volumes of HF, HCl, and HNO₃ is used in a teflon beaker and boiled with the residue. Several portions of HCl are added and evaporated to get rid of the HF and HNO₃. The solution is heated under a heat lamp for several hours to reduce the volume to 500 ml. The solution is cooled and 5 g of sodium bromate is added in small portions in order to oxidize U(IV) to U(VI). Then the solution is neutralized with concentrated ammonium hydroxide until it is slightly basic.

The solution is heated under a heat lamp for a couple of hours. The hydroxide precipitate is centrifuged and washed twice with water and then evaporated to dryness.

B. Ion-exchange Separation

A polyethylene anion-exchange column containing 30 ml of Dowex 1-X4 is set up and washed first with 150 ml 1-M HCl and then with 150 ml 10-M HCl. The dried sample obtained in the co-precipitation step is dissolved in 600 ml 10-M HCl and transferred to the ion-exchange column. The column is washed with 4-column volumes of 10-M HCl, when all the major elements and radioelements except Fe(III), Pa(V), U(VI), and Po(IV) are eluted from the column. Leaching the column is continued with a solution of 150 ml 9-M HCl plus 1-M HF to remove Pa(V). Finally uranium is stripped off from the column with 300 ml 1-M HCl. The flow rate of the elution is about 8-10 drops/min.

C. Di-isopropyl Ketone Extraction

The uranium fraction containing Fe(III) and Po(IV) is evaporated to dryness and taken to fumes with concentrated HNO_3 to eliminate the last traces of fluoride ion. The residue is dissolved in 25 ml of 6-M HCl. The solution is extracted with di-isopropyl ketone by the countercurrent extraction method, using three separatory funnels, when Fe(III) and Po(IV) go into the organic phase. The aqueous phase containing uranium is evaporated to dryness with 50 ml concentrated HNO_3 to decompose any organic matter.

D. TTA Extraction

The thenoyl-trifluoro-acetone (TTA) method has been used by Ju (5) to deposit uranium onto a planchet. The dry residue is taken up with 0.2 ml of 0.1-M HNO_3 . The purified uranium is stripped into the TTA phase in a 0.4-M TTA-benzene extraction after the pH of the aqueous phase has been adjusted to 3.0 by using a pH 3 buffer. The extractions are done by countercurrent extraction with equal volumes (1 ml each) of TTA and uranium solution.

E. Preparation of Sample for Alpha Counting

The benzene-TTA-U phase is evaporated onto a Pt or Ti disk which is washed first with acetone, then with concentrated HNO_3 , and finally with distilled water. The disk is then flamed to burn off the organic matter, giving a thin source of uranium oxide. Another method of preparation of samples is that of direct evaporation on a Ti disk of a pure uranium solution with the aid of a spreading agent -- tetraethylene glycol (TEG) (7). About 1 or 2 drops of TEG are dropped on a Ti disk, and the uranium solution is then transferred to the disk with a capillary dropper. The solution is evaporated slowly under the heat lamp to dryness. The disk is then flamed and the uranium is left as a uniform thin film.

III. Alpha-Particle Spectrometry

The alpha spectra are obtained by an alpha system consisting of a 450-mm² ORTEC detector, Instrument and Development Products preamplifier; amplifier, and a Nuclear Data 256-channel analyzer (8).

A typical spectrum of uranium from uranium nitrate ($\text{UO}_2(\text{NO}_3)_2 \cdot 6\text{H}_2\text{O}$, Baker analyzed reagent grade) is given in Figure 2. This sample contains U^{234} , U^{238} , U^{235} , and also traces of U^{236} . The U^{236} is present as a result of intense neutron irradiation, evidently in a nuclear reactor from whose spent fuel elements this uranium was recovered. The facts that the $\text{U}^{234}/\text{U}^{238}$ ratio is not unity and the $\text{U}^{235}/\text{U}^{238}$ ratio is below that in natural uranium also indicate that the sample is not of natural uranium. Because of the deficiency of U^{234} , the sample can be used for isotope dilution analysis.

The $\text{U}^{234}/\text{U}^{238}$, $\text{U}^{235}/\text{U}^{238}$, $\text{U}^{236}/\text{U}^{238}$ ratios are calculated by taking the integral of the alpha spectrum (Figure 2) from channel 96 to channel 132 for U^{238} , channel 133 to channel 155 for U^{235} , channel 156 to channel 165 for U^{236} , and channel 166 to channel 202 for U^{234} . The widths of the U^{234} and U^{238} peaks are about 5 channels (~40 keV) FWHM. A comparison of the curve in Figure 2 with the synthetic natural uranium spectra of Thomas (3), shows that the resolution is somewhat better than the 40-keV FWHM curve and definitely worse than the 20-keV FWHM curve. The instrumental resolution is thus about 35 keV.

IV. Quantitative Test of Procedures

The counting yield at different shelf positions can be calculated by using a uranium nitrate solution and assuming that the specific activity of U^{238} is 734 disintegrations/mg/min (Table 1).

The data have been collected by using a uranium nitrate solution to check the chemical yield and the reproducibility of the whole procedure. This is accomplished by performing only the last step of the procedure in the first run, and going backwards and adding one more step, proceeding to the beginning, for each successive run. For example, first only the TTA extraction is done, next the di-isopropyl ketone extraction followed by the TTA extraction, and so on. The data from successive addition of steps shows very good agreement in the $\text{U}^{234}/\text{U}^{236}$ ratio (Table 2). The chemical yield is based on a sample of uranium solution directly deposited on a Ti disk by the TEG spreading method (Table 2).

V. Plans

Because of the low-energy tailing of alpha spectra, low instrumental resolution from thick samples, and the necessity of getting higher precision, it is necessary to use a computer analysis of data. This was begun by Thomas (3) and is being developed further by Trivedi (9).

By using a U^{232} tracer through the isotope dilution method, the chemical yields at very low uranium concentration can be tested. The goal of this whole procedure to try to get the uranium content of tektites by isotope dilution and the U^{234}/U^{238} activity ratio in tektites will thus be fulfilled.

References

1. H. P. Schwarcz, Nature 194, 8-10 (1962).
2. V. Tsomi, 1967-1968 Progress Report, USAEC Report NYO-844-75, II.A.3.
3. T. J. Thomas, 1968-1969 Progress Report, USAEC Report NYO-844-76, II.A.2.
4. T. P. Sarma, Dissertation, Carnegie Institute of Technology, USAEC Report NYO-8925 (1964), pp. 24-28.
5. Teh-Lung Ku, J. Geophys. Res. 70, 3457-3474 (1965).
6. K. W. Edwards, U. S. Geol. Surv. Water-Supply paper 1696-F (1968).
7. Ismael Almodovar, Dissertation, Carnegie Institute of Technology; USAEC Contract No. AT(30-1)-844 (1960), pp. 57-59.
8. Mark Haramic, this Report, II.D.1.
9. B. M. P. Trivedi, this Report, II.D.5.

Table I
COUNTING YIELDS OF 250 μ g URANIUM DEPOSITED ON Ti
WITH TEG (SAMPLE U-15) AT DIFFERENT POSITIONS OF THE DETECTOR

Position	Activity Ratio			Counting Rate for U^{238} Peak	Counting Yield
	U^{234}/U^{238}	U^{235}/U^{238}	U^{236}/U^{238}		
Third Shelf (0.937 inch)	0.232	0.0178	0.0077	709/hr	6.4%
Second Shelf (0.687 inch)	0.241	0.0199	0.0093	1109/hr	10.1%
First Shelf (0.437 inch)	0.241	0.0198	0.0090	1872/hr	17.0%

Table II
CHEMICAL YIELDS FOR PROCEDURE STARTING
AT VARIOUS STEPS

Sample (500 μ g Uranium)	Procedure	Activity Ratio			Counting Rate for U^{238} Peak (3rd Shelf)	Chemical Yield
		U^{234}/U^{238}	U^{235}/U^{238}	U^{236}/U^{238}		
U-4	Starting with TTA extrac- tion	0.239	0.0189	0.0082	850/hr	60%
U-5	Starting with TTA extrac- tion	0.236	0.0189	0.0079	808/hr	58%
U-22	Starting with TTA extrac- tion	0.239	0.0243	0.0081	1045/hr	74%
U-20	Starting with di-isopropyl ketone ex- traction	0.233	0.0193	0.0081	579/hr	41%
U-14	Starting with ion-exchange	0.233	0.0184	0.0074	533/hr	38%
U-16	Starting with ion-exchange	0.244	0.0171	0.0067	425/hr	30%
U-17	Starting with hydroxide precipitation	0.232	0.0257	0.0118	394/hr	28%

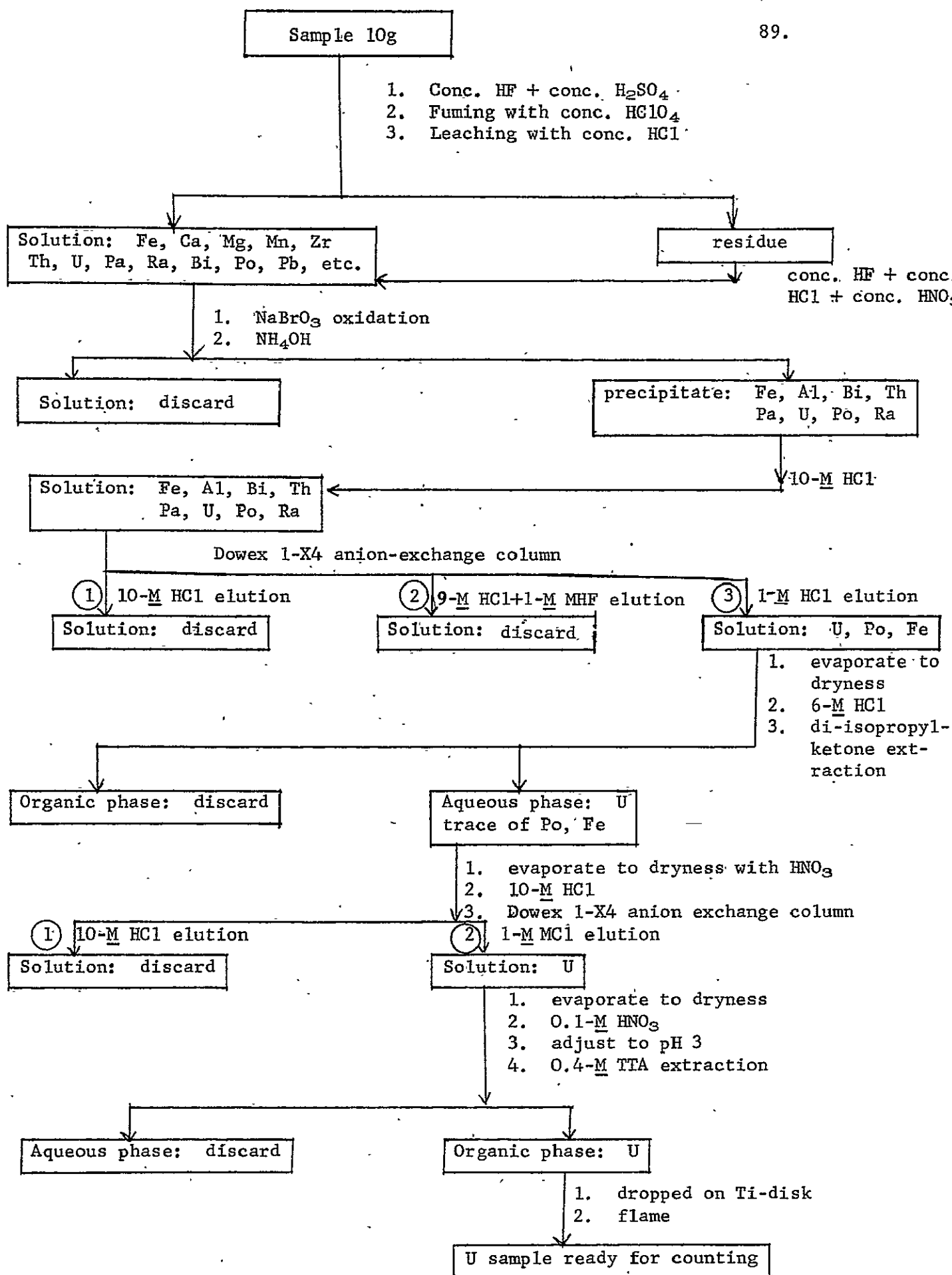


Figure 1. Chemical Procedure for Uranium

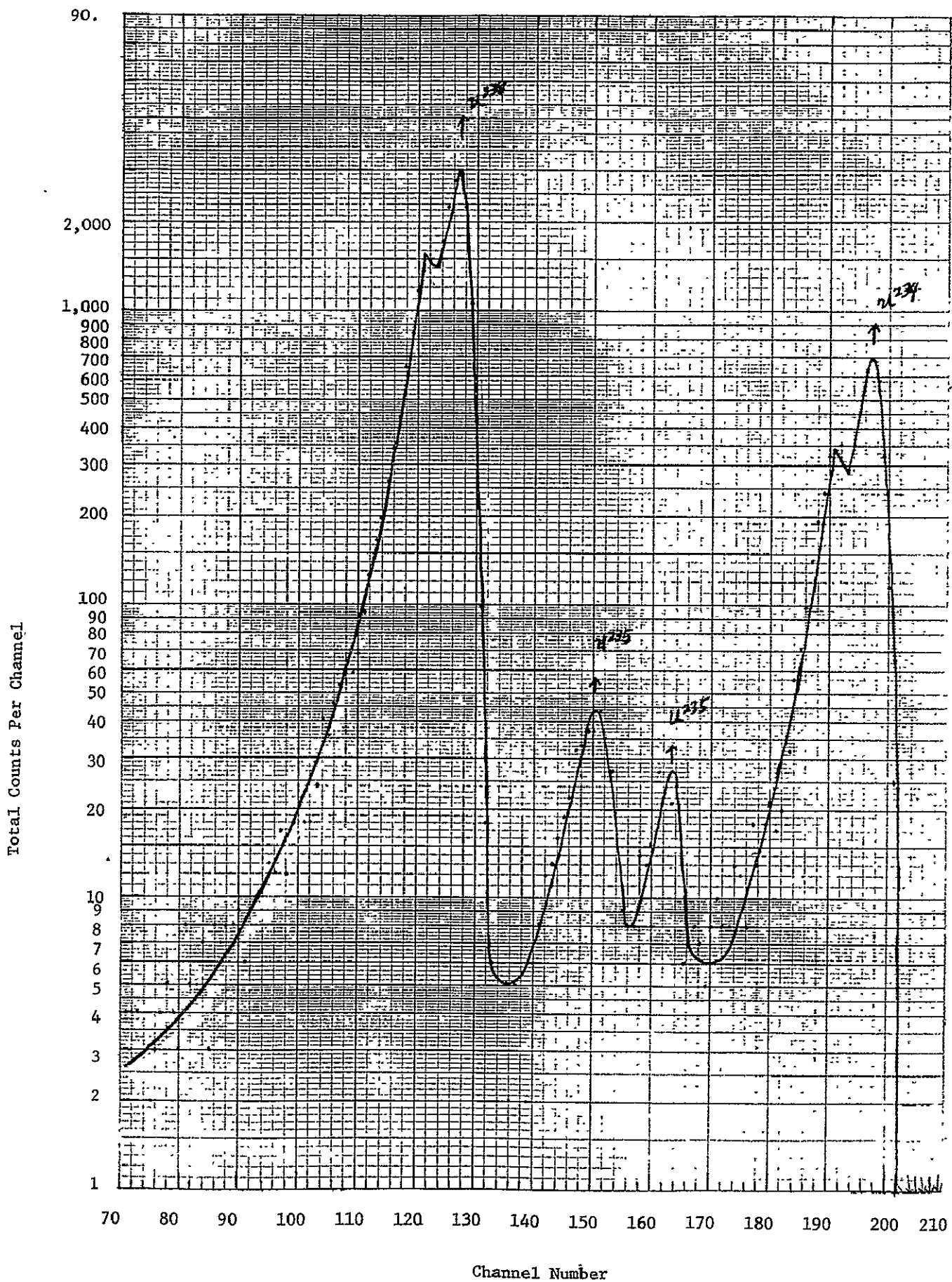


Figure 2. Alpha Spectrum of Commercial Uranium.
Sample U-16 (See Table 2 for prepara-

N71-10316

ALPHA-ISOTOPE-DILUTION ANALYSIS OF URANIUM AND THORIUM

Brij M. P. Trivedi

The present work aims at quantitative determination of uranium and thorium in natural samples, with special interest in meteorites and lunar materials by the radiometric alpha-isotope-dilution technique using U^{232} and Th^{228} as spikes.

I. Chemical ProcedureA. U^{232} and Th^{228} Tracer Solution

U^{232} solution was purchased from General Nuclear, Inc. A standard solution of $0.01 \mu\text{C}/\text{ml}$ of U^{232} was prepared by T. J. Thomas from the original standard. A portion of this solution was further diluted to give $90 \text{ dpm}/\text{ml}$ of U^{232} . About 0.1 ml of this solution was used as spike in the development of the chemical procedure. The activity ratio of (U^{232}/Th^{228}) is about 6.

B. Dissolution of Silicate Samples

A weighed quantity ($\sim 2\text{-}5 \text{ g}$) of the silicate sample is taken in a teflon beaker and spiked with 0.1 ml of U^{232} standard solution. The same amount of U^{232} solution is evaporated on a platinum planchet and counted separately to check the chemical yield. About 25 ml of hydrofluoric acid and 25 ml of nitric acid are added to the sample. The solution is evaporated to dryness and the $\text{HF} + \text{HNO}_3$ process repeated three times. The residue is dissolved in concentrated HCl . In all cases a clear solution is obtained.

C. Group Separation

Chemical procedure for separation and purification of U and Th has been developed by many investigators (1,2,3,4,5,6,7,8). Briefly, the solution obtained after dissolution of silicate material is evaporated to dryness and taken into 1.8-M HCl . The solution is passed through a Dowex 1×10 anion-exchange column (200-400 mesh, Cl^- form) 20 ml in volume. The column is washed with 1.8-M HCl (6 column volumes) when U, Th and rare earths are separated from the column and silver sticks to the column. The eluate is dried and taken into 8-M HNO_3 and passed through Dowex 1×10 column (20 ml volume). Rare earths are separated from the column by washing it with 8-M HNO_3 . Thorium is separated from the column by washing it with 10-M HCl and finally uranium is separated by washing it with 0.1-M HCl .

Purification of Thorium

The thorium fraction is evaporated to dryness and taken into 8-M HCl. The solution is passed through Dowex 50 WX4 cation-exchange column (ionic form H^+ , 50-100 mesh, 20 ml volume). Thorium sticks to the column. Thorium is desorbed from the column by washing it with 0.5-M oxalic acid. Oxalic acid in the solution containing thorium is decomposed by heating it with concentrated nitric acid. The solution is evaporated to dryness and taken into 10-M HCl and passed through Dowex 1 \times 4 anion-exchange (Cl^- form, 100-200 mesh) column (20 ml volume). Washing the column with four column volumes of 10-M HCl removes all thorium. Final purification of thorium is done by extracting it with 0.4-M solution of TTA (thenoyltrifluoroacetone) in benzene. Thorium solution is evaporated to dryness and taken into approximately half ml of 0.1-M HNO_3 . Equal volume of 0.4-M TTA solution is added and equilibrated with the aqueous solution. Thorium comes out in the organic phase and is deposited by evaporation on a platinum planchet. The platinum planchet is put to flame, when a very thin source of thorium is obtained.

E. Purification of Uranium

The uranium fraction is evaporated to dryness and taken into 6-M HCl (~ 15 ml). The solution is equilibrated with an equal volume of diisopropyl ketone. Uranium remains in the aqueous phase and is free of iron. The uranium fraction is heated with concentrated HNO_3 to decompose any organic matter and evaporated to dryness. The residue is taken into 10-M HCl and passed through Dowex 1 \times 4 anion-exchange (Cl^- form, 100-200 mesh) column (20 ml). Uranium sticks to the column and is desorbed from the column by washing it with 0.1-M HCl. The solution is evaporated to dryness and taken in about 0.2 ml of 0.1-M HNO_3 . A buffer solution (prepared from buffer tablets, Coleman) of pH 3 (~ 0.5 ml) is added to make the pH of the solution about 3. The solution is now equilibrated with equal volume of TTA (0.4-M in benzene), when uranium comes out in the organic phase. The organic phase is withdrawn and evaporated on a platinum planchet to deposit the uranium uniformly. The planchet is heated red hot, giving a thin source of uranium.

II. Alpha-Particle Spectrometry

The samples are counted in a surface barrier detector (Model No. E-022-450-300), with active area 450 mm² and sensitive depth 300 microns, purchased from ORTEC. The resolution of the detector is 35 keV and the counting yield 18%.

III. Preliminary Experiments

Preliminary experiments have been carried out with tracer alone (U^{232} and Th^{228} solution) to check the procedure. Figures (1) and (2) show the alpha spectra of U and Th, respectively, separated from a tracer

solution. Further experiments have been carried out with pure silica glass with spike added (blank run) and rock sample (Granodiorite; GSP-1) obtained from the U. S. Geological Survey. The chemical yield for each case was found to be about 50%. Figure (3) shows the alpha spectrum of uranium separated from the rock sample. The thorium sample is being purified for counting.

References

- (1) T. P. Sarma, Dissertation, Carnegie Institute of Technology, USAEC Report No. NYO-8925, pp. 24-28 (1964).
- (2) V. Tsomi, 1967-68 Progress Report, USAEC Report No. NYO-844-75 II. A. 3.
- (3) J. T. Tanner, Semi-Annual Progress Report to NASA, Contract NAS-9-8073 (1 May 1968 - 31 October 1968), Report CMU-NASA-21-1, Section IV.
- (4) J. N. Roshalt, B. R. Doe and M. Tatsumoto, Bull. Geol. Soc. Amer., 77, 987-1004 (1966).
- (5) D. L. Thurber, J. Geophys. Res., 67, 4518-4520 (1962).
- (6) J. M. Huey, R. G. Ostic and T. J. Thomas, Semi-Annual Progress Report to NASA, Contract NAS-9-8073 (1 May 1968 - 31 October 1968), Report CMU-NASA-21-1, Section VIII.
- (7) Teh-Lung Ku, J. Geophys. Res., 70, 3457-3475 (1965).
- (8) H. Itochi, This Report, II. D. 2.

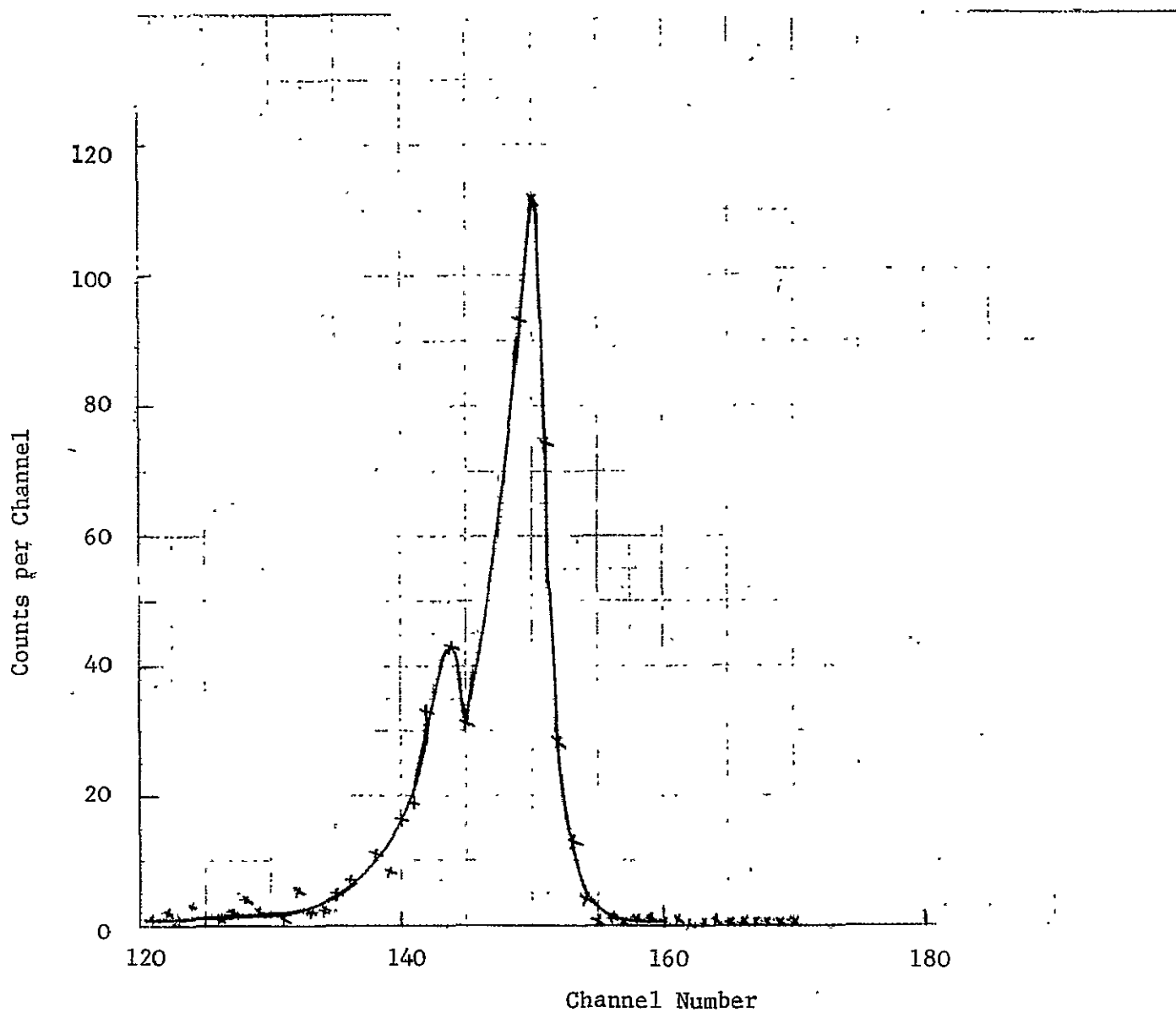


Figure 1. Alpha spectrum of U^{232} separated from a tracer solution containing U^{232} and Th^{228} and its decay products.

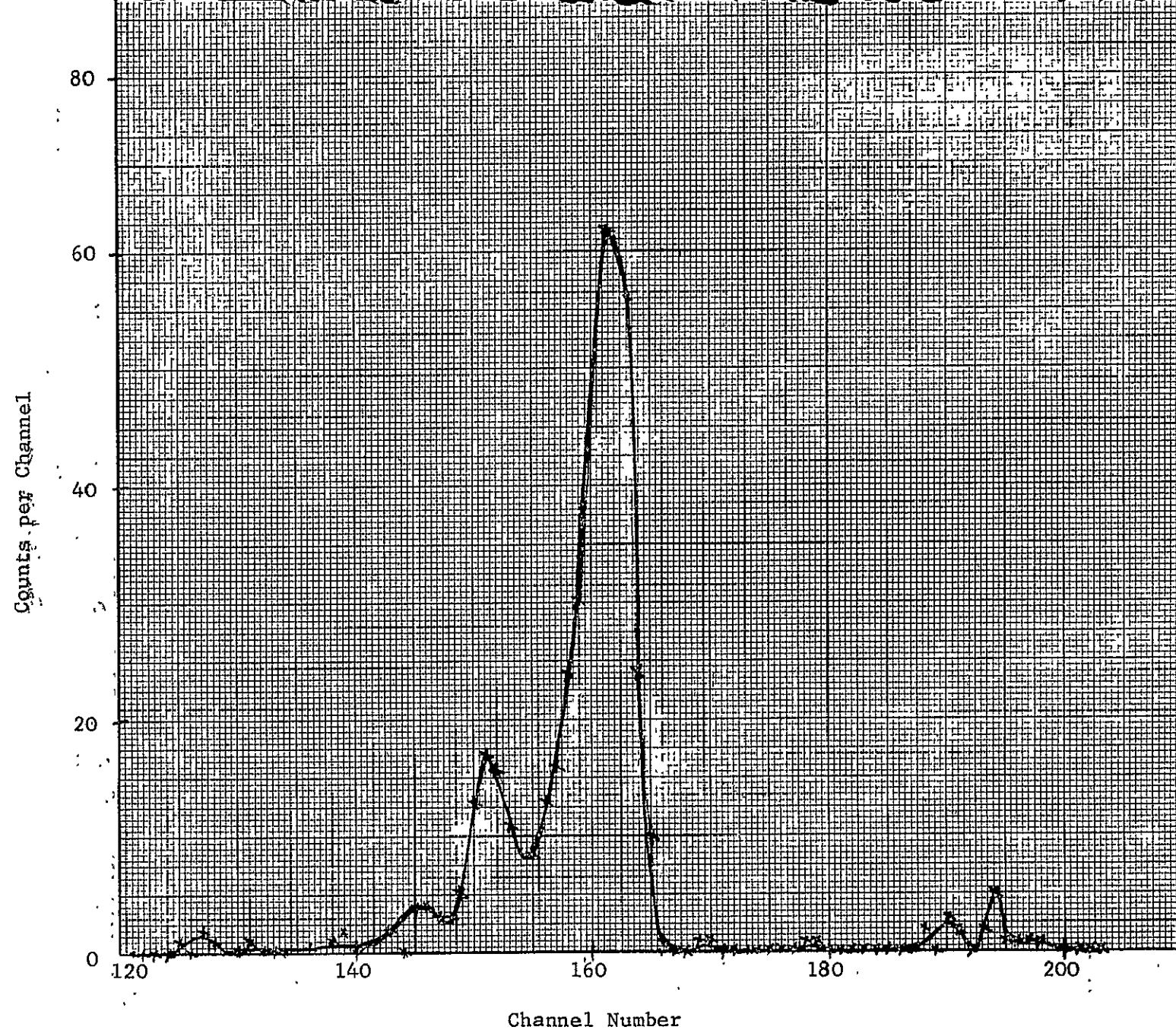


Figure 2. Alpha spectrum of Th^{228} separated from a tracer solution containing U^{232} and Th^{228} and its decay products.

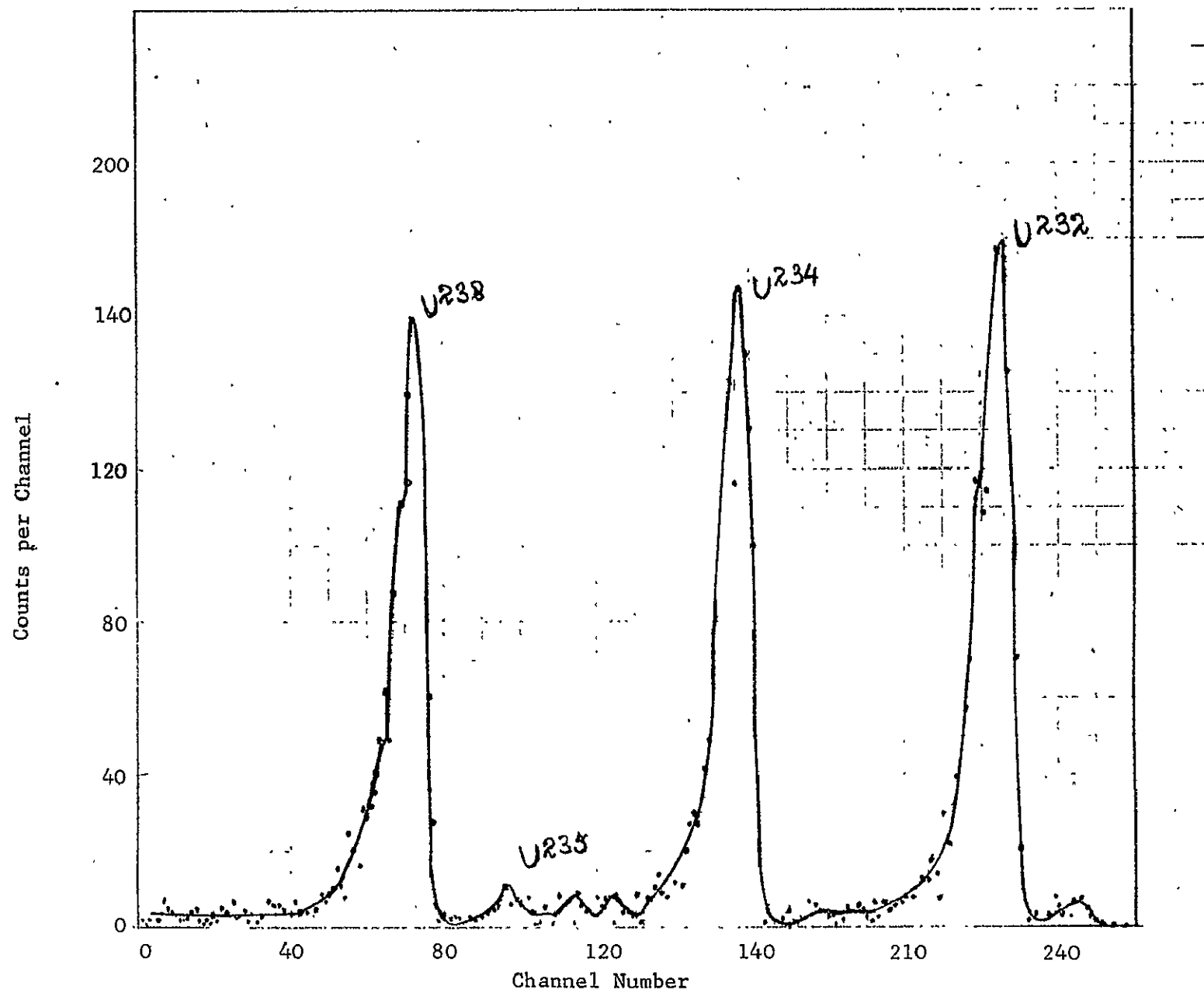


Figure 3. Alpha spectrum of natural uranium (plus U²³² spike) from a Granodiorite.

N71-10317

II. D. 6

LEAST-SQUARES ANALYSIS OF EXPERIMENTAL ALPHA SPECTRA

Brij M. P. Trivedi

For precise determination of the U^{234}/U^{238} ratio of uranium from natural materials (tektites, rocks, lunar samples, etc.) and for alpha-isotope-dilution analysis of uranium and thorium using U^{232} or U^{235} and Th^{228} or Th^{230} , respectively as spikes, a rigorous least-squares program has been developed to analyze the alpha spectra of these elements.

Observed spectra of the samples show considerable low-energy tailing because of energy loss from the finite thickness of the sample, back scattering of alpha particles from the supporting material, and the range of angles at which the particles pass through the window of the semiconductor detector in high counting geometry. The alpha spectra are therefore represented by a modified Gaussian function of the form:

$$I = I_0 \exp \left[- \frac{[(E - E_0)/W]^{M_1}}{1 + [1 - \text{sign}(E - E_0)][S(E - E_0)]^{M_2}} \right] \quad [1]$$

where

I = intensity in each channel due to an alpha group

I_0 = peak intensity of an alpha group

E = Energy

E_0 = peak energy of an alpha group

W = resolution parameter

$\text{sign}(E - E_0) = 1$ if $E > E_0$

$= -1$ if $E < E_0$

$= 0$ if $E = E_0$

S = skewing parameter. S is derived from another parameter Q , called tailing parameter, equal to ratio of peak height to low energy asymptote of tail.

$$Q = \exp. (1/2W^2S^2)$$

Equation [1] was first used by Huey et al. (1), keeping $M_1 = M_2 = 2$. It was modified by Thomas (2) by keeping $M_1 = 2$ but allowing M_2 to be variable. Equation [1] is a more generalized form of these equations.

Because the spectra are taken in a multichannel analyzer, the energy E is expressed in terms of the channel number of the analyzer:

$$E = C_1 + C_2 X$$

where

C_1 = zero channel energy intercept
(bias) of the multichannel analyzer

C_2 = energy increment per channel

and

X = channel number

The parameters to be adjusted in equation [1] are the intensities of the individual alpha emitters (I_{232} , I_{234} , I_{235} , I_{236} , I_{238} , or I_{228} , I_{230} , I_{232}) for uranium or thorium samples, respectively, and the spectrum parameters W , S , C_1 , C_2 , M_1 and M_2 . Henceforth, the intensity and the spectrum parameters will be collectively referred to as parameters. The peak intensity of each group is derived from its known branching fraction and the total intensity of the emitter to which it belongs.

For the least-squares analysis, the values of the above-mentioned parameters are first approximately guessed. The function I (I_{232} , I_{234} , I_{235} , I_{236} , I_{238} , W , S , C_1 , C_2 , M_1 , M_2) is expanded about these parameters in a Taylor series, keeping only the first terms:

$$I = (I)_0 + \left(\frac{\partial I}{\partial I_{232}} \right)_0 \Delta I_{232} + \left(\frac{\partial I}{\partial I_{234}} \right)_0 \Delta I_{234} + \dots \quad [2]$$

$(I)_0$ is the value of the function I for the initial (guessed) set of parameters. The derivatives $\left(\frac{\partial I}{\partial I_{232}} \right)_0$, etc. are evaluated numerically using the following equation and its analogs for other arguments:

$$\left(\frac{\partial I}{\partial I_{232}} \right)_0 = \frac{I(I_{232} + \Delta I_{232}, I_{234}, \dots) - I(I_{232}, I_{234}, \dots)}{\Delta I_{232}} \quad [3]$$

ΔI_{232} is a small increment (for the present case it was 0.1% of the original value) given to the parameter I_{232} .

The condition of least-square fitting adopted is (3):

$$\chi^2 = \sum_i \frac{1}{\sigma_i^2} \left[I_i - (I_{\text{obs}})_i \right]^2 = \min. \quad [4]$$

Summation is over all the observations i . $\sigma_i^2 = (I_{\text{obs}})_i$ (see for example Bevington 1969). For the present calculations σ_i^2 was set equal to $(I_{\text{cal}})_i$. This change was done to avoid the division of the function $[I_i - (I_{\text{obs}})_i]$ by zero when $(I_{\text{obs}})_i$ equals zero. This change is justified for the cases where I_i is not much different from $(I_{\text{obs}})_i$. However, when the difference $[I_i - (I_{\text{obs}})_i]$ is large, $\sigma_i^2 = (I_{\text{obs}})_i$ should be used and σ_i^2 should be put equal to unity for the cases where $(I_{\text{obs}})_i$ equals zero. Other weighting factors have also been suggested in the literature (4,5,6).

Equation [4] can be written as:

$$\begin{aligned} \chi^2 &= \sum_i \frac{1}{\sigma_i^2} \left[\left\{ (I)_o + \left(\frac{\partial I}{\partial I_{232}} \right)_o \Delta I_{232} + \left(\frac{\partial I}{\partial I_{234}} \right)_o \Delta I_{234} \right. \right. \\ &\quad \left. \left. + \dots \right\}_i - (I_{\text{obs}})_i \right]^2 = \min \\ &= \sum_i \frac{1}{\sigma_i^2} \left[\epsilon_i + \left(\frac{\partial I}{\partial I_{232}} \right)_o \Delta I_{232} + \left(\frac{\partial I}{\partial I_{234}} \right)_o \Delta I_{234} + \dots \right]^2 \quad [5] \end{aligned}$$

where $\epsilon_i = [(I)_o - I_{\text{obs}}]$ for the channel i .

Differentiating equation [5] with respect to ΔI_{232} we get:

$$\begin{aligned} \frac{\partial \chi^2}{\partial \Delta I_{232}} &= \sum_i \frac{2}{\sigma_i^2} \left[\epsilon_i + \left(\frac{\partial I}{\partial I_{232}} \right)_o \Delta I_{232} + \left(\frac{\partial I}{\partial I_{234}} \right)_o \Delta I_{234} \right. \\ &\quad \left. + \dots \right] \left(\frac{\partial I}{\partial I_{232}} \right)_o = 0 \end{aligned}$$

Similar equations are obtained for other parameters. These equations are linear in parameters (ΔI_{232} , ΔI_{234} , etc.) and can be solved for them by using matrix algebra.

The goodness of fit at each step is judged from χ_v^2 value defined as (3):

$$\chi_v^2 = \frac{\chi^2}{N-n} = \frac{1}{N-n} \sum_i \frac{1}{\sigma_i^2} (I - I_{\text{obs}})^2$$

where

N = total number of observations

and

n = total number of parameters

The computer program has been written in ALGOL for the CMU computer center UNIVAC 1108 computer. It accepts as input the approximate values of the initial parameters (I_{232} , I_{234} , I_{235} , I_{236} , I_{238} , W , S , C_1 , C_2 , M_1 , M_2) and the observed intensity in each channel. It calculates total intensity in each channel; compares with the observed values; finds an improved set of parameters; and goes through several cycles to determine the best set. So far each program was run only for five cycles, and the parameters were taken for lowest value of χ_v^2 . The program gives as output the calculated intensity in each channel, the improved set of parameters and their standard derivatives, and the value of χ_v^2 for each cycle of repetition. The method seems to converge in about 5-6 cycles if the initial parameters are properly guessed.

Results

The program has been tested by using experimental data on the measurement of uranium from tektites. The samples for these data were prepared by Tsomi (7) and counted by Thomas (2). Two such fitted spectra are shown in Figures 1 and 2. For Figure 1 the observed spectrum was taken for a single run. For Figure 2, the same sample was counted at different times and the activity in different channels were added to give one spectrum. This might result in a poor spectrum when there is a large drift. Figure 1 shows the alpha spectrum of U from a moldavite [sample T-5-I-b; Tsomi (7), Thomas (2)] and Figure 2 shows the alpha spectrum of U from a philippinite [sample T-24-V; Tsomi (7), Thomas (2)]. Table I shows the initial set of parameters and the successively adjusted parameters for each cycle for Figure 1. Also shown are the values of χ_v^2 for each cycle at the bottom.

In Table II are given the derived activity ratios of (U_{234}/U_{238}) and (U_{235}/U_{238}) for the two tektites. For comparison these ratios are given for equilibrium natural uranium. The isotopic ratios in tektites seem close to natural uranium isotopic ratio considering their relatively large uncertainties. More samples are being analyzed in this laboratory for isotopic studies (8). The method will be applied to isotope-dilution analysis of uranium and thorium from silicate materials (special interest is in lunar samples) (9).

Discussion

For a good fit, the value of χ_v^2 should be close to unity (a value between 1 and 1.5 is reasonable). For the sample T-24-V, χ_v^2 seems to be significantly different from unity. This might be due to the following reasons: (1) The method of analytical expansion of the function I converges very fast only near the point of minimum of χ^2 and not from far off points. In other words, if the initial set of parameters are not close to the true parameters, the method cannot be expected to converge with any reliability. This difficulty can be overcome by using another method, which converges fast when away from χ^2 minimum but very slowly near χ^2 minimum, to derive the initial set of parameters (3). In this method the function χ^2 is minimized with respect to each parameter

separately keeping all others constant. The parameters giving the minimum value of χ^2 can then be used as the initial parameters in the analytical expansion method. (2) Use of weighting factor ($W_i = \frac{1}{\sigma_i^2} = \frac{1}{I_{cal}}$) may not be the best. Other weighting factors ($W_i = \frac{1}{(I_{obs})^2}$; $\frac{1}{(I_{obs} \times I_{cal})}$) will be tried in the future. (3) Incorrect nuclear data (especially branching ratio of U_{234} alphas). This discrepancy is obvious from both Figure 1 and 2. (4) Variable resolution (functions of energy).

The computer program developed is still in the initial stage. All the correction factors will be introduced so that it can be used with full reliability.

References

- (1) J. M. Huey, R. G. Ostic and Thomas J. Thomas, Semi-Annual Progress Report to NASA, Contract NAS-9-8073 (1 May 1968 - 31 October 1968), Report CMU-NASA-21-1, Section VIII.
- (2) T. J. Thomas, 1968-69 Progress Report, USAEC Report NYO-844-76, II. A. 2.
- (3) P. R. Bevington, Data Reduction and Error Analysis for the Physical Sciences, (McGraw-Hill Book Co., 1969).
- (4) H. Kim, J. Chem. Ed., 47, 120 (1970).
- (5) T. P. Kohman, 1968-69 Progress Report, USAEC Report NYO-844-76, II. D. 4; J. Chem. Ed., 47, in press (1970).
- (6) W. E. Wentworth, J. Chem. Ed., 42, 96 (1965).
- (7) V. Tsomi, 1967-68 Progress Report, USAEC Report NYO-844-75, II. A. 3.
- (8) N. Kan, This Report, II. D. 4.
- (9) B. M. P. Trivedi, This Report, II. D. 5.

TABLE I
ADJUSTED PARAMETERS FOR SAMPLE NO. T-5-I-b

Parameter	Initial Input Estimate	Adjusted Value After Cycle No.					Standard Deviation ±
		1	2	3	4	5	
W	0.024	0.021	0.020	0.020	0.021	0.021	0.0000
S	12.30	15.38	18.81	19.89	19.64	19.55	1.61
C ₁	3.360	3.357	3.355	3.354	3.353	3.352	0.0000
C ₂	0.008	0.008	0.008	0.008	0.008	0.008	0.0000
M ₁	2.0	1.92	2.09	2.22	2.25	2.26	0.18
M ₂	2.0	1.82	1.90	2.06	2.11	2.12	0.08
I ₂₃₄	260	243.4	250.4	250.7	245.6	245.5	11.7
I ₂₃₅	14	14.34	14.90	14.63	14.17	14.07	2.13
I ₂₃₈	260	218.7	223.0	223.2	218.9	218.8	10.4
χ_v^2	2.63	1.54	2.97	1.72	1.46	1.36	

TABLE II
ACTIVITY RATIO OF URANIUM ISOTOPES IN TEKTITES

Sample Number	T-5-I-b		T-24-V		Natural U
No. of Iterations	5		4		
W	0.021	± 0.0000	0.022	± 0.0000	
S	19.55	± 1.61	14.97	± 0.32	
C ₁	3.352	± 0.0000	3.326	± 0.0000	
C ₂	0.008	± 0.0000	0.008	± 0.0000	
M ₁	2.26	± 0.18	1.85	± 0.039	
M ₂	2.12	± 0.08	1.72	± 0.023	
I ₂₃₄	245.5	± 11.7	2012.0	± 32.03	
I ₂₃₅	14.07	± 2.13	86.9	± 5.64	
I ₂₃₈	218.8	± 10.4	2015.1	± 32.01	
χ_v^2	1.36		5.94		
I ₂₃₄ /I ₂₃₈	1.122	± 0.075	0.997	± 0.022	1.000
I ₂₃₅ /I ₂₃₈	0.0643	± 0.0099	0.0458	± 0.00302	0.0459

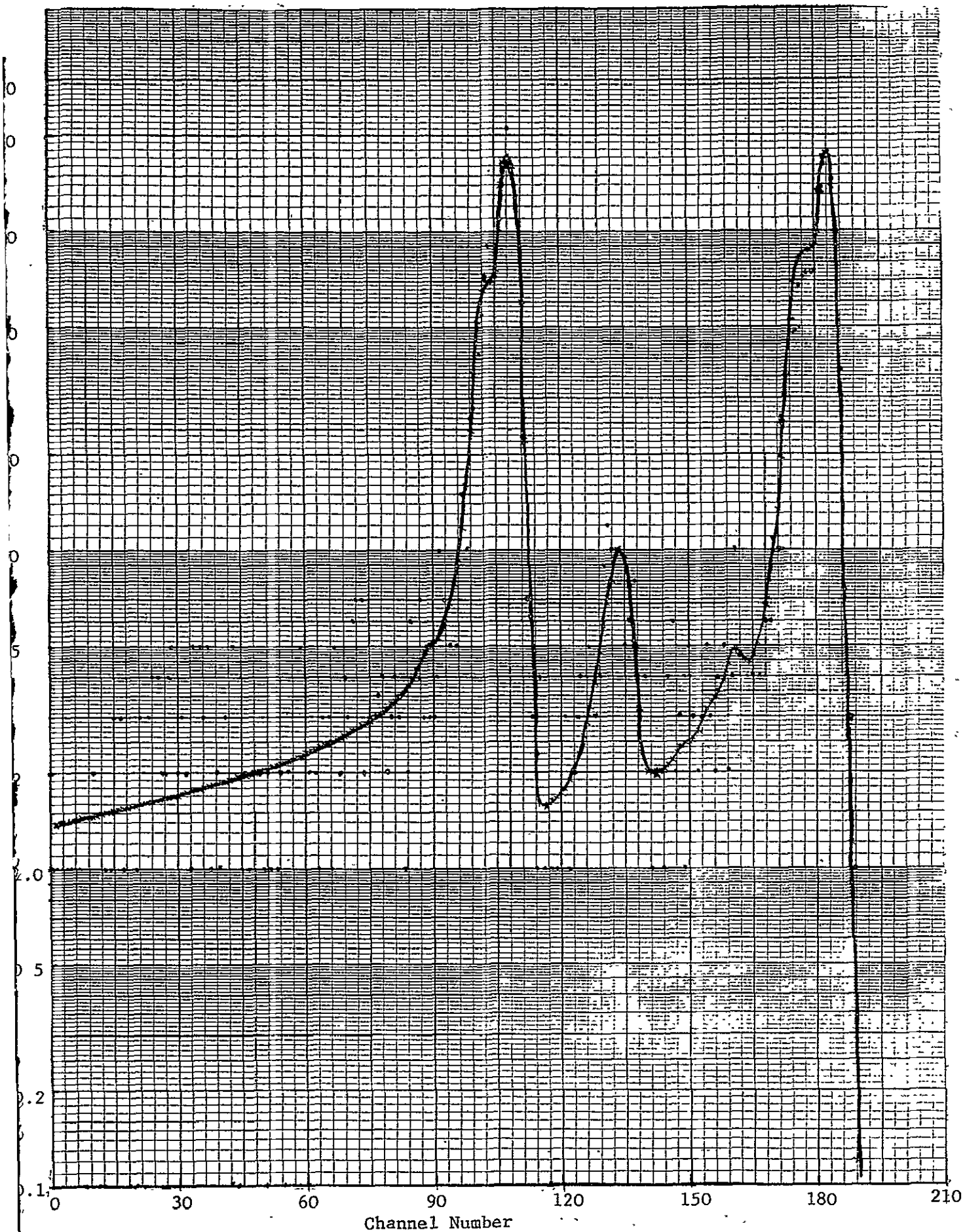


Figure 1. Experimental (points) and fitted (curve) spectra of uranium from a moldavite sample (T-5-I-h).

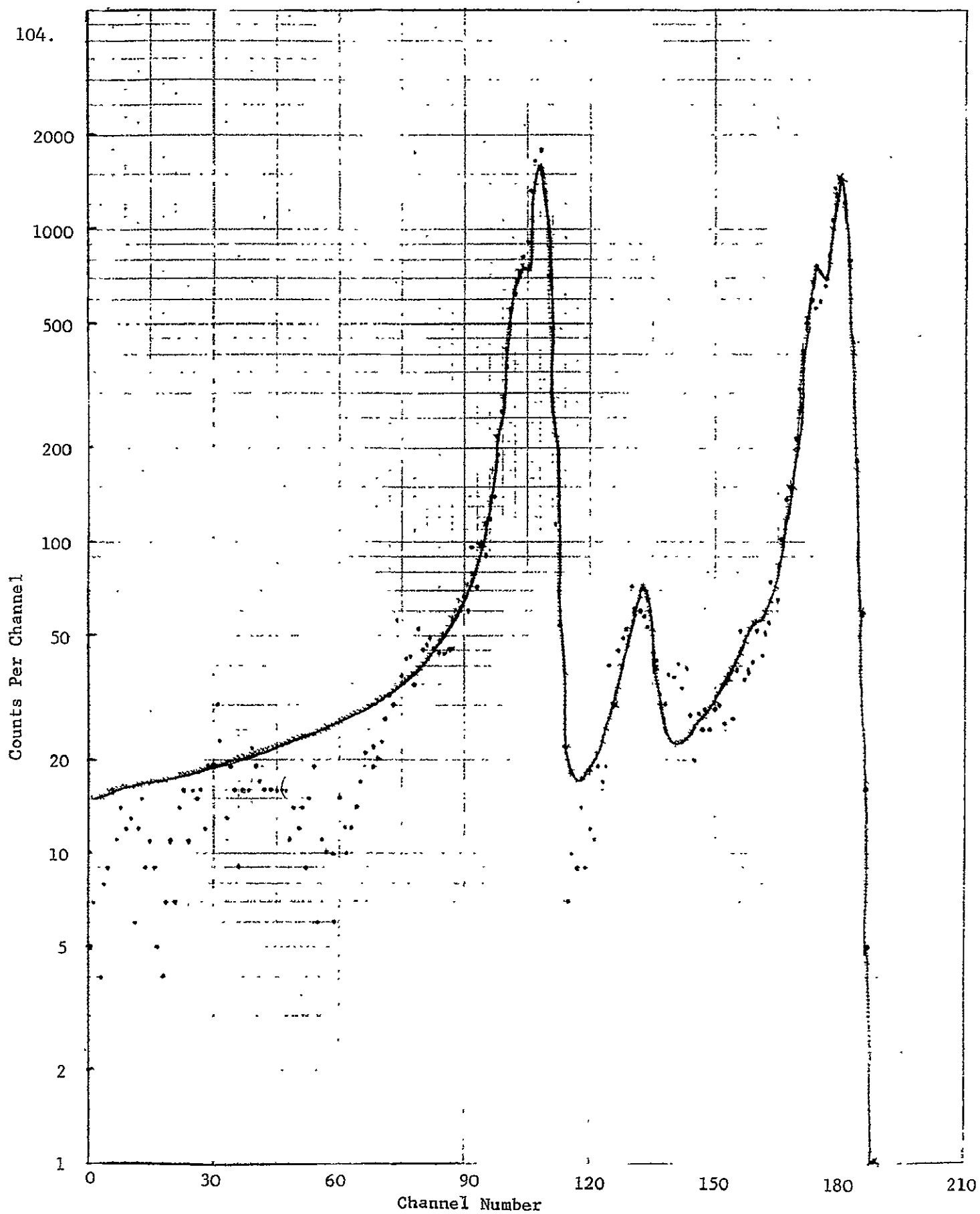


Figure 2. Experimental (points) and fitted (curves) spectra of uranium from a philippinite sample (T-24-V).

II. D. 7.

DESIGN AND CONSTRUCTION OF A POSITION-SENSITIVE PROPORTIONAL COUNTER

John R. Yocum, Jr. and John F. Monahan

I. Introduction

The objective of this project is to design and build a proportional counter which will record the location of an event in the counter as well as its magnitude. In addition, we hope to make the counter light enough to be used in unmanned spacecraft.

The basis for our interest in position sensitive proportional detectors is that they would enormously decrease the complexity and instrumentation of any proportional array and would tend to increase its sensitivity. In a normal array, the smallest increment of position is the size of the individual detectors. However, the position increment of a position sensitive device is dependent only on the uniformity of the detector, a factor which can easily be controlled. There is a practical minimum size for proportional detectors at this time; but, theoretically at least, there is no limit to the accuracy of a position sensitive device.

Another valuable point is that in order to achieve the accuracy now obtainable, many small detectors, each with its own voltage supply, preamplifier, amplifier, and recording equipment, must be used. If a large-position sensitive device were used in place of each line of small detectors, the same or greater accuracy in positioning and recording the pulses could be obtained, at a much lower cost in instrumentation, weight, and power.

Two types of position-sensitive proportional detectors have been considered.

The first, a semiconductive detector, has been in use for several years; however, it has many serious limitations. It has very good accuracy on higher energy pulses, but it also has an extremely high noise factor which blanks out lower energy pulses. The size of one of these detectors is not very large, so an array of them would require the same amount of instrumentation as any other type of detector. The use of semiconductive detectors on unmanned spacecraft would be very limited, because detectors of this type require a low temperature to operate and are very sensitive to temperature change. Due to the latter consideration, cryogenic equipment must be used, adding to weight problems.

The other alternative, a resistive proportional tube, is the main focus of our efforts at this time. In this type of proportional tube, the conductive center wire is to be replaced by a wire with a resistance of approximately twice the input impedance of one of the preamplifiers used with it.

818 01-17N

The tube is to be operated by placing a high positive potential on the center wire from both ends of the wire. An amplifier and preamplifier would also be attached to each end of the wire so that the circuit would be similar to Fig. 1.

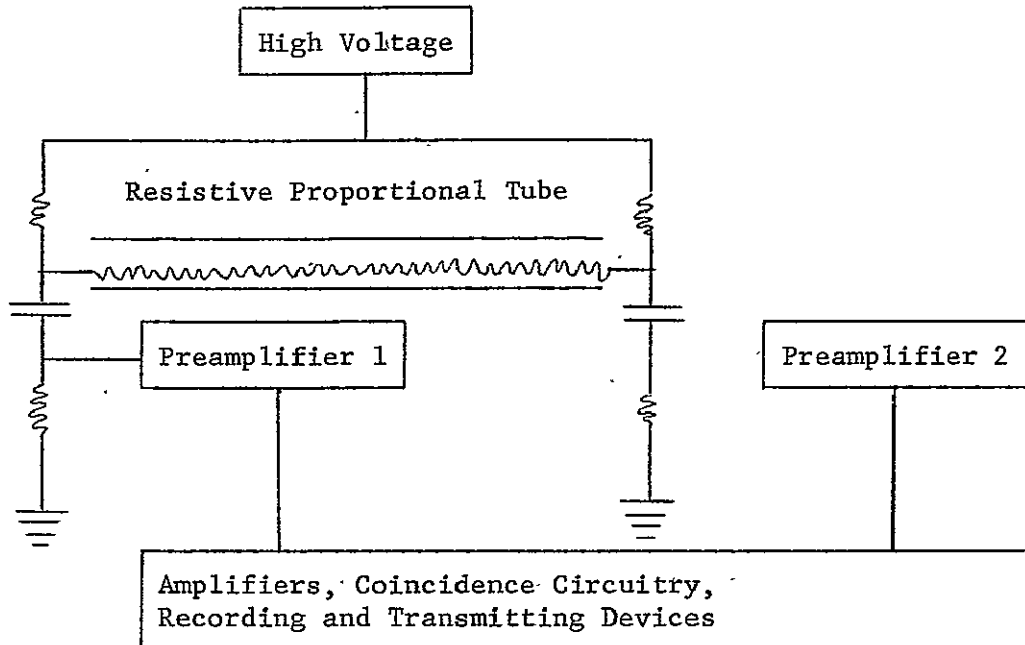


Figure 1

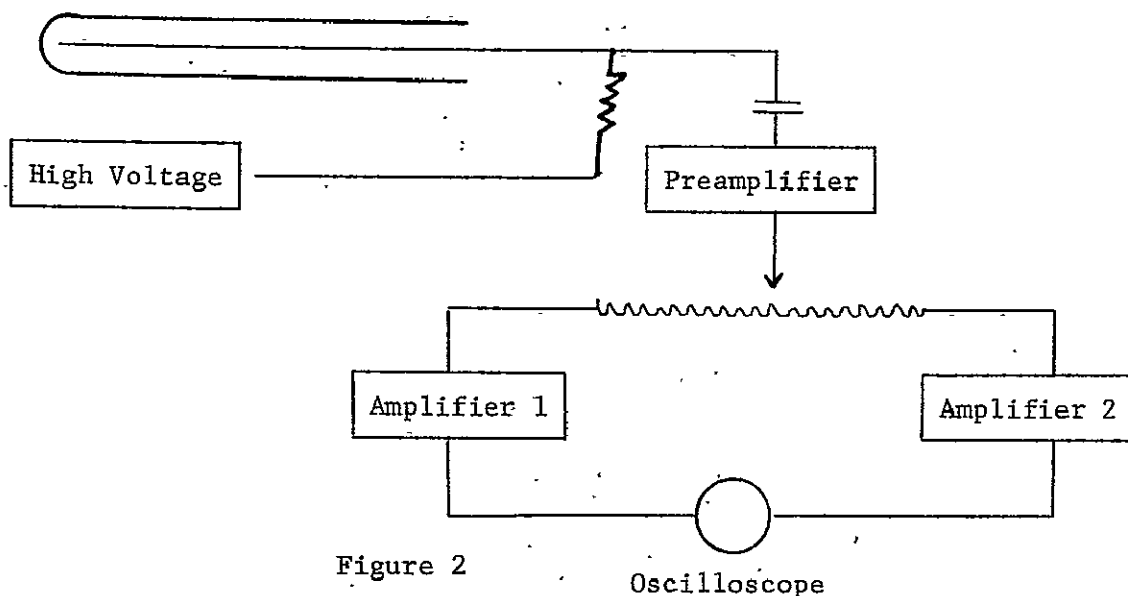
Any pulses occurring nearer one end of the tube than the other, would be larger on that end because of the lower resistance path. By recording the sum of the two pulses, the magnitude of the event could be determined. The ratio of the two would indicate where the event occurred.

The resistive proportional tube would have a wide range of applications. Presently our interest extends mainly to cosmic X-ray mapping from unmanned spacecraft. Other uses in fields such as Medicine could also use the resistive proportional tube for cobalt therapy and organ scans.

II. Experiments

A. Resistive Proportional Tube Simulation

In the resistive proportional tube simulation, a normal proportional tube and preamplifier were attached to the center tap of a potentiometer and two amplifiers were connected to the other leads, as in Fig. 2.



The proportional tube used for the simulation was filled with a 90% Kr - 10% CH₄ mixture at 73 cm pressure. Its operating voltage was 1800 volts DC. Since the tube was especially designed for x-rays, we used a Co⁵⁷ source.

By varying the setting of the potentiometer, the amount of signal reaching each amplifier could be altered. If the total resistance of the potentiometer is twice the input impedance of each amplifier and if the potential is assumed to be distributed according to resistance only, the signal amplitude should vary from $\frac{1}{4}$ the normal value at one end of the scale to $\frac{3}{4}$ value at the other. In the middle, each amplifier should receive $\frac{1}{2}$ the normal pulse amplitude.

Two display techniques have been developed. One places each amplifier output on a beam of a twin-beam oscilloscope. Differences in pulse height and shape are very clearly indicated. The other method places one output on the horizontal deflection plates of an oscilloscope and the other output on the vertical. In theory, the result should be a sloping line whose length corresponds to the size of the pulse and whose slope corresponds to the ratio between the outputs. However, due to inequities in the two amplification systems, noise and similar factors, the actual picture is very complex. Reduction of noise and more careful adjustment of the amplifiers should alleviate this difficulty. We expect both of these display methods to evolve in ensuing research.

B. Production of High-Resistance Center Wire

The high-resistance center wire necessary for the position-sensitive proportional tube must have a reasonable length and strength and must have a low-temperature coefficient of resistance.

Two techniques of making the high-resistance center wire are being considered: carbon films and vacuum deposition of metal films.

The carbon film is the first to be considered and is the more promising of the two methods. Carbon films are not as expensive to make, and they are more easily applied than metallic films. The thickness - hence, the resistance - of the film is easily adjusted, and it will not react with proportional counter gases such as argon-methane.

Carbon films also have drawbacks, however. The primary difficulty is their low adherence to a glass or quartz fiber. Since glass or quartz will probably be used as the substrate for deposition, a method of making the carbon film adhere to the substrate must be found if it is to be used.

The actual deposition would probably be done from a gas; however, the details of this operation have not yet been worked out (1,2).

If the carbon film proves unworkable, a nickel-chromium alloy deposited on a glass or quartz strand will probably be the second alternative chosen. The film would be vacuum deposited on an SiO_2 strand 15 cm in length to a depth such that the resistance would be approximately $2 \times 10^5 \Omega$ with a temperature coefficient of resistance of $< .1\%$. The ratio of nickel and chromium would probably be 4:1 (3-6).

Two methods of producing the film appear suitable.

Flash evaporation calls for vaporizing small amounts of the metallic powders in the correct ratio in very short periods of time. The best way would be to pour a slow stream of the powder onto a tantalum strip heated to about 1600°C by a tungsten radiant heater underneath. The Nichrome mixture will vaporize almost as soon as it touches the tantalum strip and will deposit on the glass substrate.

Separate filament evaporation requires two tungsten filaments, one wrapped with nickel, the other with chromium. Both are resistance-heated until the two metals vaporize. This method would not give as uniform a film as the other because of the difference in boiling points, etc., of the two metals.

The substrate will be a very fine strand of SiO_2 about 10^{-2} cm in diameter. As has been done in nearly all previous cases, the glass will be heated by a radiant heater for better adhesion and uniformity. While deposition is taking place, a vacuum tube voltmeter will be connected across the substrate to measure its resistance and to act as a control on the metallic evaporation.

III. Possible Future Activity

Our attention in the future will be focused on the actual construction of the resistive proportional tube. It should differ little from the construction of a normal proportional tube except that the strand may be fragile and require special consideration as far as installation.

The first step will be the fabrication and testing of the resistive wire outside the tube.

After the assembly of the tube with several types of wires and variations in constructional details, the differences will be evaluated and the most stable and best resistive values will be tested further. When the resistive proportional tube is developed to a workable state, we will use it to design analytical systems for recording magnitude and position readings. During this stage, the tube will also probably evolve to a much higher degree.

When these systems are in working order, several resistive proportional tubes will be linked into an array to determine whether they would be suitable for use in arrays. Following this, the array will be connected to telemetry equipment for broadcast of information.

The next step will be to miniaturize the equipment in size and weight and to increase the strength and stability of the resistive proportional tube to withstand the rigors of space flight. Finally, the device will be flown in an unmanned satellite for cosmic x-ray observation.

References

- (1) H. G. Marfield, *Electronic Engineering*, 588-594 (Sept. 1963).
- (2) P. Huijer, et al., *Philips Technical Review* 24, 144-149 (1962-63).
- (3) L. Holland, ed, This Film Microelectronics (New York, 1965).
- (4) L. Holland, *Vacuum Deposition of Thin Films* (London, 1956).
- (5) R. H. Alderton and F. Ashworth, *British Journal of Applied Physics*, 207 (May 1957).
- (6) G. Sidall and B. A. Probyn, *British Journal of Applied Physics* 12, 668-673 (1965).

E. Miscellaneous

II. E. 1.

A UNIVERSAL MAGNITUDE SYSTEM FOR ASTRONOMICAL OBJECTS

Truman P. Kohman

The great variety of magnitude scales in use in astronomy is confusing, partly because of their arbitrariness, and particularly because of the lack of a logical relationship between the scales for different quantum energies. A universal system of magnitudes based on power flux is proposed.

This proposal is based on the concept of the expression of spectral (monochromatic) power flux as the logarithmic derivative with respect to any spectral parameter:

$$I^* = \left| \frac{dI}{d \ln \lambda} \right| = \left| \frac{dI}{d \ln \nu} \right| = \left| \frac{dI}{d \ln \sigma} \right| = \left| \frac{dI}{d \ln \epsilon} \right|$$

The logarithmic derivative is related to the simple derivatives by

$$I^* = \lambda I'_\lambda = \nu I'_\nu = \sigma I'_\sigma = \epsilon I'_\epsilon$$

and is proposed as a natural universal system for power fluxes.

The universal integral and spectral magnitudes are respectively defined by:

$$\bar{m} = -\frac{5}{2} \log \frac{I}{I_0} \quad \text{and} \quad \bar{m}^* = -\frac{5}{2} \log \frac{I^*}{I_0^*}$$

It is proposed that the scale be normalized by adopting as the fluxes for zero magnitude:

$$\bar{I}_0 = 10^{-7.6} \text{ W m}^{-2} = 2.512 \times 10^{-8} \text{ W m}^{-2}$$

$$\bar{I}_0^* = 10^{-7.6} \text{ W m}^{-2} \text{ un}^{-1} = 2.512 \times 10^{-8} \text{ W m}^{-2} \text{ un}^{-1}$$

Alternate concise formulations of the definitions of integral and spectral magnitudes on the universal scale become:

$$\bar{m} = -\frac{5}{2} \log \frac{I}{\text{W m}^{-2}} - 19 \quad \text{and} \quad \bar{m}^* = -\frac{5}{2} \log \frac{I^*}{\text{W m}^{-2} \text{ un}^{-1}} - 19$$

The system is readily extended to include partial-integral magnitudes, luminance magnitudes, and absolute magnitudes.

This system realizes a definite physical relationship between magnitudes and power fluxes, facilitates meaningful intercomparisons of power fluxes or magnitudes in all parts of the electromagnetic spectrum from radio to gamma radiation, and simplifies calculations and data presentations.

A number of examples from various branches of astronomy illustrate the applicability and advantages of the system.

This paper was presented at the meeting of the American Astronomical Society in Boulder, Colorado, on 1970 June 10, and draft copies (NYO-844-80) were given or have been sent to a number of astronomers with requests for comments. After consideration of comments already received and to be received, a final version will be submitted to the Astronomical Journal for publication.